

Measured Enthalpy and Derived Thermodynamic Properties of Crystalline and Liquid Potassium Chloride, KCl, from 273 to 1174 K

Thomas B. Douglas and Ann W. Harman

Institute for Materials Research, National Bureau of Standards, Washington, D.C. 20234

(April 19, 1974)

The enthalpy of KCl relative to that at 273.15 K was precisely measured by drop calorimetry from 273 to 1174 K, and smooth thermodynamic functions were derived for this temperature range. The heat capacities found for the crystalline phase join smoothly the most precise published data for lower temperatures; those for the liquid phase are temperature-independent within the precision of measurement over the 120° range covered. It is concluded that the broad exponential upturn of the heat-capacity curve below the melting point, if attributed to lattice vacancies, indicates a predominance of large vacancy clusters.

Key words: Heat of fusion; high-temperature drop calorimetry; lattice vacancies; muriate of potash; potassium chloride; sylvite; thermodynamic properties.

1. Introduction

The experimental data on potassium chloride reported in this paper were obtained by the authors at the National Bureau of Standards in 1954. Although the results based on an earlier smoothing were incorporated in the various JANAF tables for this substance [23]¹, they have not been previously published otherwise. Since the original records were thoroughly annotated and these data appear to be still unexcelled in accuracy for the particular properties they represent, it seemed worthwhile to carry out a complete and careful reanalysis, and to present the results here. The heat capacities can be merged with the precise low-temperature values of Berg and Morrison [4] for the temperature range 2.8–270 K without any compromise of either set of data, and both the JANAF tables [23] and the present paper have chosen to carry out this merging, in order to base the enthalpy on 0 K and to obtain Third-Law entropies, as a firm basis in calculating thermodynamic equilibria involving crystalline or liquid potassium chloride. In fact, even though the small corrections to both pieces of work from the International Practical Temperature Scale of 1948 to that of 1968 (the most recent such scale) have been applied, the present smoothed values differ little from those in the latest JANAF tables (the largest discrepancy amounting to 0.5 percent in the heat of fusion, largely attributable to a different procedure of

extrapolating to the melting point). The present authors did not measure the melting point, but have critically selected a value from the literature.

The high practical importance of potassium chloride, not only among the alkali halides but among all inorganic substances, is well known, and stems partly from its fairly high natural abundance, its simplicity of chemical composition, and its chemical stability. There are, however, a number of basic scientific problems in which an accurate knowledge of the high-temperature equilibrium thermal properties of its condensed phases is important and directly applicable. Chief among such problems which motivated the present work are: (1) the abundance and nature of the lattice vacancies in the pure crystal; (2) the thermodynamic properties of solid and liquid solutions containing potassium chloride as one component; and (3) the thermodynamic properties and composition of gaseous potassium chloride. In connection with the third item, one of the present authors concluded twenty years ago that the best available vapor pressures and thermodynamic properties of the solid and liquid were consistent with reasonable electrostatic models of the postulated gas species only if saturated potassium chloride vapor near the melting point contains, in addition to the monomer, KCl, at least 8 mole percent of the dimer, K₂Cl₂. At that time no direct evidence existed for the association of alkali-halide vapors, but the subsequent mass and infrared spectroscopy of other investigators [23] established the truth of this indirect conclusion for potassium chloride.

¹ Figures in brackets refer to literature references at the end of this paper.

2. Sample and Container

A single sample—A.C.S. Reagent Grade potassium chloride from the General Chemical Division of the Allied Chemical & Dye Corporation, New York²—was used. The salt was not further purified except by fusing it quickly while contained in platinum (exposed to the atmosphere) to remove any occluded water. Two specimens of this material (each approximately 6.4 g, or 0.086 GFW), subsequently designated “samples 1 and 2”, were sealed in cylindrical containers of pure silver (“0.999 fine”) for the calorimetric measurements. Each silver container had a mass as close to 12 g as practical, and consisted of a cylinder of $\frac{5}{8}$ in diameter, 0.015 in wall thickness, and approximately 2 in length, with a tight-fitting silver cap sealed in each end by an oxy-gas flame, the final seal being made while the KCl sample was molten. In the subsequent enthalpy measurements each sample was suspended in the furnace by a wire of thermocouple-grade 90 Pt–10 Rh (o.d., 0.015 in) bearing two horizontal thin circular platinum radiation shields and a small hook of 80 Ni–20 Cr, all with controlled masses. The small mass of silver (a few tenths of a mg) lost in such a sealing process was determined by sealing other dry containers having no sample present, and applied as a correction in deducing by difference the exact mass of each sample.

The results of analyzing the sample are recorded in table 1. The qualitative spectrochemical analysis was performed on a typical specimen by the Spectrochemical Analysis Section of the Bureau. Hot KCl is slightly hydrolyzed by such an exposure to moist air as described above; therefore after all the calorimetric measurements on sample 1 (the principal specimen) it was dissolved in CO₂-free water and titrated with standard HCl solution and phenolphthalein, giving (after applying the blanks) the equivalent of 0.04 weight percent of KOH.

TABLE 1. Chemical and spectrochemical analysis of the sample^a

Impurity	Weight percent	Method of analysis
KOH	0.04	Titration with acid
Na	0.001–0.01	
Al	} 0.0001–0.001 (each)	} Qualitative spectrochemical
Ba		
Ca		
Rb		
Si		
Cu		
Mg	< 0.0001 (each)	

^a In addition B. P. and 44 other metals were sought spectrochemically but not detected.

² Mention of a specific commercial organization does not imply recommendation by the National Bureau of Standards of its goods or services.

3. Enthalpy Measurements

3.1. Calorimetric Procedure

The enthalpy of the sample and its container relative to that at 0 °C was measured by “drop” calorimetry, which is described in great detail elsewhere [12]. The particular procedure followed in the present case was briefly as follows. The sample in its container was held in an atmosphere of helium in a vertical silver-core furnace for a time sufficient to allow it to reach the (constant) furnace temperature, and was then dropped into a Bunsen ice calorimeter, which measured its loss of heat (enthalpy) in cooling from the furnace temperature to 0 °C. To account accurately for the heat lost by the container itself, during the drop and to the calorimeter, the measurement was repeated at the same furnace temperature on one or more identical empty containers.³

To create a very nearly isothermal environment, the sample or empty container was suspended in the furnace inside a central core of pure silver 10 in long, with o.d. 2 in and wall thickness $\frac{1}{2}$ in. Insulated from this core above and below were two shorter “guard” segments of silver (o.d., also 2 in) controlled by separate heaters to the temperature of the central core. The temperature of the suspended sample or container was taken to be that of the closest portion of the central core. In general, aside from the possible effects of sample composition or indefiniteness of physical state, the measurement of furnace temperature is usually the most serious source of systematic error in high-temperature drop calorimetry. The steps taken toward accurate temperature measurement are outlined in the following section.

3.2. Furnace Thermometry

Up to and including 600 °C (873 K), the furnace temperature was measured by one of two strain-free platinum resistance thermometers (ice-point resistance, approximately 25 ohms) that had been independently calibrated at the Bureau at the ice, steam, and sulfur points on the International Temperature Scale of 1948 (with later conversion to the IPTS–68 [20, 10]). When these thermometers were intercompared in the furnace just before the enthalpy measurements began, their temperature indications were discordant by + 0.036° (at 200 °C), – 0.035° (at 400 °C), and – 0.002° (at 600 °C). The ice-points of both thermometers were periodically redetermined and found not to have changed appreciably. As a precaution against an unsuspected deterioration of the tempering of the thermometer in the furnace, a thermometer reading was always accompanied by a *precise* thermocouple reading.

³ The preferable use of the same container for these two measurements would have been inconvenient, and is believed unnecessary anyhow because all containers were constructed from adjacent parts of the component materials and because the principal material, silver, has highly reproducible thermal properties when pure and annealed.

Above 600 °C, measurement of the furnace temperature had to rely on thermocouples, these being Pt/90 Pt-10 Rh (0.015-in.-diameter wires). One thermocouple had undergone a standard NBS calibration, and to minimize subsequent changes in its calibration it was used only to calibrate the "working thermocouple" (that used in the enthalpy measurements), by comparison of simultaneous readings when the junctions of both couples were in contact in the center of the furnace. A similar comparison of the "working" thermocouple with the "working" thermometer showed higher temperature readings of the thermocouple (on the basis of its calibration as described above) by 0.26° at 200 °C, 0.10° at 400 °C, and 0.17° at 600 °C. Because the thermometer is the more accurate instrument and there is no monotonic trend in these discrepancies, their mean (0.2°) was subtracted from all thermocouple readings above 600 °C. Otherwise, the graphical smoothing of the thermocouple readings from standard tables (for interpolation purposes) did not compromise any unsmoothed calibration value by more than 0.05°.

Despite the favorable conditions for an isothermal furnace region implied by the dimensions of the silver core (described in sec. 3.1), the structure of the furnace was such as to obviously permit considerable heat conduction out the ends of the core. For this reason "immersion" tests were performed, while the furnace was held at a constant temperature of about 600 °C, to test the temperature gradients around the position of the sample. Raising the thermometer or thermocouple sensing element by one cm raised the temperature reading by 0.0025° or 0.3 °C, respectively; but moving the thermocouple up and down, then rotating, and finally restoring the original level produced no net change. Raising the temperature of the *bottom* silver guard segment by 0.5° produced no effect on the thermometer and thermocouple readings, but raising the temperature of the *top* segment by 1.2° increased the thermometer reading by 0.0075° (the thermocouple *decrease* by 0.05° suggests an error in the test); these small effects are generally not unexpected, since the thermometer and thermocouple leads passed out the top of the furnace core.

3.3. Enthalpy Data

a. Empty Containers

The results of enthalpy measurements on empty containers are given in table 2. The principal series of measurements, designated "1a," was made just before the enthalpy measurements on the potassium chloride samples. Two additional series, "1b" and "2" (on the same and on a new container, respectively), were made several months after the completion of the KCl measurements, and at only three temperatures. The values of individual measurements (unsmoothed, but otherwise fully corrected) are given in the third column, in chronological order for each temperature. However, the heats actually observed

have been divided by 0.085554, the number of moles of potassium chloride in sample no. 1. By thus giving the values to be subtracted from those for container-plus-sample on the same basis, the effect of imprecision at a given temperature on the net enthalpy per mole of potassium chloride is directly obvious.

The mean measured empty-container enthalpy for each series at each temperature is given in the fourth column of table 2, and a small largely systematic difference will be noted among the three series at the three temperatures involving all series. It was decided to derive smooth values using the "series 1a" values only, partly because this series was measured closest in time to the potassium chloride samples (tending toward a greater cancellation of instrumental errors), and partly because the container surface in series 1a was believed more comparable to that for the KCl samples. (Each series of empty-container measurements was made at increasing temperatures, except that the highest temperature, 1174 K, was run first, with the belief that this might stabilize most quickly the crystal growth, and hence the radiative emissivity, of the surface.)

The empirical equation derived to represent the smoothed empty-container relative enthalpies from series 1a (in joules per mole of KCl sample No. 1, at temperature T K(IPTS-68)) is

$$H_T - H_{273.15} = 37.8035(T - 273.15) + 4.6024(10^{-4})(T - 273.15)^2 + 2.4227(10^{-6})(T - 273.15)^3 - 584.84(T - 273.15)/T. \quad (1)$$

Values from eq (1) are given in the fifth column of table 2, and the differences of the mean measured values from these, in the last column.

b. KCl Samples

Table 3 records the enthalpy results on potassium chloride. A second specimen of the salt ("sample No. 2") was measured in a different container at two temperatures (primarily to guard against an appreciable error in the mass of the principal specimen, sample No. 1, that would not otherwise be revealed by inconsistencies in the data). The individual enthalpy measurements are recorded in chronological order for each temperature. For sample No. 1, the liquid range (above 1045 K) was measured first, the crystalline range 373-974 K next, then 1009 K, and finally 1039 K. For sample No. 2 (run shortly after sample No. 1) the two measurements at 1034 K intervened between the second and third at 1009 K.

The container of sample No. 1 proved to be sealed completely tight, and the total mass changed by only about one mg during the whole series of measurements. In sealing sample No. 2, however, a small hole was blown in the top of the container, resulting in an immediate mass loss of 8.6 mg, which was assumed to be half KCl and half molten silver (introducing an

TABLE 2. Enthalpy data on typical empty containers

Temperature, $T(K)^a$	Container and series	Relative enthalpy, $H_T - H_{273.15}$ (in J per mole of KCl)					
		Measured	Mean measured	Smoothed (eq (1))	Difference		
373.15	1a	$\begin{Bmatrix} 3,629 \\ 3,631 \end{Bmatrix}$	3,630	3,631	-1		
473.19	1a	$\begin{Bmatrix} 7,346 \\ 7,366 \end{Bmatrix}$	7,356	7,353	+3		
573.22	1a	$\begin{Bmatrix} 11,144 \\ 11,140 \end{Bmatrix}$	11,142	11,144	-2		
673.23	1a	$\begin{Bmatrix} 15,003 \\ 15,007 \end{Bmatrix}$	15,005	15,005	0		
773.23	1a	$\begin{Bmatrix} 18,943 \\ 18,952 \end{Bmatrix}$	18,947	18,945	+2		
		$\begin{Bmatrix} 18,983 \\ 18,983 \end{Bmatrix}$				18,983	+38
	2	$\begin{Bmatrix} 18,958 \\ 18,954 \end{Bmatrix}$	18,956		+11		
873.30	1a	$\begin{Bmatrix} 22,947 \\ 22,981 \\ 22,978 \end{Bmatrix}$	22,969	22,976	-7		
973.54	1a	$\begin{Bmatrix} 27,124 \\ 27,115 \end{Bmatrix}$	27,119	27,115	+4		
		$\begin{Bmatrix} 27,155 \\ 27,179 \end{Bmatrix}$				27,167	+52
	2	$\begin{Bmatrix} 27,126 \\ 27,099 \end{Bmatrix}$	27,107		-8		
1008.64				28,590			
1033.70				29,653			
1038.72				29,866			
1053.76				30,509			
1073.82	1a	$\begin{Bmatrix} 31,368 \\ 31,376 \end{Bmatrix}$	31,372	31,370	+2		
1093.87				32,236			
1133.99				33,985			
1174.10	1a	$\begin{Bmatrix} 35,737 \\ 35,738 \\ 35,755 \\ 35,762 \\ 35,780 \end{Bmatrix}$	35,754	35,755	-1		
		$\begin{Bmatrix} 35,824 \\ 35,795 \end{Bmatrix}$				35,810	+55
	2	$\begin{Bmatrix} 35,727 \\ 35,723 \end{Bmatrix}$	35,725		-30		

^a International Practical Temperature Scale of 1968 [20].

uncertainty of 0.04 percent in the net enthalpies for KCl from this sample, owing to the widely different specific heats of these two substances). Furthermore, during the enthalpy measurements on it sample No. 2 steadily lost mass (to a total of 4 mg), which was corrected for on the assumption that minute amounts of KCl had escaped by evaporation.

The thermal values in table 3 (as well as those in table 2) are based on 270.48 J per g of mercury as the ideal calibration factor of the ice calorimeter [12]. The mass of KCl sample No. 1 was 6.3781 g (0.085554

“mol” on the basis of a molecular weight or GFW of 74.551 [2]). The mass of sample No. 2 varied with time from 6.4183 to 6.4141 g, but the gross enthalpies for this sample as recorded in the third column of table 3 have been increased by small amounts (about 0.2 percent) so that their means in the fourth column, as well as those for sample No. 1, may be decreased by the corresponding empty-container values (fifth column of table 2) to give all the mean net molar enthalpies of KCl listed in the fifth column of table 3. All enthalpies in tables 2 and 3 include very small

TABLE 3. Enthalpy data on samples of potassium chloride (KCl)

Temperature, T(K) ^a	Sample no.	Relative enthalpy, $H_T - H_{273.15}$ (J mol ⁻¹) ^b				
		KCl+ container		KCl only		
		Measured	Mean measured	Measured	Smoothed ^c	Difference
373.15	1	{8,805 8,827}	8,816	5,185	5,182	+3
473.19	1	{17,884 17,880}	17,882	10,529	10,529	0
573.22	1	{27,185 27,182}	27,183	16,038	16,040	-2
673.23	1	{36,714 36,727}	36,720	21,715	21,714	+1
773.23	1	{46,507 46,497}	46,502	27,557	27,560	-3
873.30	1	{56,588 56,611}	56,599	33,623	33,621	+2
973.54	1	{67,154 67,139}	67,146	40,032	40,025	+7
1008.64	{1 2}	{70,963 70,990}	70,976	42,386	42,391	{-5 -20}
		{70,965 70,958 70,959}	70,961	42,371		
1033.70	2	{73,798 73,787}	73,792	44,139	44,133	+6
1038.72	1	{74,727}	-----	(44,861)	44,488	{ d(+373) d(+295) d(+228) d(+156)
		{74,649}	-----	(44,783)		
		{74,582}	-----	(44,716)		
		{74,510}	-----	(44,644)		
1053.76	1	{102,268 102,228 102,228}	102,241	71,731	71,731	0
1093.87	1	{106,899 106,923 106,908}	106,910	74,674	74,675	-1
1133.99	1	{111,631 111,582 111,611}	111,608	77,623	77,620	+3
1174.10	1	{116,315 116,322}	116,318	80,563	80,564	-1

^a International Practical Temperature Scale of 1968 [20].

^b Molecular weight ("GFW") = 74.551 [2].

^c Calculated below 1045 K from eq (2) (crystal), and above 1045 K from eq (3) (liquid).

^d See discussion in sec. 3.3.b.

corrections for adjustment to a standard mass of each nonsample material (silver, 80 Ni-20 Cr, 90 Pt-10 Rh, and air inside the container). No correction was made for the heat of forming or condensing potassium chloride vapor inside a container, as this heat was calculated not to exceed 0.6 joule per mole of KCl sample [23]. No corrections for furnace temperature were needed, as these temperatures were always constant and within 0.01° of those listed in the tables. Previous tests had shown the time of the sample in the furnace (20 to 80 min) to be adequate for thermal equilibrium;

however, at 1054 K the sample was only 9° above the melting point, so to hasten the complete input of the heat of fusion the sample was preliminarily heated at 1094 K for at least 30 min.

For 1039 K the individual net enthalpies for the sample (table 3, fifth column) show a large drift with time which invites separate explanation (see below). The values for the lower temperatures, however, show no drift with time beyond what may be attributed to accidental error, and indicate a heat-capacity curve for the crystal which varies nearly linearly with

increasing temperature except with an accelerated upturn as the melting point is approached. It was found that these data could have been fit satisfactorily by correcting for premelting caused by 0.015 mole percent of liquid-soluble solid-insoluble impurity. However, according to table 1 the only impurities present in comparable abundance are KOH and some sodium salt (presumably NaCl), and the phase diagrams of the KCl-KOH and KCl-NaCl systems [29] show such large solid solubilities (for compositions near pure KCl) as to suggest no premelting at any temperature in table 3. Consequently, the plausible alternative attribution of the above heat-capacity upturn to the effect of lattice vacancies was adopted instead (calling for one or more exponential terms in the enthalpy-temperature function). Moreover, all enthalpy values observed for 1039 K were omitted from the data fit because it is plausible to assume that this near the melting point the sample actually may have undergone extensive premelting which decreased in successive enthalpy measurements: the sample had earlier been fused and rapidly crystallized, and it seems reasonable to assume that the total of 190 min of holding the sample at 1039 K was required for about half the impurity to diffuse into the crystalline KCl. With all premelting ignored in the data fitting, the additive corrections for the impurities would be well within the uncertainties of the final results and were ignored.

Excepting the values for 1038.72 K, the mean corrected unsmoothed relative enthalpy found for potassium chloride at each furnace temperature (from table 3, fifth column) was given equal weight in the method of least squares to derive the coefficients and the exponential argument of the following empirical enthalpy equations (in J mol⁻¹ at *T* K, IPTS-68) for the crystal below the melting point and the liquid above the melting point:⁴

$$\begin{aligned} \text{KCl, } T = 273.15 - 1045 \text{ K: } H_T(c) - H_{273.15}(c) = & 46.5369 T \\ & + 8.1720(10^{-3})T^2 + 9.0725(10^7) \exp(-12300/T) \\ & - 13321.3 \quad (2) \end{aligned}$$

$$\begin{aligned} \text{KCl, } T = 1045 - 1174.10 \text{ K: } H_T(\ell) - H_{273.15}(c) \\ = 73.3994 T - 5614.1 \quad (3) \end{aligned}$$

Values from eqs (2) and (3) are given in the sixth column of table 3, and the differences of the mean measured values from these, in the last column.

Equations (2) and (3) are based solely on the authors' own data. The final equations recommended to cover these temperature ranges (sec. 4.3) involve small changes to effect a smooth join to good data below room temperature.

⁴ The least-squaring of the crystal-state data was actually carried out for fixed values of the exponential argument varying from $-11500/T$ to $-13500/T$ in steps of $-200/T$; the standard deviations not being very sensitive to this argument in this range. On repetition except allowing in the enthalpy a polynomial term in $1/T$, the best fit was inferior to that without this term, and besides, gave a negative coefficient for the $1/T$ term, whereas it was desired to represent all the positive curvature of the heat capacity-temperature curve in the exponential term.

4. Smooth Thermodynamic Functions

4.1. The Melting Point

The authors have not measured the melting point of pure potassium chloride. Nine values reported in the literature are listed later (table 8, sec. 5.1). Of these, the value of Roberts [43] was adopted—because it appears to be based on careful experimental work and because he documented his temperature scale with several fixed-point values, which are compared with those on the International Practical Temperature Scale of 1968 in table 4. Adding 1.7° (interpolated from the last column) to his reported melting point, 770.3° ± 0.5 °C, gives for the adopted melting point 772.0 °C, which may be rounded to 1045 K (IPTS-68).

TABLE 4. Values of thermometric fixed points on the IPTS-68 and as reported by Roberts

Fixed point	Value reported by		Difference
	IPTS-68 [20]	Roberts [43]	
	°C	°C	°C
Melting point of ice	0	^a (0)	0.0
Normal boiling point of water	100	^a (100)	0.0
Freezing point of lead	327.502	327.3	+0.2
Freezing point of zinc	419.58	419.4	+0.2
Freezing point of aluminum	660.37	658.7	+1.7
Freezing point of gold	1064.43	1062.6	+1.8
Freezing point of palladium	1554.	1551.5	+2.5

^a Not stated but inferred.

4.2. Joining With Low-Temperature Results

In order to arrive at what they regard as the most reliable formulation of the thermodynamic properties of potassium chloride over the temperature range of their measurements (273–1174 K), the authors carefully examined all available published results at both low and high temperatures (details are given later, in sec. 5.1), and decided to join their values smoothly with those of Berg and Morrison [4], whose measurements of heat capacity cover the range 2.8–270 K. (This compromise led to a small modification of eq (2) up to 373.15 K, noted later.) The decision to give full weight to the low-temperature heat capacities of Berg and Morrison was made because of the following facts about those values. (a) They are of relatively high precision, the (less precise) values of Southard and Nelson [48], Clusius et al. [8], and Strelkov et al. [49] scattering above and below them. (b) They are thoroughly documented in all details pertaining to their accuracy. Their stated estimated accuracy of 0.2 percent (in the range 25–270 K) is supported by agreement of comparably measured heat capacities of Al₂O₃ with the precise values of Furukawa et al. [17]—“excellently” over 78–150 K, though 0.1–0.2 percent higher over 150–270 K. (c) As will presently

be shown, Berg and Morrison's heat capacity-temperature function for KCl may be merged smoothly with the authors' without compromising either set of data.

Using the notation T_1 (ΔT) T_2 for the temperatures from T_1 to T_2 at constant intervals of ΔT , the smooth heat-capacity values of Berg and Morrison are for 2.5, 3, 5 (5) 30 (10) 60 (20) 100 (25) 250, and 270 K. By interpolating their Debye temperatures, the present authors interpolated heat capacities for 45, 55, 65, 70, 75, and 90 K also. In addition, in order to be consistent with the present work, small corrections have been applied to all values derived from their data in order to place the values on the basis of the International Practical Temperature Scale of 1968 [20, 10]⁵. The values of heat capacity listed by Berg and Morrison at the three highest temperatures in their table (225, 250, and 270 K), after conversion to IPTS-68, are represented exactly (in $\text{J mol}^{-1} \text{K}^{-1}$) by the monotonic equation

$$C_p = 98.9551 - 105.2107/T^{0.13897}. \quad (4)$$

The temperature derivative of eq (2), based on the authors' data, cannot be expected to represent accurate heat capacities in its lowest interval 273.15 to 373.15 K because there the enthalpy was measured only over the whole interval. However, to merge smoothly the authors' results at still higher temperatures with Berg and Morrison's results below 273.15 K, an empirical polynomial equation was derived for the heat capacity over the temperature interval 270–373.15 K (eq (9) of sec. 4.3). The five coefficients of the equation were determined from C_p and dC_p/dT as given by eq (4) at 270 K and as given by eq (2) at 373.15 K, and from $(H_{373.15} - H_{273.15})$ as given by eq (2). The deviations (in terms of heat capacity) of eqs (2) and (4) from the new equation are plotted in figure 1. Although both eqs (2) and (4) give lower heat capacities than the adopted equation between 305 and 345 K, this results from forcing the new equation to reproduce the (smoothed) measured enthalpy increment, and also it should be noted that the entire curve labeled "Berg and Morrison" is an extrapolation beyond the temperature range of their measurements.

Berg and Morrison's heat capacities were integrated to give the enthalpy and entropy increments over the interval 0–270 K. The major contributions were evaluated from three approximate empirical equations derived to cover the respective temperature ranges 0–20 K, 20–80 K, and 80–270 K with continuity in C_p and dC_p/dT (except for a 15 percent discontinuity in dC_p/dT at 20 K); the minor residual contributions equivalent to the deviations of these equations from the heat-capacity curve were determined graphically. The entropy of KCl(c) is certainly zero at 0 K, and the results are

$$H_{270}^{\circ} - H_0^{\circ} = \int_0^{270} C_p dT = 9934.6 \text{ J mol}^{-1}; \quad (5)$$

$$S_{270}^{\circ} = \int_0^{270} (C_p/T) dT = 77.490 \text{ J mol}^{-1} \text{K}^{-1}. \quad (6)$$

The values of eqs (5) and (6) include corrections of -0.4 J mol^{-1} and $+0.004 \text{ J mol}^{-1} \text{K}^{-1}$, respectively, for the conversion to the basis of IPTS-68 [10].

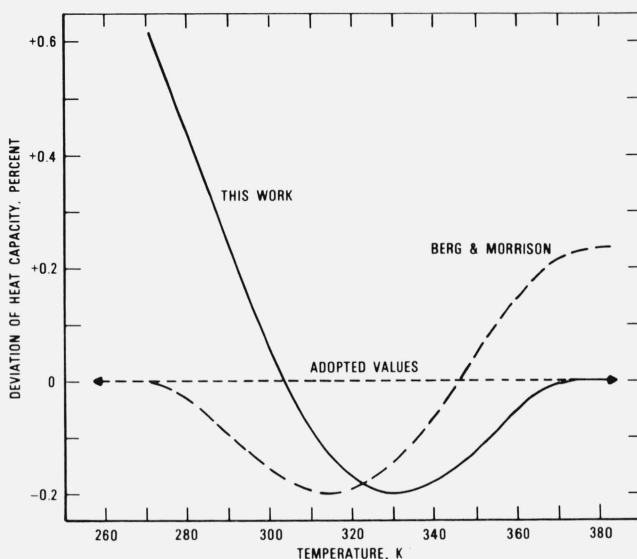


FIGURE 1. Compromise of KCl heat capacity in the temperature range 270–373.15 K.

The "Adopted Values" are those given by eqs (9) and (12) or by tables 5 and 6. The curve labeled "This Work" refers to the derivative of eq (2), and the curve labeled "Berg and Morrison" follows eq (4) as an extrapolation of their values [4].

4.3. Final Thermodynamic Functions

After the treatment of the temperature range 270–373.15 K described in sec. 4.2, and using eqs (5) and (6) and the requirement of continuity in enthalpy and entropy to supply the integration constants, the authors derived numerical equations to represent their final values for the common thermodynamic properties of crystalline and liquid potassium chloride from 270 to 1200 K. These numerical equations are given below as eqs (8)–(17). The Gibbs-energy function is then obtainable from the thermodynamic relation

$$-(G^{\circ} - H_0^{\circ})/T = S^{\circ} - (H^{\circ} - H_0^{\circ})/T. \quad (7)$$

The values above 1174.10 K involve an extrapolation up to 1200 K of the data on the liquid on which eq (3) is based; otherwise, the equations should be considered applicable only in the respective temperature ranges stated. The energy unit is J mol^{-1} (1 "mole" = 74.551 g), at the temperature T K (IPTS-68). The enthalpy is formulated as that relative to the crystal at 0 K. "ln" signifies the natural logarithm (i.e., to the base e). In general, eight significant figures should be retained in each coefficient of eqs (8)–(10), to avoid loss of significance in the computed thermodynamic functions.

⁵ The corrections below 90 K assume that Berg and Morrison [4] adopted the following fixed points of Los and Morrison [31]: normal boiling points of $e\text{-H}_2$ and O_2 , 20.273 and 90.190 K, respectively; triple point of O_2 , 54.363 K.

KCl(c), 270–373.15 K	}	$H^\circ - H_0^\circ = 241.29052T - 1.265787640T^2$	
		$+ 4.100661148(10^{-3})T^3$	
		$- 6.5082939(10^{-6})T^4$	
		$+ 4.08177711(10^{-9})T^5 - 14,920.39$	(8)
		$C_p = 241.29052 - 2.53157528T$	
		$+ 1.23019834(10^{-2})T^2$	
		$- 2.60331756(10^{-5})T^3$	
		$+ 2.04088856(10^{-8})T^4$	(9)
		$S^\circ = 241.29052 \ln T - 2.53157528T$	
		$+ 6.15099172(10^{-3})T^2$	
$- 8.6777252(10^{-6})T^3$			
$+ 5.10222139(10^{-9})T^4 - 894.5502$	(10)		
KCl(c), 373.15–1045 K	}	$H^\circ - H_0^\circ = 46.5369T + 8.1720(10^{-3})T^2$	
		$+ 9.0725(10^7)\exp(-12300/T)$	
		$- 3227.08$	(11)
		$C_p^\circ = 46.5369 + 1.63439(10^{-2})T$	
		$+ [1.1159(10^{12})/T^2]\exp(-12300/T)$	(12)
Fusion, 1045 K	}	$S^\circ = 46.5369 \ln T + 1.63439(10^{-2})T$	
		$+ 7377[1 + (12300/T)]\exp(-12300/T)$	
		$- 187.4624$	(13)
$\Delta H^\circ = 26,153.11; \Delta S^\circ = 25.0269$	(14)		
KCl(l), 1045–1200 K	}	$H^\circ(\ell) - H_0^\circ(c) = 73.3994T + 4480.10$	(15)
		$C_p^\circ = 73.3994$	(16)
		$S^\circ = 73.3994 \ln T - 331.3696$	(17)

Values calculated from eqs (8)–(13) and (15)–(17) are given for round temperatures in table 5 in terms of the joule as the energy unit, and in table 6 in terms of the commonly used “defined thermochemical calorie.”

Although table 6 is based on the International Practical Temperature Scale of 1968 and the latest existing JANAF tables for KCl [23] are based on the scale of 1948, the changes resulting from the temperature-scale conversion are quite small in the present case, and it is of interest to ignore these changes and compare the two tables because they are based on

the same experimental data. The values of ($H_{298.15}^\circ - H_0^\circ$) and $S_{298.15}^\circ$ are identical within rounding error, reflecting the agreement in integrating Berg and Morrison’s [4] heat capacities. The heat-capacity values of table 6 are higher at 298, 500, 1000, and above 1045 K (liquid) by +0.2, –0.1, +1.5, and –0.3 percent respectively; and the heat of fusion in table 6 is 0.5 percent lower, principally because of the exponential terms in eqs (11) and (12) instead of a simple correction for pre-melting reflected in the JANAF tables. The Gibbs-energy function (for the same temperatures, and based

TABLE 5. Thermodynamic functions for potassium chloride (KCl), crystalline and liquid phases (in terms of **JOULES** per mole) (1 mol = 74.551 g; International Practical Temperature Scale of 1968; H_0° refers to the enthalpy of the crystal at 0 K)

T	$H^\circ - H_0^\circ$	C_p°	S°	$-(G^\circ - H_0^\circ)/T$
K	J mol ⁻¹	J mol ⁻¹ K ⁻¹	J mol ⁻¹ K ⁻¹	J mol ⁻¹ K ⁻¹
Crystalline				
270	9934	50.63	77.49	40.70
273.15	10094	50.71	78.08	41.12
280	10442	50.89	79.34	42.04
290	10952	51.16	81.13	43.36
298.15	11370	51.37	82.55	44.41
300	11465	51.42	82.87	44.65
310	11980	51.65	84.56	45.91
320	12498	51.86	86.20	47.14
330	13017	52.04	87.80	48.35
340	13538	52.19	89.36	49.53
350	14061	52.32	90.87	50.69
360	14585	52.45	92.35	51.83
370	15110	52.59	93.78	52.94
380	15637	52.75	95.18	54.04
400	16695	53.08	97.89	56.16
420	17760	53.40	100.49	58.21
440	18831	53.73	102.98	60.19
460	19909	54.06	105.38	62.11
480	20994	54.38	107.69	63.96
500	22085	54.71	109.91	65.75
520	23182	55.04	112.07	67.49
540	24286	55.37	114.15	69.18
560	25397	55.69	116.17	70.83
580	26514	56.02	118.13	72.42
600	27638	56.35	120.03	73.98
620	28767	56.68	121.89	75.50
640	29904	57.01	123.69	76.97
660	31047	57.35	125.45	78.42
680	32198	57.69	127.17	79.83
700	33355	58.03	128.85	81.20
720	34519	58.39	130.49	82.55
740	35691	58.76	132.09	83.87
760	36870	59.14	133.66	85.16
780	38056	59.55	135.20	86.42
800	39252	59.98	136.72	87.66
825	40758	60.57	138.57	89.18
850	42281	61.24	140.39	90.65
875	43821	61.99	142.17	92.10
900	45381	62.85	143.93	93.51
925	46964	63.85	145.67	94.89
950	48574	65.01	147.39	96.25
975	50216	66.37	149.09	97.59
1000	51895	67.96	150.79	98.89
1025	53616	69.82	152.49	100.18
1045	55029	71.52	153.86	101.19
Liquid				
1045	81183	73.40	178.89	101.19
1050	81550	73.40	179.24	101.57
1100	85219	73.40	182.65	105.17
1150	88889	73.40	185.91	108.61
1200	92559	73.40	189.04	111.90

TABLE 6. Thermodynamic functions for potassium chloride (KCl), crystalline and liquid phases (in terms of **CALORIES** per mole) (1 cal = 4.1840 J; 1 mol = 74.551 g; International Practical Temperature Scale of 1968; H_0° refers to the enthalpy of the crystal at 0 K)

T	$H^\circ - H_0^\circ$	C_p°	S°	$-(G^\circ - H_0^\circ)/T$
K	cal mol ⁻¹	cal mol ⁻¹ K ⁻¹	cal mol ⁻¹ K ⁻¹	cal mol ⁻¹ K ⁻¹
Crystalline				
270	2374.5	12.101	18.520	9.726
273.15	2412.6	12.120	18.661	9.828
280	2495.8	12.162	18.962	10.048
290	2617.7	12.226	19.390	10.363
298.15	2717.6	12.277	19.729	10.614
300	2740.3	12.288	19.805	10.670
310	2863.4	12.344	20.209	10.972
320	2987.1	12.394	20.602	11.267
330	3111.3	12.437	20.984	11.555
340	3235.8	12.473	21.356	11.838
350	3360.7	12.505	21.718	12.115
360	3485.9	12.535	22.070	12.387
370	3611.4	12.568	22.414	12.653
380	3737.3	12.607	22.750	12.914
400	3990.3	12.685	23.399	13.423
420	4244.8	12.763	24.020	13.913
440	4500.8	12.841	24.615	14.386
460	4758.3	12.919	25.188	14.843
480	5017.5	12.997	25.739	15.285
500	5278.3	13.075	26.271	15.714
520	5540.6	13.154	26.786	16.130
540	5804.5	13.232	27.284	16.534
560	6069.9	13.310	27.766	16.927
580	6336.9	13.388	28.234	17.309
600	6605.4	13.467	28.689	17.681
620	6875.5	13.546	29.132	18.043
640	7147.3	13.625	29.563	18.396
660	7420.6	13.705	29.984	18.741
680	7695.5	13.787	30.394	19.078
700	7972.1	13.869	30.795	19.407
720	8250.4	13.954	31.187	19.729
740	8530.2	14.042	31.571	20.044
760	8812.0	14.134	31.946	20.352
780	9095.7	14.231	32.315	20.654
800	9381.4	14.335	32.676	20.950
825	9741.5	14.476	33.120	21.312
850	10105.4	14.634	33.554	21.666
875	10473.3	14.814	33.981	22.012
900	10846.2	15.020	34.401	22.350
925	11224.7	15.259	34.816	22.681
950	11609.6	15.537	35.226	23.006
975	12002.0	15.863	35.634	23.325
1000	12403.1	16.243	36.040	23.638
1025	12814.6	16.686	36.447	23.945
1045	13152.3	17.093	36.773	24.188
Liquid				
1045	19403.1	17.543	42.755	24.188
1050	19490.8	17.543	42.839	24.276
1100	20367.9	17.543	43.655	25.139
1150	21245.1	17.543	44.435	25.961
1200	22122.2	17.543	45.181	26.746

on either H_0° or $H_{298.15}^\circ$) is virtually identical for the crystal, and only about $0.01 \text{ cal mol}^{-1}\text{K}^{-1}$ lower for the liquid in table 6.

5. Discussion

5.1. Comparison with Other Investigators

The investigations measuring the relative enthalpy or heat capacity of potassium chloride (a) below room

temperature and (b) above room temperature are outlined in chronological order in table 7. The individual unsmoothed values of enthalpy from most of these investigations, including those of the present authors (table 3), were adjusted to the basis of the International Practical Temperature Scale of 1968 and to the base enthalpy at 273.15 K as well as possible, and are compared with the final smooth values of this paper in figure 2.

TABLE 7. Reported measurements of the enthalpy or heat capacity of potassium chloride (KCl)

Authors	Year published	Reference	Temp. range (K)	H or C_p measured?
(a) BELOW ROOM TEMPERATURE				
Nernst	1911	[36]	22-90	} C_p
Nernst & Lindemann	1911	[37]	22-90	
Lindemann & Schwern	1913	[30]	22-90	
Southard & Nelson	1933	[48]	17-285	
Keesom & Clark	1935	[25]	2.3-17	
Feodosiev	1938	[16]	86-298	
Clusius et al.	1949	[8]	10-270	
Sayre & Beaver	1950	[45]	69-81	
Keesom & Pearlman	1953	[26]	1-5	
Strelkov et al.	1954	[49]	12-300	
Webb & Wilks	1955	[55]	1-40	
Berg & Morrison	1957	[4]	2.8-270	
Sokolov & Sharpataya	1964	[47]	88-299	
(b) ABOVE ROOM TEMPERATURE				
Plato	1906	[40]	293-999, 1080-1208	H
Russell	1912	[44]	275-317	?
Magnus	1913	[33]	289-823	H
Brönsted	1914	[6]	273-293	?
Lyashenko	1935	[32]	291-1127	H
Popov et al.	1940	[41]	293-923	H
Mustajoki	1951	[35]	334-721	C_p
Skuratov & Lapushkin	1951	[46]	293-933	H
Dworkin & Bredig	1964	[13, 14]	1323-1373	H
Palkin et al.	1965	[39]	296-299	C_p
Bloom & Tricklebank	1966	[5]	300-1123	H
Vasil'kova et al.	1969	[53]	402-1045	H
Leadbetter & Settatre	1969	[27, 28]	314-641	C_p
Marchidan & Ciopec	1970	[34]	400-700	H
Thompson & Flengas	1971	[51]	298-1306	H
Douglas & Harman	1974	This work	273-1174	H

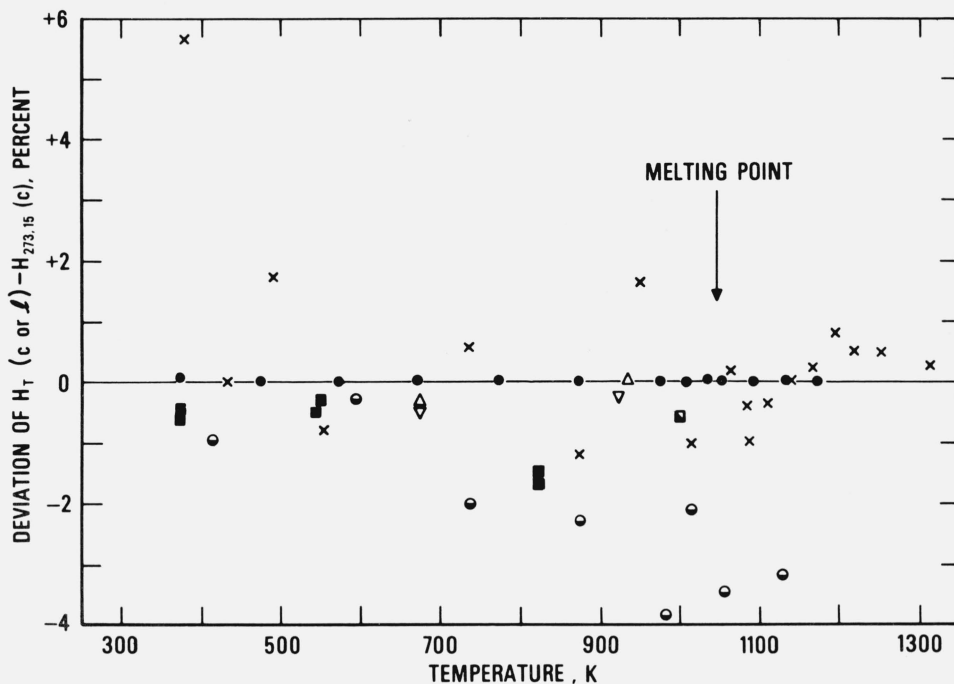


FIGURE 2. Percentage deviation of KCl unsmoothed relative enthalpy, $H_T(c \text{ or } \ell) - H_{273.15}(c)$, of various investigators from those adopted in this paper.

See fig. 3 for legend of symbols.

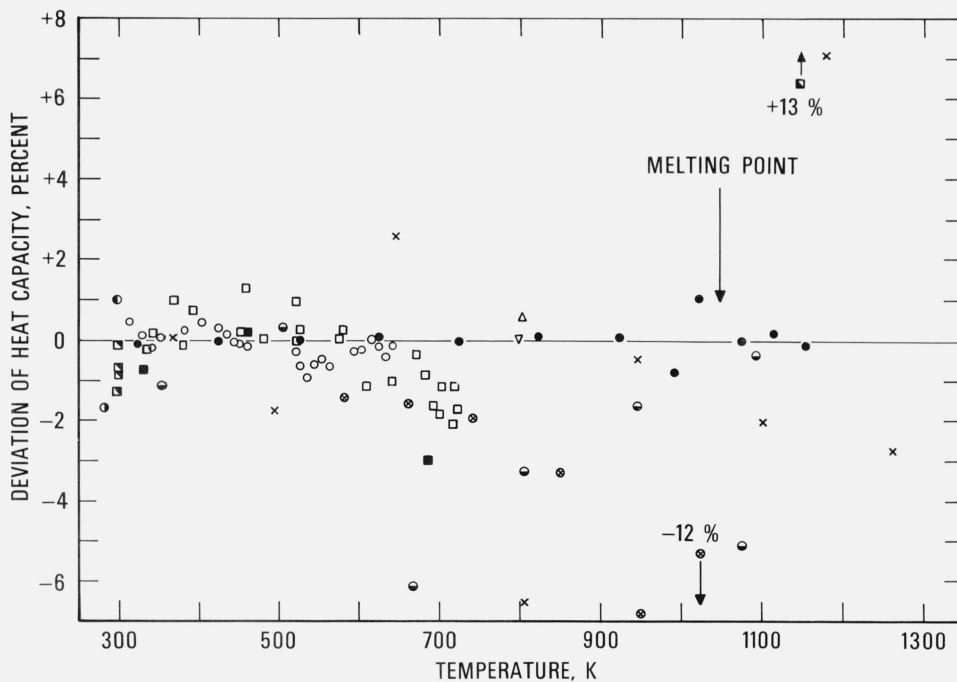


FIGURE 3. Percentage deviation of unsmoothed heat capacity, C_p , of various investigators from those adopted in this paper.

Base line: Eqs (8)-(17) or tables 5 and 6 (this work).

● : Douglas and Harman (1974)	This work	□ : Mustajoki (1951)	[35]
× : Thompson and Flengas (1971)	[51]	▽ : Popov et al. (1940)	[41]
○ : Leadbetter and Settaree (1969)	[27, 28]	● : Lyashenko (1935)	[32]
⊗ : Vasil'kova et al. (1969)	[53]	○ : Brönsted (1914)	[6]
⊙ : Palkin et al. (1965)	[39]	■ : Magnus (1913)	[33]
◐ : Dworkin and Bredig (1964)	[13, 14]	⊙ : Russell (1912)	[44]
△ : Skuratov and Lapushkin (1951)	[46]	■ : Plato (1906)	[40]

TABLE 8. Reported measurements of the melting point and heat of fusion of KCl

Authors	Year published	Reference	Melting point °C	Heat of fusion cal mole ⁻¹ ^b
Carnelley.....	1877.....	[19, 7].....	770.....	
Ramsay.....	1896.....	[19, 42].....	762.....	
Jaeger.....	1914–1915.....	[19, 21].....	771.....	
Jaeger.....	1917.....	[19, 22].....	768.....	
von Wartenberg & Albrecht.....	1921.....	[19, 54].....	768 ± 3.....	
Roberts.....	1924.....	[43].....	^a 770.3 ± 0.5.....	
Ginnings & Phipps.....	1930.....	[18].....	770.....	
Lyashenko.....	1935.....	[19, 32].....		6290
Johnson & Bredig.....	1958.....	[24].....	769.5.....	
Dworkin & Bredig.....	1960.....	[14].....		6340
Aukrust et al.....	1960.....	[23, 3].....	770.....	^c 6400
Bloom & Tricklebank.....	1966.....	[5].....		6200
Vasil'kova et al.....	1969.....	[53].....		6430
Thompson & Flengas.....	1971.....	[51].....		6250
Douglas & Harman.....	1974.....	This work.....		6250

^a See table 4 for values found for thermometric fixed points.

^b In those cases where defined, 1 cal = 4.184 J.

^c This is the *calorimetric* value reported. A value derived from phase diagrams also was reported, but is not tabulated here.

A similar comparison of unsmoothed heat capacities above 273 K is shown in figure 3.⁶ This comparison includes not only the heat capacities measured directly by some authors, but also the heat capacity corresponding to the difference between the observed relative enthalpies for two adjacent temperatures of measurement,⁷ after applying a small correction for curvature when this was significant. The accounting for the curvature correction was done by using the approximate equation [38]

$$C_p = (\Delta H/\Delta T) - [(\Delta T)^2/24][\partial^2 C_p/\partial T^2], \quad (18)$$

where C_p and $\partial^2 C_p/\partial T^2$ apply at the middle of the temperature interval corresponding to ΔT ($\partial^2 C_p/\partial T^2$ was computed from eq (9) or (12)). The great majority of points in figure 3 fall within 1 percent of the base line, though above 700 K there are fewer investigations and also the scatter is greater.

The reported values for the melting point and heat of fusion found in the literature are summarized in table 8 in chronological order. The heat-of-fusion values range from 1 percent lower to 3 percent higher than the authors' value. Noncalorimetric heat-of-fusion values have been excluded from the table because in general other methods (particularly, derivation from phase diagrams) are less reliable and sometimes misleading.

⁶ A few data are omitted from figure 2 (but included in fig. 3) because the temperature intervals covered did not include room temperature. The results of Vasil'kova et al. [53] are represented in figure 3 by selected smoothed values only.

⁷ When the temperature interval would otherwise be quite small, individual enthalpies and their temperatures were averaged such that the temperature interval ΔT used would be of the order of that for the authors' data (100° more or less), so as to make the precision of different investigations more nearly comparable in figure 3.

5.2. Reliability of the Results

The discussion of reliability will be limited to the final values of heat capacity above 273 K and to the heat of fusion (tables 5 and 6, or eqs (9), (12), (16), and (14)). As usual, the limits of absolute accuracy are difficult to ascertain closely, but may be estimated after careful consideration of the identifiable individual sources of systematic error, the measurement precision, and a comparison with high-accuracy results of other investigators.

Several systematic errors prove to be of relatively minor consequence. The furnace temperatures measured only by thermocouple may be in error by amounts up to 0.2°, which corresponds to an error of less than 0.03 percent of the net enthalpy relative to 273 K (and probably also of the heat capacity) of potassium chloride above 873 K. Inconstancy from one container to another of the heat lost during the drop into the calorimeter was estimated to be even less serious. The assumed calibration factor of the ice calorimeter is believed to be accurate to ±0.01 percent, affecting the relative enthalpy and heat capacity by the same percentage. Although the ambiguity in the mass of KCl sample 2 mentioned in sec. 3.3.b contributes an uncertainty of 0.04 percent to the KCl heat capacity calculated for this sample, the corresponding uncertainty for the sample usually used (sample 1) was estimated to be only 0.005 percent. The sample impurities (table 1) were estimated [23] to cause errors in the heat capacity varying from 0.02 to 0.04 percent (aside from any premelting; see below); however, no such corrections were applied to the data, owing to considerable uncertainty in the applicability of the additivity assumption on which this estimate is based.

The standard deviation of the mean net heat capacity of potassium chloride, as determined from the reproducibility (tables 2 and 3), is 0.2 percent over the liquid range covered, and averages the same over any 100-deg interval in the crystalline range.

The equations given in this paper to represent the enthalpy data for KCl being reported were derived on the assumption that the samples underwent no pre-melting below the melting point (except for the data at 1038.72 K, which were not included in the fit). Except in a rather short temperature region below the melting point (above 974 K), where the fit is within the precision, this smoothing did not compromise the unsmoothed mean heat capacities for pairs of successive temperatures by more than about 0.1 percent. Yet it was found that the crystal enthalpy data could have been fit almost as well if alternatively the samples were assumed to contain a small amount (empirically assumed to be 0.015 mole percent) of liquid-soluble, crystal-insoluble impurity, with subtraction of the corresponding enthalpies of premelting before the fitting. The results derived from this alternative fitting would correspond to heat capacities of pure KCl different by never more than 0.3 percent below 925 K (or above the melting point, 1045 K), but averaging 2 percent less over the interval 925–1045 K, and almost 5 percent less at 1045 K. As a consequence the heat of fusion would have been 0.5 percent greater than that derived assuming no premelting.

The purity of the samples, while high, was not sufficiently high to rule out unequivocally the possibility of a comparatively small amount of impurity causing premelting to the extents alternatively hypothesized above, and as a consequence the above differences between the two sets of results were retained in considering the reliability of the values derived for pure potassium chloride. Nevertheless, the occurrence of appreciable premelting (except at 1038.72 K, as discussed in sec. 3.3.b) is considered improbable for two reasons. In the first place, the accelerated upturn of the *observed* C_p -versus- T curve below the melting point can be explained by the effect of lattice vacancies whose existence is indicated by other properties (discussed in section 5.3), without the assumption of any premelting; and in the second place available phase diagrams [29] suggest, after use of an earlier analogous treatment [11], solubilities of the known impurities in the KCl (c) too great to cause any melting of the sample at as low a temperature as 1033.7 K (the highest temperature at which accepted enthalpy measurements were made below the melting point). It is true that a small amount (up to about 0.05 mole percent) of silver chloride may have formed according to the reaction



when the sample containers were sealed (sec. 3.3.b) and that an early phase diagram of the KCl-AgCl system [29] shows no solid solubility. However, it was estimated that the solidus curve of this system would have to be at least 60 times as steep as the liquidus

curve (near 100 percent KCl) for the solidus curve to be crossed at or below 1033.7 K for the present samples, and the ratio of the molar volume of AgCl to that of KCl is not so different from unity that the solid solubility of AgCl in KCl (c) would seem to be actually so small.

On the basis of the foregoing considerations it was estimated that the values adopted in this paper for the heat capacity of KCl (c) are probably not in error by more than amounts varying from 0.2 percent at 273 K to 0.5 percent at 925 K to 5 percent at 1045 K, and with assigned uncertainties of 0.5 percent for the heat of fusion and 0.4 percent for the mean heat capacity of KCl (ℓ) over the range measured (1045–1174 K). However, if there are errors of such magnitude in the heat capacity just below the melting point, they are nearly compensated by a corresponding error of opposite sign in the heat of fusion, so that the enthalpy interval KCl (c) (925 K) to KCl (ℓ) (1045 K) is probably represented accurately to 0.2 percent. These accuracy estimates are consistent with figure 1, according to which the (extrapolated) smoothed heat-capacity values of neither set of observers differ from the adopted values by more than 0.2 percent above 295 K (and Berg and Morrison's estimated accuracy up to 270 K was 0.2 percent). The heat-capacity values of other observers (see fig. 3) were considered too imprecise to aid in assessing the present work.

5.3. Contributions From Lattice Vacancies

In one investigation [50] the results of the thermal analysis of several binary systems and of potassium chloride of different purities were interpreted as indicating that this substance transforms at 753–755 K (presumably at atmospheric pressure) into a polymorphic crystalline modification whose melting point was said to be some 200° lower than that ordinarily encountered (1045 K). This is the only reported evidence of a polymorphic transformation of KCl (except the long-known one to the CsCl-type structure at quite high pressures) of which the authors are aware.

According to Ubbelohde [52], adiabatic elastic constants and linear-thermal-expansion data have been used to convert earlier C_p data on KCl to C_v values which, unlike C_p , were found to show no "premonitory" rise with temperature, within experimental error, below the melting point [15]. The "premonitory" rise of the crystal C_p referred to is clearly shown in figure 4, where the C_p of both crystalline and liquid KCl, as evaluated in the present investigation (eqs (4), (9), (12), and (16)) is plotted against temperature. According to eq (12), the C_p - T curve is very nearly linear from 373 K up to above 700 K, a fact which invites an attempt to interpret quantitatively the upturn of the curve at higher temperatures as represented by the exponential term in the equation. Such an upturn has been found for many crystalline substances, and is too pronounced and too broad to be explainable by premelting (see sec. 5.2), but has generally been accepted as representing the energy needed to create an increasing number of lattice vacancies (or other lattice defects) as the melting point is approached. It may be pointed

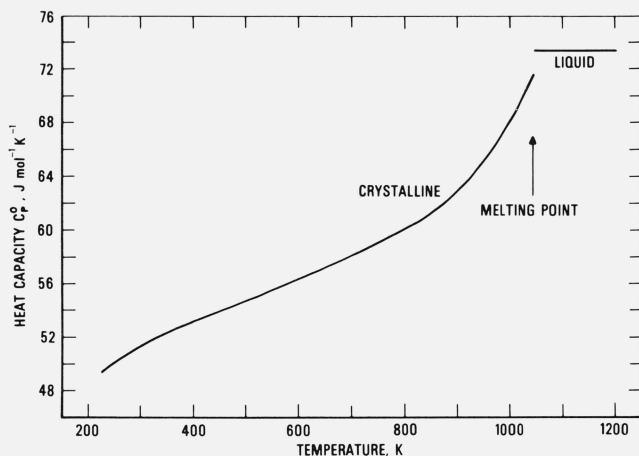


FIGURE 4. The heat capacity of potassium chloride from 225 to 1200 K.

The values are given below 270 K by eq (4), and above 270 K by eqs (9), (12), and (16) or by table 5.

out that the cooling of the sample in the ice calorimeter in the present work is believed to be too slow by many orders of magnitude to prevent the maintenance of virtual equilibrium with respect to these vacancies (at least in the high-temperature "intrinsic" region where vacancies (Schottky defects) predominate numerically over lattice-site impurities).

In a pure typically ionic equi-valent salt such as KCl in which interstitial lattice defects are highly unfavorable energetically, there will be equal numbers of cation and anion vacancies which in some important respects simulate a gas of ions. For example, a major energetic effect is a strong Coulombic attraction between vacancies of opposite charge, leading to the extensive formation of vacancy clusters or aggregates (pairs, quartets, etc.). Unless one type of cluster is known to predominate under all conditions of interest, it is appropriate to assume (somewhat arbitrarily at high vacancy concentrations) that for each temperature and pressure there is a definite number of each type of vacancy cluster in thermodynamic equilibrium. Then for each such cluster type (considering isolated cation and anion vacancies as separate types) we can write to a good approximation

$$x_i = g_i \exp(-E_i/RT), \quad (20)$$

and

$$H_i = g_i E_i \exp(-E_i/RT), \quad (21)$$

where x_i and H_i are — per mole (GFW) of salt (KCl) — the number of moles of the vacancy clusters of type i and their enthalpy of formation, respectively; E_i is the energy of formation of one mole of such clusters from perfect crystal; R is the gas constant; and g_i is the degeneracy of the cluster type (in the simplest case, the number of distinguishable orientations). In general, the total enthalpy of vacancy formation will be given by a sum of many terms of the form of eq (21), though at a given temperature only one or two terms may be of appreciable magnitude. Furthermore, taking the

pair cluster as an example, we may divide these into separate cluster types depending on the pair distance (and consequently on the energy E_i), and this will be approximately equivalent to neglecting all pairs except those with the largest value of x_i .

Comparing the exponential enthalpy term of eq (11), $9.073 (10^7) \cdot \exp(-12300/T)$ J/mole of KCl, with eq (21) gives from the data of this paper ⁸

$$E_i = 1.06 \text{ eV and } g_i = 887. \quad (22)$$

Using these values, eq (20) gives as the vacancy-aggregate concentration, per mole of KCl, a value from 0.001 mole at 900 K to 0.007 mole at 1045 K, the melting point. However, owing to the imprecision of the experimental enthalpy data (small but real), the parameters of eqs (22) cannot be considered to be determined by these data except within wide ranges: allowing a 50 percent greater standard deviation of fit than the best fit, which gave eqs (22), would give a spread from $E_i = 0.97$ eV ($g_i \approx 400$) to $E_i = 1.18$ eV ($g_i \approx 3000$). Furthermore, in view of the large magnitudes of the preexponential factor g_i , the interpretation in terms of lattice vacancies only must indicate the importance of large vacancy clusters (see below), and hence the probability that the single empirical exponential term in the enthalpy equation represents a composite of several vacancy types.

Various investigators have employed other methods — particularly ionic conductivity, diffusion with isotopic tracers, charged dislocations, and dielectric relaxation — to measure the concentrations and energies of lattice vacancies in ionic crystals, and we may summarize some results for KCl as given in a fairly recent review [1]. The temperature dependence cited as typical for the first two methods is close to that of eqs (22) (being equivalent to values of E_i from 1.11 to 1.16 eV), but the accompanying preexponential factors cited are much smaller (equivalent to values of g_i from 15 to 44). However, the overall spread of parameter values that have been found for KCl by different methods is very wide. Some of this spread may be due to the wide range of temperatures (from 543 to 1043 K) of the measurements, and some may be due to the customary interpretation of the parameter E_i in eq (20) as half the energy of formation of a mole of vacancy pairs. It may be that at low temperatures where the total vacancy concentration is quite small, this interpretation is valid; and that at high temperatures the electric field involved in such techniques as ionic conductivity effectively dissociates many vacancy clusters which, in the absence of a field, seem to be present during the enthalpy measurements.

One of the authors has used classical ionic-crystal theory (and arbitrary cutoffs) to compute the energy of replacing a single ion of a perfect alkali-halide crystal by another ion of the same charge [9], and the agreement with all comparable calorimetric results was excellent (being within experimental error). In principle, the same approach should be successful in

⁸ One eV is equivalent to $9.64867 (10^7)$ J mol⁻¹.

computing the energies of isolated vacancies and vacancy clusters in potassium chloride, and such computations⁹ were begun in the hope of reproducing within a reasonable approximation the empirical parameter values of eqs (22). These computations were soon abandoned, for two reasons. In the first place, calculations involving alternative cutoffs at 2, 4, 6, and 10 independent relaxation parameters (respectively 2, 4, 5, and 8 ion shells surrounding the vacancy) gave isolated-vacancy energies successively decreasing from 2.14 to 1.75 eV, but showing no sign of convergence, a failure possibly caused by the long-range nature (not present in the earlier situation [9]) of the Coulombic potential around the vacancy. In the second place, the indicated extension to vacancy clusters would encounter much lower symmetry than for isolated vacancies, and thereby present a problem of great complexity in evaluating the equilibrium relaxation and resulting energy effects of enough ions in the neighborhood of such vacancy clusters.

Very rough estimations did lead to the conclusion, however, that in order to explain the parameters of eqs (22) derived from the authors' enthalpy data—particularly the large multiplicity (value of g_i)—vacancy pairs having energies in the range of the stated value of E_i (eqs (22)) would have far too small values of g_i , but that the given parameter values may be consistent with a predominance of much larger vacancy clusters (e.g., quadrupoles, octapoles, etc.) for which the number of different geometric arrangements is far greater.

6. References

- [1] American Institute of Physics Handbook, 3rd ed. (McGraw-Hill Book Co., New York, 1972), pp. 9–74 to 9–85.
- [2] Atomic weights of the elements 1971 (IUPAC Comm. on Atomic Weights), Pure Appl. Chem. **30**, 637–649 (1972).
- [3] Aukrust, E., Björge, B., Flood, H., and Forland, T., Ann. N.Y. Acad. Sci. **79**, 830–837 (1960).
- [4] Berg, W. T., and Morrison, J. A., Proc. Royal Soc. (London) **A242**, 467–477 (1957).
- [5] Bloom, H., and Tricklebank, S. B., Australian J. Chem. **19**, 187–196 (1966).
- [6] Brönsted, J. N., Z. Elektrochem. **20**, 555ff (1914).
- [7] Carnelley, T., J. Chem. Soc. **31**, 381ff (1877).
- [8] Clusius, K. von, Goldmann, J., and Perlick, A., Z. Naturforsch. **4A**, 424–432 (1949).
- [9] Douglas, T. B., J. Chem. Phys. **45**, 4571–4585 (1966).
- [10] Douglas, T. B., J. Res. Nat. Bur. Stand. (U.S.) **73A** (Phys. and Chem.), No. 5, 451–470 (1969).
- [11] Douglas, T. B., and Ditmars, D. A., J. Res. Nat. Bur. Stand. (U.S.) **71A** (Phys. and Chem.) No. 3, 185–193 (1967).
- [12] Douglas, T. B., and King, E. G., High Temperature Drop Calorimetry, Chapter 8 in Experimental Thermodynamics Vol. I (Butterworths, London, 1968); also in Precision Measurement and Calibration (Heat), D. C. Ginnings, Ed., Nat. Bur. Stand. (U.S.), Spec. Publ. 300, Vol. **6**, 181–219 (1970).
- [13] Dworkin, A. S., private communication to JANAF Thermochemical Tables, Dec. 1, 1964. (See also ref. [14].)
- [14] Dworkin, A. S., and Bredig, M. A., J. Phys. Chem. **64**, 269–272 (1960).
- [15] Enck, F. D., Phys. Rev. **119**, 1873–1877 (1960).
- [16] Feodosiev, N., Zhur. Fiz. Khim. (J. Phys. Chem., Russian) **12**, 291ff (1938).
- [17] Furukawa, G. T., Douglas, T. B., McCoskey, R. E., and Ginnings, D. C., J. Research NBS **57**, 67–82 (1956) RP2694.
- [18] Ginnings, D. C., and Phipps, T. E., J. Amer. Chem. Soc. **52**, 1340–1345 (1930).
- [19] Gmelins Handbuch anorg. Chem. System, Verlag Chemie, Berlin, 1938, 22 (K), p. 374.
- [20] The International Practical Temperature Scale of 1968, Metrologia **5**, 35ff (1969).
- [21] Jaeger, F. M., Akad. Amsterdam Versl. **23**, 360 (1914–1915).
- [22] Jaeger, F. M., Z. anorg. Chem. **101**, 185ff (1917).
- [23] JANAF Thermochemical Tables, 2nd ed., Nat. Stand. Ref. Data Ser., Nat. Bur. Stand. (U.S.), **37**, 1141 pages, 1971.
- [24] Johnson, J. W., and Bredig, M. A., J. Phys. Chem. **62**, 604–607 (1958).
- [25] Keesom, W. H., and Clark, C. W., Physica **2**, 698ff (1935).
- [26] Keesom, P. H., and Pearlman, N., Phys. Rev. **91**, 1354ff (1953).
- [27] Leadbetter, A. J., private communication, July 26, 1967 (see ref. [28]).
- [28] Leadbetter, A. J., and Settartree, G. R., Proc. Phys. Soc., London, Solid State Phys. [2] **2**, 385–392 (1969).
- [29] Levin, E. M., Robbins, C. R., and McMurdie, H. F., Phase Diagrams for Ceramists, M. K. Reser, Ed. (Am. Ceram. Soc., Columbus, O., 1964): KCl-KOH, Fig. 1733 (p. 483); KCl-NaCl, Figs. 1258 and 1259 (p. 376); KCl-AgCl, Fig. 1215 (p. 368).
- [30] Lindemann, F. A., and Schwers, F., Physik. Zeit. **14**, 766ff (1913).
- [31] Los, J. M., and Morrison, J. A., Canad. J. Phys. **29**, 142ff (1951).
- [32] Lyashenko, W. S., Metallurg. **10** [11], 89ff (1935).
- [33] Magnus, A., Physik. Zeit. **14**, 5ff (1913).
- [34] Marchidan, D. I., and Ciopec, M., Rev. Roum. Chim. **15**, 1177–1180 (1970) (in English) (see Chem. Abstr. **74**, 35358 (1971)).
- [35] Mustajoki, A., Ann. Acad. Sci. Fennicae, Ser. A, I, **98**, 7–45 (1951).
- [36] Nernst, W., Ann. Physik [4] **36**, 395ff (1911).
- [37] Nernst, W., and Lindemann, F. A., Z. Elektrochem. **17**, 817ff (1911).
- [38] Osborne, N. S., Stimson, H. F., Sligh, T. S., and Cragoe, C. S., BS Sci. Pap. **20**, 65ff (1925) S501.
- [39] Palkin, V. A., Kuz'mina, N. N., and Chernyaev, I. I., Zhur. Neorg. Khim. (J. Inorg. Chem., Russian) **10**, 41–48 (1965).
- [40] Plato, W., Zeit. physik. Chem. **55**, 721–737 (1906).
- [41] Popov, M. M., Skuratov, S. M., and Nikonova, I. N., Zhur. Obschei Khim. (J. Gen. Chem., Russian) **10**, 2017–2022 (1940).
- [42] Ramsay, W., and Eumorphopoulos, N., Phil. Mag. [5] **41**, 365ff (1896).
- [43] Roberts, H. S., Phys. Rev. **23**, 386ff (1924).
- [44] Russell, A. S., Physik. Zeit. **13**, 62ff (1912).
- [45] Sayre, E. V., and Beaver, J. J., J. Chem. Phys. **18**, 584–594 (1950).
- [46] Skuratov, S. M., and Lapushkin, S. A., Zhur. Obschei Khim. (J. Gen. Chem., Russian) **21**, 2217–2220 (1951).
- [47] Sokolov, V. A., and Sharpataya, G. A., Zhur. Neorg. Khim. (J. Inorg. Chem., Russian) **9**, 1542–1546 (1964).
- [48] Southard, J. C., and Nelson, R. A., J. Amer. Chem. Soc. **55**, 4865–4869 (1933).
- [49] Strelkov, P. G., Itskevich, E. S., Kostryukov, V. N., and Mirskaya, C. G., Zhur. Fiz. Khim. (J. Phys. Chem., Russian) **28**, 645–649 (1954).
- [50] Sumarokova, T. N., and Modestova, T. P., Izv. Akad. Nauk Kaz. SSR, Ser. Khim. **14**, 26–33 (1964) (Russian); Chem. Abstr. **62**, 3632 (1965).
- [51] Thompson, W. T., and Flengas, S. N., Canad. J. Chem. **49**, 1550–1563 (1971).
- [52] Ubbelohde, A. R., Melting and Crystal Structure, Oxford Univ. Press, 1965, p. 231.
- [53] Vasil'kova, I. V., Podzorov, B. N., and Shapkin, P. S., Zhur. Neorg. Khim. (J. Inorg. Chem., Russian) **14**, 1732ff (1969).
- [54] Wartenberg, H. von, and Albrecht, P., Zeit. Elektrochem. **27**, 164ff (1921).
- [55] Webb, F. J., and Wilks, J., Proc. Royal Soc. (London) **230A**, 549ff (1955).

⁹ Using the justifiable simplification of a single inverse-power repulsive term, consistent with the known lattice energy of a perfect KCl crystal, for the non-Coulombic part of the potential function.

Publications of the National Bureau of Standards*

Citations with Selected Abstracts

J. Res. Nat. Bur. Stand. (U.S.), **78A** (*Phys. and Chem.*), No. 3, (May-June 1974), SD Catalog No. C13.22/sec.A:78/3.

Photoionization of CO₂-CO-O₂ mixtures. Formation and reactions of ion clusters, L. W. Sieck and R. Gorden, Jr.

Analysis of low temperature viscosity data for three NBS standard glasses, A. Napolitano, J. H. Simmons, D. H. Blackburn, and R. E. Chidester.

PVT relationships for liquid and glassy poly(vinyl acetate), J. E. McKinney and M. Goldstein.

Correction and extension of van der Poel's method for calculating the shear modulus of a particulate composite, J. C. Smith.

The formation of curved polymer crystals: Polychlorotrifluoroethylene, J. D. Barnes and F. Khoury.

Enthalpy of formation of phosphorus pentachloride; derivation of the enthalpy of formation of aqueous orthophosphoric acid, R. H. Schumm, E. J. Prosen, and D. D. Wagman.

Heat capacities of polyethylene from 2 to 360 K. II. Two high density linear polyethylene samples and thermodynamic properties of crystalline linear polyethylene, S. S. Chang.

The specific heats, C_p, C_v, of compressed and liquefied methane, B. A. Younglove.

An improved procedure for synthesis of DL-4-hydroxy-3-methoxymandelic acid (DL-"vanillyl"-mandelic acid, VMA), A. J. Fatiadi and R. Schaffer.

Single particle motions in liquids: Qualitative features of memory functions, R. D. Mountain.

The infrared spectra of matrix isolated uranium oxide species, S. Abramowitz and N. Acquista.

J. Res. Nat. Bur. Stand. (U.S.), **78B** (*Math. Sci.*), No. 2, (Apr.-June 1974), SD Catalog No. C13.22/sec.B:78/2.

Rational equivalence of unimodular circulants, S. Pierce.

How to determine the accuracy of the output of a matrix inversion program, M. Newman.

A conjecture on a matrix group with two generators, M. Newman.

A property of equivalence, M. Newman.

Comments on the discrete matrix model of population dynamics, R. Freese and C. R. Johnson.

Fixed-point solution of plant input/location problems, A. J. Goldman.

A new proof of Pick's theorem, S. Minsker.

Monogr. 125. **Thermocouple reference tables based on the IPTS-68**, R. L. Powell, W. J. Hall, C. H. Hyink, Jr., L. L. Sparks, G. W. Burns, M. G. Scroger, and H. H. Plumb, Nat. Bur. Stand. (U.S.), Monogr. 125, 410 pages (Mar. 1974) SD Catalog No. C13.44:125, \$4.55.

Key words: base metal alloys; noble metal alloys; temperature scale; temperature standards; thermocouples; thermometry.

Revision of the International Practical Temperature Scale requires that there be changes for all accurately tabulated thermophysical values. Revised reference data for thermocouples have been generated in a cooperative program between groups of the National Bureau of Standards in Boulder and Gaithersburg. This Monograph contains tables, analytic expressions, various approximations, and explanatory text. Only the standard letter-designated thermocouples are described: noble metal Types S, R, and B and base metal Types E, J, K, and T. Their appropriate "single-leg" or thermoelement versus Pt-67 values are also included. The new reference data reflect not only revisions in the temperature scale, but also slight changes in the materials themselves and improvements in data fitting methods. The temperature ranges vary for different types, from a low of -270 °C for Type E to a high of 1820 °C for Type B. The main functions and tables are given in terms of Celsius degrees and microvolts. Tables in the appendices represent the data with less precision, in millivolts, and in degrees Fahrenheit as well as Celsius. Approximate quadratic, cubic, and quartic analytic expressions are also given for each thermocouple type in various temperature ranges. Supersedes NBS Circular 561.

SP369. **Soft x-ray emission spectra of metallic solids: Critical review of selected systems and annotated spectral index**, A. J. McAlister, R. C. Dobbyn, J. R. Cuthill, and M. L. Williams, Nat. Bur. Stand. (U.S.), Spec. Publ. 369, 176 pages (Jan. 1974) SD Catalog No. C13.10:369, \$1.85.

Key words: alloys; critical review; emission spectra; intermetallic compounds; metals; soft x ray; spectra.

Theory and experimental practice in the field of soft x-ray emission from metallic solids are briefly reviewed, and measurements on a number of systems are critically evaluated and compared with the results of other techniques and theory, with a view to establishing the pertinence of the soft x-ray measurements and indicating specific guidelines for further enhancing their value. In addition, an exhaustive annotated index of measured spectra is provided. Supersedes NBS Monograph 52 in part, for emission spectra only.

SP382. **Hydraulic research in the United States and Canada, 1972**, G. Kulin and P. H. Gurewitz, Eds., Nat. Bur. Stand. (U.S.), Spec. Publ. 382, 340 pages (Jan. 1974) SD Catalog No. C13.10:382, \$3.00.

Key words: fluid mechanics; hydraulic engineering; hydraulic research; hydraulics; hydrodynamics; model studies; research summaries.

Current and recently concluded research projects in hydraulics and hydrodynamics for the years 1971-1972 are summarized. Projects

*Publications with prices and SD Catalog numbers may be purchased directly from the Superintendent of Documents, U.S. Government Printing Office, Washington, D.C. 20402 (foreign: one-fourth additional). Microfiche copies are available from the National Technical Information Service (NTIS), Springfield, Va. 22151. Reprints from outside journals and the NBS Journal of Research may often be obtained directly from the authors.

from more than 250 university, industrial, state and federal government laboratories in the United States and Canada are reported.

SP390. Index of international standards, S. J. Chumas, Ed., Nat. Bur. Stand. (U.S.), Spec. Publ. 390, 222 pages (Mar. 1974) SD Catalog No. C13.10:390, \$5.60.

Key words: analyses; International Commission on Rules for the Approval of Electrical Equipment; International Electrotechnical Commission; International Organization for Standardization; International Organization of Legal Metrology; International Special Committee on Radio Interference; recommendations; specifications; standards; test methods.

This computer-produced Index, based on the Key-Word-In-Context (KWIC) system, contains over 2,700 standards titles of the International Organization for Standardization (ISO), the International Electrotechnical Commission (IEC), the International Commission on Rules for the Approval of Electrical Equipment (CEE), the International Special Committee on Radio Interference (CISPR), and the International Organization of Legal Metrology (OIML).

SP392. Vibrationally excited hydrogen halides: A bibliography on chemical kinetics of chemiexcitation and energy transfer processes (1958 through 1973), F. Westley, Nat. Bur. Stand. (U.S.), Spec. Publ. 392, 81 pages (Apr. 1974) SD Catalog No. C13.10:392, \$1.30.

Key words: bibliography; chemical kinetics; chemiexcitation; gas phase; halogens; hydrogen; hydrogen halides; laser; quenching; vibrational energy transfer.

A bibliography, a reaction oriented list of references, is provided for published papers and reports containing rate data for reactions of halogen atoms with hydrogen-containing compounds, or of H (D, or T) atoms with halogen-containing compounds to form vibrationally chemiexcited hydrogen halides. The reactions for vibroexcitation of hydrogen halides through unimolecular or photochemical elimination, as well as the processes for vibrational energy transfer between hydrogen halides and various second bodies are also included. In addition, four lists of theoretical papers and a list of critical reviews and bibliographies are provided. Over 300 papers covering 50 types of reactions are listed. The period covered extends from 1958 through 1973.

SP393. Colorimetry and spectrophotometry: A bibliography of NBS publications January 1906 through January 1973, K. L. Kelly, Nat. Bur. Stand. (U.S.), Spec. Publ. 393, 54 pages (Apr. 1974) SD Catalog No. C13.10:393, 95 cents.

Key words: bibliography; color; color codes; colorimetry; color measurement; spectrophotometry; vision.

This bibliography of publications will serve as the key to the large amount of research into color measurement and specification, and color vision carried out by the staff of the National Bureau of Standards (NBS) in colorimetry and spectrophotometry. These 623 publications appeared in NBS publications and outside scientific and technical journals between January 1906 and January 1973. This material has been in constant demand by Bureau members as well as by outside individuals and organizations. The practical value of this wealth of information lies in its ready accessibility to the scientific and technical fraternity by title, by key words or by author, in the Library of Congress and in depository libraries such as large public and university libraries. A short organizational chronology of the colorimetry and spectrophotometry program is included.

SP400-1. Semiconductor measurement technology. Quarterly report, July 1 to September 30, 1973, W. M. Bullis, Ed., Nat. Bur. Stand. (U.S.), Spec. Publ. 400-1, 68 pages (Mar. 1974) SD Catalog No. C13.10:400-1, \$1.15.

Key words: contact resistance; die attachment; dopant profiles; electrical properties; electronics; gold-doped silicon; hermeticity;

metallization; methods of measurement; microelectronics; microwave diodes; mobility; MOS devices; oxide films; photomasks; photoresist; resistivity; resistivity standards; scanning electron microscopy; semiconductor devices; semiconductor materials; semiconductor process control; sheet resistance; silicon; S-parameters; spreading resistance; test patterns; thermal resistance; thermally stimulated capacitance; thermally stimulated current; wire bonds.

This quarterly progress report, twenty-first of a series, describes NBS activities directed toward the development of methods of measurement for semiconductor materials, process control, and devices. Principal accomplishments during this reporting period include (1) extension of the technique for measuring thermally stimulated current and capacitance to include measurements on MOS capacitors, (2) completion of the development of the thermal response method for evaluation of transistor die attachment, (3) analysis of the interlaboratory comparison of transistor scattering parameter measurements, (4) preliminary review of measurement problems in the photolithographic aspects of semiconductor device processing, of problems associated with certain hermeticity testing procedures, and of methods for evaluating metallization step coverage, and (5) initiation of new activity on characterization of oxide films in MOS structures and analysis of diffusion profiles. Results are also reported on spreading resistance, capacitance-voltage, and sheet resistance measurements; the activation energy of the gold acceptor in silicon; evaluation of the base-to-metal contact resistor test structure; metallurgical systems for ultrasonic bonding; burn-out characteristics of fine gold and aluminum bonding wire; transistor thermal resistance measurements; and microwave diode conversion loss measurements. Supplementary data concerning staff, publications, workshops and symposia, standards committee activities, and technical services are also included as appendices.

NSRDS-NBS48. Radiation chemistry of ethanol: A review of data on yields, reaction rate parameters, and spectral properties of transients, G. R. Freeman, Nat. Stand. Ref. Data Ser., Nat. Bur. Stand. (U.S.), 48, 43 pages (Feb. 1974) SD Catalog No. C13.48:48, 80 cents.

Key words: chemical kinetics; data compilation; ethanol; G; radiation chemistry; rates; review; spectra.

The yields (G) for products and intermediates formed by irradiation of ethanol, in the solid, liquid and gaseous state, have been compiled and reviewed. Rates of reactions of transient ions and radicals and spectroscopic parameters, including optical and esr spectra, are also included.

BSS49. Laboratory studies of the hydraulic performance of one-story and split-level residential plumbing systems with reduced-size vents, R. S. Wyly, G. C. Sherlin, and R. W. Beausoliel, Nat. Bur. Stand. (U.S.), Bldg. Sci. Ser. 49, 53 pages (Mar. 1974) SD Catalog No. C13.29/2:49, 95 cents.

Key words: hydraulic criteria for plumbing; hydraulic test loads; plumbing-vent sizing; reduced-size vents; sanitary DWV systems; secondary ventilation; testing plumbing systems; vents for plumbing.

A laboratory study on one-story and split-level experimental drainage systems where the vents in some cases were varied from one to six pipe-sizes smaller than those presently specified by codes showed satisfactory hydraulic and pneumatic performance under various loading conditions. The research was originally sponsored by the National Association of Home Builders and the National Bureau of Standards and more recently by a program of the Department of Defense through the Tri-Services Investigational Committee on Building Materials. This paper presents criteria recommended for the design and evaluation of systems using reduced-sized vents and a sizing table for one- and two-story systems. The laboratory work also contributed to the development of analytical and test procedures needed for evaluating the application of reduced-size venting to a

broad range of innovative drain-waste-vent designs for buildings of any height.

This work indicates that, in some circumstances, reduced-size venting might be a good alternative to other types of drainage systems for multistory buildings which use either conventional or innovative venting concepts. Because this study involved only a limited number of drainage system designs, it is recommended that ongoing field and laboratory studies be explored if code changes are contemplated to permit the use of smaller vents.

BSS51. Structural evaluation of steel faced sandwich panels, J. H. Pielert, T. W. Reichard, and L. W. Masters, Nat. Bur. Stand. (U.S.), Bldg. Sci. Ser. 51, 43 pages (Apr. 1974) SD Catalog No. C13.29/2:51, 90 cents.

Key words: accelerated aging; adhesive bond; ductility; flexural shear; housing systems; local buckling; material variability; moisture conditioning; Operation BREAKTHROUGH; paper honeycomb; structural sandwich; sustained load.

A series of structural evaluation tests performed on components and materials intended for use in one of the Operation BREAKTHROUGH housing systems is described. Four samples of steel faced, paper honeycomb, sandwich panel material and four full size prototype roof panels were evaluated.

The samples of sandwich panel material were used to evaluate the variability of panel material properties and the effect of aging on tensile and shear strength. The roof panels were used to determine the behavior in service considering the effects of adverse environmental conditions on ultimate strength and mode of failure. In addition, the performance of one panel under sustained loading was evaluated.

FIPS PUB28. Standardization of data elements and representations, H. S. White, Jr., Nat. Bur. Stand. (U.S.), Fed. Info. Process. Stand. Publ. (FIPS Pub.) 28, 12 pages (1973) SD Catalog No. C13.52:28, 60 cents.

Key words: computers; data elements and representations; data processing systems; Federal Information Processing Standards; management information systems; standards; U.S. Government.

Pursuant to the authority delegated to the Secretary of Commerce by Executive Order 11717 (38 FR 12315, dated May 11, 1973), Subtitle A of Title 15 of the Code of Federal Regulations has been amended to add a new Part 6 which implements the provisions of Section III (f) (2) of the Federal Property and Administrative Services Act of 1949, as amended (79 Stat. 1127). This new Part 6 supersedes and replaces in its entirety the provision of Office of Management and Budget Circular A-86 entitled, "Standardization of data elements and codes in data systems," dated September 30, 1967 which was rescinded by the Director of the Office of Management and Budget on August 29, 1973. Part 6 provides policy and identifies responsibilities of executive branch departments and independent agencies for a government-wide program for the standardization of data elements and representations used in Federal automated data systems. This publication provides a copy of Part 6 and other documents relating to this amendment.

PS59-73. Prefinished hardboard paneling. (ANS A135.5-1973), K. G. Newell, Jr., Technical Standards Coordinator, Nat. Bur. Stand. (U.S.), Prod. Stand. 59-73, 7 pages (Feb. 1974) SD Catalog No. C13.20/2:59-73, 45 cents.

Key words: hardboard paneling; paneling, hardboard; prefinished hardboard paneling.

This Voluntary Product Standard covers requirements and methods of test for the dimensions, squareness, edge straightness, and moisture content of prefinished hardboard paneling; for the physical properties of the hardboard substrate; and for the finish of the paneling. Methods of identifying products which conform to the requirements of the standard are included.

PS60-73. Hardboard siding. (ANS A135.6-1973), K. G. Newell, Jr., Technical Standards Coordinator, Nat. Bur. Stand. (U.S.) Prod. Stand. 60-73, 7 pages (Feb. 1974) SD Catalog No. C13.20/2:60-73, 40 cents.

Key words: hardboard siding; siding, hardboard.

This Voluntary Product Standard covers requirements and methods of test for the dimensions, straightness, squareness, physical properties, and surface characteristics of hardboard siding. Definitions of trade terms used and methods of identifying products that comply with the standard are included.

TN594-6. Optical radiation measurements: The present state of radiometry and photometry, B. Steiner, Nat. Bur. Stand. (U.S.), Tech. Note 594-6, 56 pages (Mar. 1974) SD Catalog No. C13.46:594-6, 95 cents.

Key words: measurement system; photometry; professional societies; radiometry; standards.

The electro-optics industry and the public that depends on it are part of an informal but influential system for optical radiation measurement. The growth of this industry and of public concerns related technically to it have put severe new strains on this measurement system. The system itself must therefore be analyzed. The state of the art, on which the measurement system depends, is surveyed in terms of basic measurement parameters. The measurement system is analyzed in terms of its three basic components: the flow of physical standards, the generation of procedural standards, and the funding framework. The roles of the professional society and of the Council for Optical Radiation Measurement are reviewed. New requirements of the system are identified. Finally, the methodology of the study is reviewed in detail.

TN594-7. Optical radiation measurements: Approximate theory of the photometric integrating sphere, W. B. Fussell, Nat. Bur. Stand. (U.S.), Tech. Note 594-7, 39 pages (Mar. 1974) SD Catalog No. C13.46:594-7, 75 cents.

Key words: illuminance distribution; integrating sphere; lamp comparisons; photometric accuracy; photometry; total luminous flux.

An approximate mathematical theory of the photometric integrating sphere is developed. The analysis is accurate to the first order in the ratio of the baffle area to the sphere wall area. The sphere is assumed to be occupied by a circular baffle and a spherical lamp; the centers of the baffle and the lamp lie on a diameter of the sphere. The surfaces of the sphere and the baffle are assumed to reflect in a uniformly diffuse manner. The lamp is assumed to absorb a fraction of the radiation incident upon it, and to transmit (or specularly reflect) the remainder. The luminance distribution at the sphere window is derived for a general source input at any point of the sphere wall. A model lamp illuminance distribution is assumed, and a formula for the fractional error in comparing the total luminous fluxes of two lamps in the integrating sphere, is derived. The physical significance of the formula is described.

TN616. Revised March 1974. Frequency standards and clocks: A tutorial introduction, H. Hellwig, Nat. Bur. Stand. (U.S.), Tech. Note 616 (Revised), 72 pages (Mar. 1974) SD Catalog No. C13.46:616 (Rev.), 70 cents.

Key words: cesium beam; clocks (atomic); crystal oscillator; frequency accuracy; frequency stability; frequency standards; hydrogen maser; quartz crystal; rubidium gas cell; timekeeping.

The topic of frequency standards and clocks is treated in a tutorial and nonmathematical way. The concepts of time, frequency stability, and accuracy are introduced. The general physical principles and design features of frequency standards and clocks are described. The design, performance, and limitations of quartz crystal oscillators and atomic devices (cesium, hydrogen, rubidium) are discussed in detail.

and critically compared for laboratory devices as well as for devices intended for field usage.

TN647. Microwave attenuation measurement system (series substitution), W. Larson and E. Campbell, Nat. Bur. Stand. (U.S.), Tech. Note 647, 28 pages (Feb. 1974) SD Catalog No. C13.46:647, 35 cents.

Key words: attenuation; measurement; rotary-vane attenuator; series substitution.

A dual detection microwave bridge circuit has been incorporated in a series substitution system for the measurement of microwave attenuation devices. The use of an optical rotary-vane attenuator in the system yields practical resolution and stability of 0.00005 dB from zero to 30 dB. The dual detection system has several favorable features: (1) it employs a single microwave source which reduces cost, (2) measurements are obtained without power stabilization of the microwave signal source, and (3) this waveguide configuration enables measurements of attenuation devices at any length with minimum of effort and movement of waveguide components.

The system configuration is convenient for both attenuation difference, and insertion loss measurements from zero to 70 dB over the WR90 waveguide band of 8.2 to 12.4 GHz.

TN649. The standards of time and frequency in the U.S.A., J. A. Barnes and G. M. R. Winkler, Nat. Bur. Stand. (U.S.), Tech. Note 649, 91 pages (Feb. 1974) SD Catalog No. C13.46:649, \$1.00.

Key words: astronomical time measurements; clock synchronization; clocks; Coordinated Universal Time (UTC); frequency; frequency standards; International Atomic Time (TAI); International Radio Consultative Committee (CCIR); International Scientific Radio Union (URSI); International Time Bureau (BIH); international time organizations; leap seconds; national time/frequency standards; NBS time and frequency; Precise Time and Time Interval (PTTI); time; time coordination; time interval; time scales; Treaty of the Meter (standards); U.S.A. standard time zones; USNO time and frequency.

This paper describes the national responsibilities for standards of time and frequency in the U.S.A. The National Bureau of Standards (NBS) and the U.S. Naval Observatory (USNO) are the two organizations chiefly involved in distributing accurate and precise time and frequency information within the U.S.A. The NBS is responsible for the "custody, maintenance, and development of the national standards" of frequency and time (interval) as well as their dissemination to the general public. The mission of the USNO includes the "provision of accurate time" for electronic navigation systems, communication, and space technology. This is an integral part of its work concerned with the publication of ephemerides which are used in support of navigation and in the establishment of a fundamental reference system in space.

Both agencies provide the U.S. contribution to the Bureau International de l'Heure (BIH) [International Time Bureau], which has the responsibility of publishing definitive values of Universal Time (UT), International Atomic Time (TAI), and Coordinated Universal Time (UTC).

TN651. Scattering-matrix description and near-field measurements of electroacoustic transducers, D. M. Kerns, Nat. Bur. Stand. (U.S.), Tech. Note 651, 40 pages (Mar. 1974) SD Catalog No. C13.46:651, 50 cents.

Key words: electroacoustic transducer measurement techniques; near-field measurement techniques; scattering matrix description of electroacoustic transducers.

Recently developed and successfully applied analytical techniques for the measurement of microwave antennas at reduced distances are "translated" into corresponding techniques for the measurement of electroacoustic transducers in fluids. The basic theory is formulated

in scattering-matrix form and emphasizes the use of plane-wave spectra for the representation of sound fields. This theory, in contrast to those based on asymptotic description of transducer characteristics, is suitable for the formulation and solution of problems involving interactions at arbitrary distances. Two new techniques (in particular) are described: One, utilizing deconvolution of planar scanning data, taken with a known transducer at distances d which may be much less than the Rayleigh distance d_R ($\equiv D^2/2\lambda$), provides a means of obtaining complete effective directivity functions, *corrected for the effects of the measuring transducer*. Applicability of a (two-dimensional, spatial) sampling theorem and the "fast Fourier transform" algorithm, which greatly facilitate the necessary computations, is shown. The second technique provides a means of extrapolating received signal as a function of distance (observed with $d \sim d_R$) to obtain on-axis values of effective directivity. Other possible applications are indicated. These techniques rigorously utilize observed output of nonideal (but linear) measuring transducers.

TN803. A guide to networking terminology, A. J. Neumann, Nat. Bur. Stand. (U.S.), Tech. Note 803, 29 pages (Mar. 1974) SD Catalog No. C13.46:803, 80 cents.

Key words: computer networks; glossary; telecommunications; teleprocessing; terminology; vocabulary.

A selected set of terms and definitions relating to computer networking is presented in a coherent manner. An introduction gives the rationale for the glossary, defines the scope by a brief tutorial overview, and states the glossary format and conventions. The glossary is arranged alphabetically and contains about 140 definitions and associated terms. The sources of many terms are cited and modifiers indicate the status of definitions. A complete listing of source material is appended.

TN811. Evaluation of the column connections used in a precast concrete modular housing system, F. Y. Yokel and T. W. Reichard, Nat. Bur. Stand. (U.S.), Tech. Note 811, 63 pages (Mar. 1974) SD Catalog No. C13.46:811, \$1.00.

Key words: building system; column connection; concrete tri-axial strength; ductility; neoprene bearing pad; Operation Breakthrough; performance test; precast concrete; structural design.

The column connections used in a housing system employing stacked precast concrete box modules were tested to evaluate their structural performance. The system was proposed for construction in Operation Breakthrough, a research and demonstration program sponsored by the Department of Housing and Urban Development. The system uses innovative structural design concepts, which include: confinement of the concrete in the vicinity of the column bearings by reinforcing ties in order to increase concrete compressive strength; neoprene pads between column bearings in the upper stories; steel-neoprene-steel sandwich in the lower stories; and a grouted dowel through the center of the columns to provide resistance to tension and shear.

The test program included the following: tests to determine the effect of various bearing pads on the load capacity of the connection; tests to determine the load-deformation characteristics of the neoprene pads; a test to determine the performance of a lower-story connection using a steel-neoprene-steel sandwich and a grouted dowel; and tests to evaluate the strength and ductility of the connections when subjected to a shear force. The test results are presented and interpreted and the findings are summarized. Supersedes NBSIR 73-148 (PB 220366/7).

TN812. Tensile behavior of boron/epoxy-reinforced 7075-T6 aluminum alloy at elevated temperatures, D. J. Chwirut and G. F. Sushinsky, Nat. Bur. Stand. (U.S.), Tech. Note 812, 31 pages (Mar. 1974) SD Catalog No. C13.46:812, 65 cents.

Key words: aluminum alloy; boron/epoxy; co-cure; composite materials; fabrication process; load-deformation characteristics;

residual stress; rule of mixtures; sandwich specimen; stress-strain curves; tensile properties.

Static tensile tests were performed on specimens of 7075-T6 aluminum alloy, 0° unidirectional boron/epoxy, and 7075-T6 aluminum alloy reinforced on the surface with 0° unidirectional boron/epoxy laminate, at four temperatures up to 300 °F (149 °C). Analytical load-strain curves are formulated for the reinforced-metal specimens using the rule of mixtures, assuming that the longitudinal strains in the composite and the metal remain equal, and taking account of the residual stresses caused by the fabrication process. Two analytical curves are plotted for each reinforced-metal specimen, one based on the measured ply thickness of the composite, and one based on a nominal 0.005-in (0.13-mm) ply thickness. In general, the experimental load-strain curves fall between the two analytical curves for each specimen.

TN817. Kitchen ranges in fabric fires, A. K. Vickers, Nat. Bur. Stand. (U.S.), Tech. Note 817, 23 pages (Apr. 1974) SD Catalog No. C13.46:817, 60 cents.

Key words: accidents; burns; FFACTS; flammable fabrics; garments; ignition sources; injuries; kitchen ranges.

Kitchen ranges played a major role in the 1616 fabric accident case histories recorded in the Flammable Fabrics Accident Case and Testing System as of May 1972. They accounted for 214 or 35 percent of the direct garment ignitions in FFACTS. Female victims outnumbered males by 3 to 1; females under 16 and over 65 were particularly heavily represented. Reaching over and leaning against the range caused the majority of the garment ignitions. Shirts, robes, pajamas, nightgowns and dresses were the most frequently ignited garments. Thirty-four victims died from injuries resulting from garment ignitions from ranges; 24 of these fatalities were people over 65 years old.

TN819. A technical index of interactive information systems, D. W. Fife, K. Rankin, E. Fong, J. C. Walker, and B. A. Marron, Nat. Bur. Stand. (U.S.), Tech. Note 819, 73 pages (Mar. 1974) SD Catalog No. C13.46:819, \$1.20.

Key words: bibliographic systems; computer programs; computer systems; data base; data management; information retrieval; information services; interactive system; query language; software selection; text processing.

This report constitutes a reference to technical features and operational status of interactive information systems, i.e. those providing a "conversational" usage mode to a "non-programmer" through a data terminal device. It is aimed at the ADP service manager, for his use in the state-of-the-art assessments preparatory to a detailed system selection process. It contains an index that describes 46 systems in terms of a list of over 50 technical features plus descriptive, identification, and background information. In addition, there are aids and examples contributing to the intended use of the index.

TN820. Complete clear text representation of scientific documents in machine-readable form, B. C. Duncan and D. Garvin, Nat. Bur. Stand. (U.S.), Tech. Note 820, 55 pages (Feb. 1974) SD Catalog No. C13.46:820, 90 cents.

Key words: graphic character sets; information analysis centers; information interchange codes; recording typewriters; scientific computer technology.

Science and technology use a large variety of symbols to represent physical properties, chemical formulas and mathematical expressions.

Data centers that codify and evaluate physical properties need to use this conventional symbolism in their work. It is recommended that these data centers adopt the symbols and terminology specified by the various International Unions both in manual operations and in the creation of machine-readable data bases.

It is demonstrated that these conventional symbols can be produced by modern communications devices that are compatible

with the international standard codes for information interchange. A set of characters suitable for representing scientific data and text is presented and proposed as an extension of the ISO information interchange code.

The use of this extended character code by computer oriented data centers at the National Bureau of Standards is described. The equipment needed for this level of performance and criteria for their selection are outlined.

TN821. Photometric data variability of automotive lighting components, B. G. Simson and J. Mandel, Nat. Bur. Stand. (U.S.), Tech. Note 821, 15 pages (Mar. 1974) SD Catalog No. C13.46:821, 60 cents.

Key words: Federal Motor Vehicles Safety Standards; inter-laboratory test evaluation; motor vehicles; photometric testing; safety standards.

Four automotive lighting components were tested in three commercial testing laboratories to estimate the degree of photometric data repeatability and reproducibility. The laboratories used the photometric testing techniques required by Federal Motor Vehicle Safety Standard No. 108. The precision of this test method was placed in a range of about 10 percent coefficient of variation. However, this value should be considered more as an indication of existing conditions than as a predictive parameter.

TN822. A review of Federal and military specifications for floor coverings, W. C. Wolfe, Nat. Bur. Stand. (U.S.), Tech. Note 822, 99 pages (Apr. 1974) SD Catalog No. C13.46:822, \$1.50.

Key words: carpets; floor coverings; government; performance; procurement; specifications; standards; tests; user needs.

In this manual, which is organized so as to aid ready reference, requirements and test methods in Federal and military specifications for flooring, or floor coverings are combined, indexed and reviewed. The manual covers carpet, resilient flooring, monolithic surfacings or seamless flooring, and polyurethane coatings related to seamless flooring. It also covers all serviceability requirements except those relating to flammability, fire safety and acoustical properties.

Physical and material requirements in Federal specifications for floor coverings are considered in separate sections. Military specifications for monolithic surfacings and Federal specifications for floor coverings and polyurethane coatings are summarized in comprehensive tables. Under each physical requirement, comments indicate whether it is a quality control or a performance requirement. Each comment is followed by a list of those Federal specifications which include the requirement and a brief description of the criteria and test methods in the specifications. Comments on materials requirements relate to their adequacy and applicability to the product for which they were written. Finally, recommendations are made for improvements in performance requirements which should be considered for inclusion in future flooring and floor covering specifications.

TN823. Cryogenic Physics Section, summary of activities 1973, R. J. Soulen, Jr., Ed., Nat. Bur. Stand. (U.S.), Tech. Note 823, 23 pages (Mar. 1974) SD Catalog No. C13.46:823, 60 cents.

Key words: Josephson junctions; noise thermometer; nuclear orientation; paramagnetism; superconductivity; temperature.

This report summarizes the research activities of the Cryogenic Physics Section which specifically relate to thermometry. The topics range from superconductive fixed points to nuclear orientation thermometry, as well as Josephson junction noise thermometry and paramagnetism.

TN824. A laboratory study of some performance characteristics of an aluminum oxide humidity sensor, S. Hasegawa, L. Greenspan, J. W. Little, and A. Wexler, Nat. Bur. Stand. (U.S.), Tech. Note 824, 28 pages (Mar. 1974) SD Catalog No. C13.46:824, 65 cents.

Key words: aluminum oxide sensor; humidity; humidity sensor; hygrometer; measurement of frost points; moisture measurement; water vapor measurement.

A laboratory study was made of the performance of aluminum oxide humidity sensors over a range of ambient temperatures from +20 °C to -60 °C encompassing dew points from +13 °C to frost points of -100 °C. Information was obtained on such characteristics as sensitivity, hysteresis, temperature effect, pressure-altitude effect and short-term and long-term repeatability. The sensors were found to be capable of detecting frost points as low as -100 °C at ambient temperatures of -40 °C and -60 °C. It is estimated that the total uncertainty inherent in these sensors is approximately 4 °C.

TN826. Cost-benefit analysis of computer graphics systems, I. W. Cotton, Nat. Bur. Stand. (U.S.), Tech. Note 826, 47 pages (Apr. 1974) SD Catalog No. C13.46:826, 90 cents.

Key words: computer graphics; cost-benefit analysis; cost-effectiveness; economics; performance evaluation.

This report assesses the state-of-the-art in cost benefit analyses of computer graphics systems and suggests an approach for developing improved methodology. Cost-benefit analyses are distinguished from analyses of system performance in that the latter are directed at optimizing system performance at a given level of investment, while the former are directed at justifying the investment itself.

Computer graphic system design alternatives are first outlined. Then methods of analyzing the performance and costs of computer systems in general and graphic systems in particular are discussed. With this information it is shown how cost-effectiveness analyses may be performed. The next crucial step is to conduct benefit analysis, an ill-defined art. The results of benefit analysis must be combined with cost-effectiveness analysis in order to perform the desired cost-benefit analysis.

An experimental methodology is suggested for better performing benefit analyses of computer graphic systems. A more rigorous formulation of the cost-benefit procedure is then outlined. No attempt is made in this report to actually perform such an analysis.

NBSIR 73-152. Measurement of transit time and related transistor characteristics, D. E. Sawyer, G. J. Rogers, and L. E. Huntley, 131 pages (Oct. 1973). Order from NTIS as AD 914258.

Key words: delay time; electronics; high-frequency probes; Sandia bridge; scattering; S-parameters; transistors; vector voltmeter.

Two instruments for transistor delay-time measurements, the vector voltmeter and Sandia bridge, were analyzed and comparative measurements were made on several types of commercial and two special transistors. It was found that extraneous pickup at the measurement frequency can cause large errors in measured delay time. A technique for minimizing these errors was developed and verified for the Sandia bridge by removing the frequency dependence of delay force, probe tip protrusion and lateral motion (skating) with loading were recorded for special probe assemblies to be used in an automatic wafer prober for measurements on transistors in custom-designed integrated circuit wafers. The data is used to assist in adjusting the probes. A technique was developed for determining the effects of the probe assemblies on transistor measurements made from 0.1 to 2.0 GHz. Each probe assembly may be represented by an equivalent circuit consisting of three unknowns; these unknowns are determined by making impedance measurements at the input connectors with the probe tips contacted by combinations of open circuits, short circuits, and resistors of known value. Arrays of such terminations were successfully fabricated and characterized. An S-parameter interlaboratory testing program was developed. The plan calls for six of each of three types of transistors to be measured by participants at frequencies from 0.11 to 2.0 GHz. Additionally, a 10-dB attenuator and R-C networks on TO-72 headers are to be circulated to pinpoint measurement discrepancies.

NBSIR 73-180. Testing of the NBS clinical microcalorimeter, E. J. Prosen and R. N. Goldberg, 31 pages (Apr. 1973). Order from NTIS as COM 74-10139.

Key words: clinical chemistry; clinical microcalorimetry; microcalorimeter; NBS microcalorimetry; testing of microcalorimeter.

The NBS Clinical Microcalorimeter has been tested for stability, sensitivity, ease of operation, and accuracy. The accuracy was tested by means of electrical calibration and the determination of the heat of neutralization of HCl(aq) with NaOH(aq). The heat of this reaction agrees with the best literature value within the precision of the calorimeter. The precision is about 0.6 percent when measuring about 50 mJ of heat of chemical reaction. The accuracy is estimated as 1 percent. The precision of electrical energy determination is about 0.4 percent for energies of from 1 to 1400 mJ.

NBSIR 73-199. Experimental and analytical studies of floor covering flammability with a model corridor, W. Denyes and J. Quintiere, 115 pages (May 1973). Order from NTIS as COM 74-10129.

Key words: flame spread; floor covering materials; model corridor; scaling laws; test method.

An experimental model corridor facility was designed, constructed, and instrumented. The facility examines flame spread over floor covering materials in a small scale corridor under a forced air flow condition. A gas burner flame serves as the ignition source.

A study was made of the factors influencing flame spread in the model corridor. These factors included energy release rate of the ignition source, air velocity, and model corridor geometry. Twenty-six carpet materials and 5 other floor covering materials were studied in the model corridor, and 369 flame spread runs were conducted.

It was found that flame spread behavior in the model corridor generally involves either a rapidly accelerating flame front which propagates the full 8 foot length of the test section ("flameover"), or involves a decelerating flame front which results in extinction a short distance from the ignition source. Radiant heating of the floor material due to hot products of combustion heating the ceiling is a significant factor in causing flameover. Carpet assembly was found to affect flame spread more significantly than pile fiber type.

The data have been analyzed to determine quantitatively the effects of the factors influencing flame spread. Scaling relationships have been presented to attempt to extrapolate the model corridor results to full scale corridor fires.

Finally a procedure has been suggested for using the facility in a floor covering flammability test method. The procedure is based on determining the minimum energy input rate to cause flameover.

NBSIR 73-200. A model corridor for the study of the flammability of floor coverings, W. Denyes and J. W. Raines, 40 pages (May 1973). Order from NTIS as COM 74-10478.

Key words: air flow, energy input; flameover; flame spread; floor covering flammability; model corridor; test repeatability.

A program was carried out to develop a laboratory test method that would measure the flame propagation characteristics of floor covering materials. A facility was designed which included a floor mounted specimen in a rectangular cross-sectional duct having a forced supply of air and a gas burner ignition source. The effects of variations in duct size, ignition source, and air flow were studied. Factors influencing repeatable test results were explored. Flame spread was measured by an observer and temperature and heat flux measurements were recorded on an electronic digital data acquisition system.

NBSIR 73-234. Drapery and curtain fires—data element summary of case histories, A. K. Vickers, 28 pages (July 1973). Order from NTIS as COM 74-10128.

Key words: burns; case histories; curtains; death; draperies; FFACTS; fires; flammable fabrics; houses; standards; statistical data.

A preliminary examination of 1,567 computerized case histories from the NBS Flammable Fabric Accident Case and Testing System has found 77 incidents in which curtains and draperies were involved in fires. This report is a summary of information relating to these 77 incidents, and includes the location of incidents, ignition sources, personal injury, fabrics involved and personal characteristics of victims. Fifteen people died from these fires and 32 others were injured. Curtains or draperies were the first fabric item to ignite in 28 of 55 curtain and drapery incidents in which the ignition source is known.

NBSIR 73-280. Thermodynamics of chemical species important to rocket technology, T. B. Douglas and C. W. Beckett, 109 pages (Jan. 1, 1973). Order from NTIS as COM 74-10549.

Key words: associated vapors; graphite; heat capacity; molybdenum; molybdenum pentafluoride; niobium; radiance temperature; spectral emittance; surface roughness; thermodynamic properties.

The enthalpy of high-purity molybdenum was accurately measured 273-1173 K, and joined smoothly to lower-temperature (German) and higher-temperature (NBS) results to give thermodynamic functions 273-2100 K. The heat capacity of a grade of Poco graphite was measured by a subsecond-duration pulse-heating technique 1500-3000 K (estimated inaccuracy, 3% or less). Based largely on earlier NBS IR and Raman spectroscopy, ideal-gas thermodynamic functions for MoF₅ were generated and are tabulated for 0-6000 K. Three alternative classical-thermodynamic or quasi-chemical treatments are developed for deriving thermodynamic properties from vaporization data on partially associated vapors, with calculations to illustrate experimental-error propagation for one treatment. A subsecond-duration pulse-heating technique was applied to niobium metal to measure its change in normal spectral emittance and radiance temperature at and near its melting point (wavelength, 650 nm), studying dependence on solid-state roughness (0.1 to 0.95 μ m).

NBSIR 73-281. Thermodynamics of chemical species important to rocket technology, T. B. Douglas and C. W. Beckett, 122 pages (July 1, 1973). Order from NTIS as COM 74-10550.

Key words: electrical resistivity; iron; molybdenum pentafluoride; partly associated vapors; solid-state transformations; solution calorimetry; specific heat; spectral emittance; transition alloys; vapor pressure.

Using a subsecond-duration transient technique, the specific heat, electrical resistivity, and hemispherical total emittance were simultaneously measured 1500-2800 K for iron and the alloy 80Nb-10Ta-10W (estimated uncertainties: 3%, 0.5-1%, and 3% for the respective properties). Comparisons are made with generalized approximations. At the gamma-to-delta transformation of iron (about 1680 K), the temperature, heat of transformation, specific heat, spectral emittance, and electrical resistivity were measured, thereby demonstrating the feasibility of the technique for solid-solid transformations. Two other alloys were likewise measured. Solution calorimetry involving several thermochemical steps (including oxidation by XeO₃ in aqueous HF) gave the standard heat of formation of MoF₅(c). A new static vapor-pressure method, after verification to 1 percent by I₂ and MoF₆, and after modifications to deal with the necessarily added MoF₆, gave the vapor pressure of MoF₅ at 393 K and indicated (using also earlier NBS transpiration data) 85-90 mole percent of monomer in the saturated vapor.

NBSIR 73-294. Cost sharing as an incentive to attain the objectives of shoreline protection, H. E. Marshall, 70 pages (Dec. 1973). Order from NTIS as COM 74-10541.

Key words: beach erosion control; cost sharing; economics; efficiency; equity; incentives; shoreline protection.

The nation's shorelines are being eroded by high winds and waves. Nonfederal interests have traditionally received Federal help in the form of cost sharing for protective structures. This study provides the

Army Corps of Engineers with an evaluation of alternative cost-sharing rules for shoreline protection with respect to efficiency, equity, and administrative feasibility.

Existing cost-sharing rules are described for hurricane, beach erosion, and emergency protection. The present cost-sharing system appears to induce local interests to choose (1) costly techniques of protection, e.g., engineering rather than management techniques, and (2) overbuilt projects in terms of the efficient scale.

It is concluded that the Association Rule, which requires local beneficiaries of shoreline protection to share in all of the costs of a project purpose in the proportion that local benefits bear to national benefits at the margin, should be applied to all shoreline protection programs. All techniques of protection should be subject to the same percentage cost-sharing rule. It is also concluded that *all* categories of project costs should have the same percentage cost share apply to them. Finally, Federal cost sharing might be used as an incentive to encourage local interests to comply with minimum land use requirements that would prevent shoreline damages.

NBSIR 73-297. Fracture and deformation of alumina, S. M. Wiederhorn, 14 pages (July 31, 1973). Order from NTIS as AD 772066.

Key words: electron microscopy; fracture; mechanical properties; plastic deformation; sapphire; sodium chloride.

This report summarizes work conducted during the past eight years on the fracture and deformation of ceramic materials. Accomplishments discussed in this report include: an elucidation of fracture process of aluminum oxide and sodium chloride; the development of techniques to study the deformation of aluminum oxide during abrasion; and the development of techniques for measuring fracture mechanics parameters on ceramic materials.

NBSIR 73-351. Thermal conductivity standard reference materials from 6 to 280 K: VI. NBS sintered tungsten, J. C. Hust, 58 pages (Jan. 1974). Order from NTIS as AD 775367.

Key words: cryogenics; electrical resistivity; Lorenz ratio; Seebeck effect; standard reference material; thermal conductivity; transport properties; tungsten.

Thermal conductivity, electrical resistivity, Lorenz ratio, and thermopower data are reported for two specimens of NBS sintered tungsten for temperatures from 6 to 280 K. Variability of this tungsten was studied by means of electrical resistivity and residual resistivity measurements on 39 specimens. These data indicate a material variability of about ± 10 percent in thermal conductivity at helium temperatures. Above 90 K variation in thermal conductivity is only about ± 1 percent. To reduce the uncertainty caused by specimen variation at low temperatures, characterization by residual electrical resistivity data is described. By this procedure the low temperature uncertainty is reduced to about ± 3 percent.

NBSIR 73-405. Use of organic coatings on the interior surfaces of equestrian statues at Memorial Bridge Plaza, F. Ogburn, 9 pages (Nov. 1973). Order from NTIS as COM 74-10131.

Key words: bronze statuary; organic coatings; restoration; statues.

The equestrian statues at Memorial Bridge Plaza in the District of Columbia are bronze castings. The exterior finish is subject to corrosion processes associated with pores and cracks in the castings. The interior surfaces are subjected to high humidity and condensation. Detrimental corrosion is expected only at discontinuities in the plated coatings on the exterior surfaces. Painting of interior surfaces has been recommended, but the need for painting is not clear. The NCP is advised to keep the statues under close observation till the fall of 1974 and then reconsider their course of action.

NBSIR 73-412. The incidence of hazardous material accidents during transportation and storage, W. A. Steele, D. Bowser,

and R. E. Chapman, 40 pages (Nov. 1973). Order from NTIS as COM 74-10512.

Key words: accidents; hazardous material; storage of hazardous material; transportation of hazardous material.

This report is one of a series describing background research concerning the incidence of abnormal loading. The report is organized in terms of modes of hazardous material transportation and storage. These modes—pipeline, water, motor vehicle, and railroad transportation systems—are addressed in four sections with Storage Systems discussed in a fifth. The sections depend on the amount of available data, rather than the risk involved in an accident. A summary of the results is presented in the last section. On the whole, there is little empirical evidence to substantiate a threat to buildings from hazardous materials transport. However, trends in volumes shipped in proximity to structures of interest raises the prospect of future incidents.

NBSIR 73-414. Building and evaluation of a polluted air delivery system, G. P. Baumgarten and F. W. Ruegg, 36 pages (Apr. 1974). Order from NTIS as COM 74-10866.

Key words: air pollution; critical flow; laminar flow; nozzle; porous plug; sulfur dioxide concentration.

The building and evaluation of a prototype SO₂ polluted air delivery system (PADS) is discussed. The delivery system was built to deliver sulfur dioxide (SO₂) in air at a rate of 5 liters per minute with design concentrations by volume of 1.0, 0.1 and 0.01 parts per million. It consists of a diluent air delivery system utilizing a critical flow sonic nozzle and three separate concentrated SO₂ in air flow systems utilizing laminar flow porous plugs, one plug for each desired output concentration. The delivery system is contained in a dispatch case and the two gases are delivered to it from pressurized containers through detachable supply lines. Prospective use by unskilled technicians dictated simplicity and durability and compactness.

By maintaining specific upstream pressures on the critical flow nozzle and the laminar flow porous plugs of 45 and 12 psig respectively, the prototype PADS produced average output concentrations of 0.76, 0.100 and 0.003 parts per million of SO₂ in air based on concentration measurements with an NBS calibrated analyzer. The expected output concentrations were 0.98, 0.105 and 0.010 respectively, based on flow calibrations of the individual components. The uncertainty of the output concentration is estimated to be about ± 10 percent.

NBSIR 73-416. Report on meeting of ISO/TC 6/SC 5 testing methods and quality specifications for pulp, W. K. Wilson, J. H. Schulz, C. E. Brandon, and J. L. Borstelmann, 69 pages (Nov. 16, 1973). Order from NTIS as COM 74-10511.

Key words: ISO recommendations; pulp; pulp, testing methods; testing methods for pulp.

The ninth meeting of ISO/TC 6, Paper, SC 5, Testing Methods for Pulp, was held in Madrid, Spain, November 2-8, 1973. Over 30 delegates from 11 countries discussed methods for testing of pulp and, to some extent, paper. Methods were agreed upon for the determination of saleable mass of flash dried pulp, disintegration of pulp, laboratory beating of pulp, preparation of laboratory sheets, and measurement of ISO brightness of pulp. It was agreed that ISO Recommendations for determination of saleable mass of pulp in lots, determination of dry matter content, and determination of trace metals in pulp should be revised. Plans were made to continue studies of methods for the determination of viscosity, aqueous extraction, dirt and shives, total sulphur content, saleable mass of unitized lots of pulp, statistical evaluation of number of sample bales, preparation of laboratory sheets, and fiber classification and drainability.

NBSIR 73-424. A study of young children's pull-apart strength (an addendum to NBSIR 73-156—a study of the strength capabilities of children ages two through six), W. C. Brown,

C. J. Buchanan, and J. Mandel, 17 pages (Apr. 1974). Order from NTIS as COM 74-10867.

Key words: children; children's strength; pull-apart; safety; strength; test methods; toys; toy safety.

The Child Pull-Apart Strength Study was conducted to provide information which can be used to develop reliable and realistic standards and test methods for children's toys. The study was conducted with over 500 children in the Washington Metropolitan area, and included both black and white children from varying economic and social backgrounds.

The pull-apart test device used is a prototype model designed and constructed at the National Bureau of Standards. This test device was designed to measure the force that children can exert when pulling an object apart.

The results of the pull-apart strength study are consistent with those obtained in the previous child strength study which dealt with twisting, pulling, pushing, and squeezing (NBSIR 73-156). The study provided quantitatively precise and useful information about the effects of age and sex on the pull-apart strength capability of children ages two through six. The results are exhibited in tables of averages, standard deviations, coefficients of variation, and 95th and 5th percentiles.

NBSIR 74-430. Chemical kinetics data survey VII. Tables of rate and photochemical data for modelling of the stratosphere (revised), D. Garvin and R. F. Hampson, 104 pages (Jan. 1974). Supersedes NBSIR 73-203. Order from NTIS as COM 74-10724.

Key words: atmospheric chemistry; chemical kinetics; data evaluation; energy transfer; gas phase; high temperature air chemistry; ion-molecule reactions; optical absorption cross sections; photochemistry; quantum yield; rate constants.

Chemical kinetic and photochemical data for gas phase reactions pertinent to the chemistry of the stratosphere are presented in four tables. These tables give recommended values and also cite recent experimental work. They give data in the following subject areas: chemical reactions and photochemistry of neutral species, energy transfer reactions, high temperature air reactions, and ion-molecule reactions.

NBSIR 74-432. 1972 international activities center for building technology, C. C. Raley, 68 pages (Aug. 1973). Order from NTIS as COM 74-10751.

Key words: cooperative programs; foreign visitors; information exchange; international building technology; international organization memberships; professional interaction.

This report summarizes the Center for Building Technology's 1972 international activities including formal cooperative programs, exchange programs, special projects, international organization memberships, foreign guests at CBT, and CBT foreign travel.

NBSIR 74-444. A review of natural stone preservation, G. A. Sleater, 40 pages (Dec. 1973). Order from NTIS as COM 74-10548.

Key words: air pollution; historic structures; laboratory evaluation; natural weathering; stone decay; stone preservation.

With increased interest in stone preservation, it is desirable to know what causes stone to decay, and what materials can be used to preserve stone. This review covers the following topics: causes of stone decay, including faults in the stone, salts, natural weathering factors, air pollution, living organisms, and most importantly, water action; various materials that have been used to preserve stone, including paints, waxes, oils, inorganic chemical surface treatments and impregnants, silicones, silicates, and synthetic organic polymers; methods of evaluating stone preservatives. Field and laboratory procedures for testing stone preservatives, the cleaning of stone, a glossary, and a bibliography are given in appendices.

NBSIR 74-455. **Abstracts of papers on testing and analysis of flammable fabrics October 1972 to October 1973**, J. F. Krasny, 27 pages (Mar. 1974). Order from NTIS as COM 74-10865.

Key words: burn injuries; carpets; clothing; fabrics; fire retardants; flammability testing.

This collection of abstracts covers papers on textile flammability testing and analysis of flame retardant fibers and finishes, for the period October 1972 to October 1973. It is hoped that this collection will facilitate research in this area in which there has been great interest in connection with the introduction of fabric and garment flammability standards by the Federal and several state governments. Similar collections appear in the Proceedings of the Annual Meetings of the Information Council on Fabric Flammability, available from the Council, Room 510, 1457 Broadway, New York, N.Y. 10036.

NBSIR 74-464. **The Shirley Highway Express-Bus-On-Freeway Demonstration Project—second year results**, J. T. McQueen, R. F. Yates, and G. K. Miller, 87 pages (Nov. 1973). Order from NTIS as COM 74-10785.

Key words: bus transit; busway operations; commuter travel behavior; express bus-on-freeway operations; project evaluation; transit operations.

This report contains: (a) A review of the performance of the Shirley Highway Express-Bus-On-Freeway Demonstration Project between 1969 and 1973; (b) A description of the methodology and data use to estimate project measures of effectiveness; (c) A discussion of factors considered in commuter mode choice decision making.

This column lists all outside publications by the NBS staff, as soon after issuance as practical. For completeness, earlier references not previously reported may be included from time to time.

Allan, D. W., Glaze, D. J., Machlan, H. E., Wainwright, A. E., Hellwig, H., Barnes, J. A., Gray, J. E., **Performance, modeling, and simulation of some cesium beam clocks**, *Proc. 27th Annual Symp. on Frequency Control, Philadelphia, Pa., June 12-14, 1973*, pp. 334-346 (Electronic Industries Association, Washington, D.C. 1973).

Key words: atomic clock; atomic clock modeling; atomic clock noise; atomic clock performance; atomic time scale accuracy; comparison of atomic time scales; comparison of frequency standards; frequency calibration; frequency drift; simulation of clock performance.

With the availability of a new primary frequency standard, NBS-5 at the National Bureau of Standards, we have been able to evaluate with greater confidence than in the past the performance characteristics of the commercial cesium beam clocks used in the AT(NBS) atomic time scale. Two other techniques have also been employed to evaluate a clock's performance, viz., interclock comparisons and comparisons with other national laboratories.

Utilizing the above performance data we have constructed models for the behavior of cesium beam atomic clocks. Based on these models and appropriate optimization procedures, algorithms have been developed to generate an atomic time scale, AT(NBS), from the ensemble of standards available to us. The model is shown to well fit both individual clocks as well as clock ensembles. This modeling provides a direct opportunity for clock data simulation. Simulation techniques are developed and applied in the testing of some diagnostic tests for frequency and/or time steps. The results are very encouraging as a new effort for even better clock modeling.

Rate calibrations of AT(NBS), UTC(NBS), TAI, and other national time scales are given with reference to NBS-5, and these are compared with other past primary cesium beam frequency standards. TAI was measured as too high in rate by 12 ± 5 parts in 10^{13} .

Allan, D. W., Gray, J. E., Machlan, H. E., **The National Bureau of Standards atomic time scales: Generation, dissemination, stability, and accuracy**, *IEEE Trans. Instrum. Meas.* **IM-21**, No. 4, 388-391 (Nov. 1972).

Key words: AT(NBS); clock dispersion; clock ensemble; frequency and time standards; International Atomic Time; Loran-C; model of clock stability; optimum time prediction; precision and accuracy of timing; time coordination, synchronization, and dissemination; UTC(NBS).

The independent atomic time scale at the National Bureau of Standards AT(NBS), is based upon an ensemble of continuously operating cesium clocks calibrated occasionally by an NBS primary frequency standard. The data of frequency calibrations and interclock comparisons are statistically processed to provide nearly optimum time stability and frequency accuracy. The long-term random fluctuation of AT(NBS) due to nondeterministic perturbations is estimated to be a few parts in 10^{14} , and the present accuracy is inferred to be 1 part in 10^{12} .

A small coordinate rate is added to the rate of AT(NBS) to generate UTC(NBS); this small addition is for the purpose of maintaining synchronization within a few microseconds of other international timing centers. UTC(NBS) is readily operationally available over a large part of the world via WWV, WWVH, WWVB, and telephone; also via some passive time transfer systems, e.g., Loran-C and the TV line-10 system; and also experimentally via satellite and WWVL. The precision and accuracy of these dissemination systems will be discussed.

Allan, D. W., **Statistical modeling and filtering for optimum atomic time scale generation**, (Proc. Frequency Standards and Metrology Seminar, Quebec, Canada, Aug. 30-Sept. 1, 1971), Paper in *Proceedings of the Frequency Standards and Metrology Seminar*, pp. 388-410 (Quantum Electronics Laboratory, Laval University, Quebec, Canada, 1972).

Key words: clock stability model; frequency calibration; frequency stability; international time scale; time scale accuracy; time scale stability.

Statistical models for the fractional frequency fluctuations in atomic clocks, clock ensembles, and some of the propagation media are developed. Using these models, near optimum time prediction algorithms are employed to generate time for a clock ensemble or for a set of laboratories' time scales. An example using data from the BIH Circular D bulletin is illustrated and the results compared with IAT.

Accuracy and uniformity problems are considered in light of the CCDS June 1970 recommendations. A model for an evaluable primary frequency standard is developed as well as for a time scale (flywheel frequency standard). It is shown that under certain conditions the accuracy of a time scale can be better than the accuracy of the primary standard for the current calibration, if there is a sufficient number of independent past calibrations. A method of simultaneously achieving accuracy and uniformity is discussed.

Aminadav, N., Selig, H., Abramowitz, S., **Raman spectrum of F₃NO gas**, *J. Chem. Phys.* **60**, No. 1, 325-326 (Jan. 1, 1974).

Key words: gas; ONF₃; Raman spectroscopy; thermodynamic properties; vibrational analysis.

The Raman spectrum of gaseous F₃NO has been observed allowing a definite vibrational assignment. The thermal functions have been computed using this assignment and previous microwave and electron diffraction data.

Andrews, J. R., **Inexpensive laser diode pulse generator for optical waveguide studies**, *Rev. Sci. Instrum.* **45**, No. 1, 22-24 (Jan. 1974).

Key words: fiber optics; GaAs; impulse; laser; optics; picosecond; pulse; waveguide.

An inexpensive GaAs laser diode pulse generator is presented. This generator has found application in the evaluation of optical pulse dispersion in glass fiber optical waveguide studies. It is capable of producing optical impulses as narrow as 110 psec at a wavelength of 0.9 μ and a pulse repetition rate of 50 kHz. With a slight modification, it may be used to produce optical pulses of considerably longer duration at reduced repetition rates.

Armstrong, G. T., **Recent developments in calorimetry and thermochemistry at the National Bureau of Standards**, (Proc. Plenary Lectures of 8th Symp. on Calorimetry and Thermal Analysis, Okayama, Japan, Nov. 1972), Paper in *Calorimetry, Thermometry and Thermal Analysis* **6**, 51-60 (Kagaku Gijitsu-Sha, Tokyo, Japan, 1973).

Key words: calorimetry; microcalorimetry of biological processes; standard reference materials for calorimetry; thermochemistry; thermodynamic data.

The thermochemistry work at the National Bureau of Standards provides standard reference data for the National Measurement System both in the form of critical compilations of work done elsewhere and also in the form of new measurements of key substances. A new electrolyte thermodynamic data center has been formed. On-going compilations of the properties of inorganic compounds are being systematized in the form of a catalog of thermochemical quantities. New measurements on organic halogen, nitrogen, and sulfur compounds are extending the range of certified standard reference materials for calorimetry.

A new program on the microcalorimetry of biological processes has shown the applicability of calorimetry to practically important problems of clinical chemistry, and has resulted in improvements in the accuracy of microcalorimetric measurements.

Arp, V. D., Clark, A. F., Flynn, T. M., **Superconducting levitation of high speed vehicles**, *Transp. Eng. J.* **99**, No. TE4, 873-885 (Nov. 1973).

Key words: fatigue life; magnetic properties; materials; refrigeration; superconducting magnets; suspension; transportation; urban transportation.

The current status (December 1972) of worldwide research on high speed ground transportation techniques is reviewed. Particular attention is given to studies of magnetic levitation using superconducting magnets, including comparison with alternative magnetic techniques and with air suspension systems. Superconducting levitation appears to be a strong contender in the U.S. Department of Transportation hopes to select in the late 1970's the best of the possible levitation techniques for subsequent advanced development. Cryogenic engineering research needed in support of major development of a superconducting levitated system is identified.

Barnes, I. L., Garner, E. L., Gramlich, J. W., Machlan, L. A., Moody, J. R., Moore, L. J., Murphy, T. J., Shields, W. R., **Isotopic abundance ratios and concentrations of selected elements in some Apollo 15 and Apollo 16 samples**, (Proc. 4th Lunar Science Conf., March 5-8, 1973, Houston, Tex.), *Geochimica et Cosmochimica Acta, Suppl.* **4**, 2, 1197-1207 (1973).

Key words: chromium; isotopic ratios; lead; model ages; nickel; potassium; rubidium; strontium; thorium; uranium.

The elements Pb, U, Th, Rb, Sr, K, Cr, and Ni have been determined on a series of Apollo 15 and 16 rocks and soils. The elements U, Rb, Cr, and Ni show isotopic abundances identical with those of terrestrial materials in both types of samples but the $^{39}\text{K}/^{41}\text{K}$ ratio is fractionated by about 1 percent in the soils and the extreme reversed discordancy of the Pb-U-Th ages in the Apollo 16 soils indicated that lead has also been fractionated in these.

The breccia 60335.36 has concordant Pb-U-Th model ages of 4075 MY and the basalt 15495.59 shows one slightly discordant age of

around 4480 MY. The Rb-Sr model ages are in good agreement with the Pb-U-Th model ages.

Beehler, R. E., **Recent progress on atomic frequency standards**, (Proc. 1972 Precision Electromagnetic Measurement Conf., Boulder, Colo., June 26-29, 1972), Paper in *CPEM Digest*, pp. 166-167 (IEEE, Inc., New York, N.Y., June 1972).

Key words: atomic frequency standards; cesium beam standards; hydrogen masers; rubidium standards.

A brief summary is presented of a paper reviewing progress achieved in the development of atomic frequency standards during recent years. Particular emphasis is placed on cesium, rubidium, and hydrogen maser standards.

Bennett, H. S., **Two-electron U centers in ionic crystals: Point-ion models**, *Phys. Rev. B* **6**, No. 10, 3936-3940 (Nov. 15, 1972).

Key words: BaF_2 ; CaF_2 ; CdF_2 ; ionic polarization; KCl; Mollwo-Ivey relations; NaCl; point-ion potential; SrF_2 ; U centers

The Hartree-Fock-Slater (HFS) equations for the two-electron orbitals about a proton located substitutionally at an anion site have been solved numerically in the point-ion lattice potential. The lattice relaxation of the nearest-neighbor ions is included in the model. The five lowest-lying U-center states for NaCl, KCl, CdF_2 , CaF_2 , SrF_2 , and BaF_2 have been calculated within the framework of the above model. It is found that the low-lying singlet states have the following order for increasing values of the energy: $^1\text{S}(1s, 1s)$, $^1\text{P}(1s, 2p)$, and $^1\text{S}(1s, 2s)$. The energy levels for the triplet states $^3\text{S}(1s, 2s)$ and $^3\text{P}(1s, 2p)$ lie between the energy levels for the $^1\text{S}(1s, 1s)$ and $^1\text{P}(1s, 2p)$ states. The ordering of the triplet states depends upon the host crystal and the lattice relaxation. In some cases, these triplet states may be degenerate or very nearly so. In addition, the extent to which the peak energies of the U bands obey Mollwo-Ivey relations is given for the alkali halides and for the alkaline-earth fluorides. The predictions based upon the numerical HFS wave functions are compared with the predictions based upon past variational wave functions and with experiment.

Berger, H. W., **Polarography. Constant-current coulometry. Differential thermal analysis**, Parts 10.7, 10.8 and 10.9 in *Paint Testing Manual*, Gardner/Sward, 13th Edition, G. G. Sward, Ed., *Amer. Soc. Testing Mater. Spec. Tech. Publ.* **500**, pp. 556-563 (1972).

Key words: coulometric titration; coulometry; differential thermal analysis; diffusion current; dropping mercury electrode, half-wave potential; polarography.

Polarography is an instrumental method of analysis based on the evaluation of current-voltage curves that are obtained during the electro-reduction or oxidation of a chemical compound. The limiting current is diffusion controlled and is a function of concentration. The half-wave potential is the voltage at one-half the diffusion current and is characteristic of the reaction occurring. The dropping mercury electrode, used in polarography, has the particular advantage of being constantly renewed.

Constant current coulometry is a highly accurate analytical technique based on Faraday's Law and involves measuring the number of coulombs (current \times time) that pass through a chemical cell. Coulometric titrations can be performed by electrogenerating the necessary titrant in situ.

Differential thermal analysis is used for identifying or measuring the physical and chemical changes that occur in materials as they are heated or cooled. The temperature of a test sample is compared to an inert reference and the differential temperature is recorded. Exothermic and endothermic temperature changes are related to chemical reactions or physical transformation.

Blunt, R. F., Candela, G. A., Forman, R. A., **Effect of γ irradiation on the magnetic properties of ruby**, *J. Appl. Phys.* **44**, No. 4, 1753-1755 (Apr. 1973).

Key words: aluminum oxide; chromium; color centers; magnetic susceptibility; radiation damage; ruby.

The magnetic susceptibilities of ruby samples (Cr^{3+} in $\alpha\text{-Al}_2\text{O}_3$) were measured before and after Co^{60} γ irradiation. Within the experimental error the magnetic susceptibility was found to be unchanged by the irradiation. The degree of microwave saturation possible for the Cr^{3+} spin system, when at the resonance condition for complete saturation, showed a marked decrease after irradiation. Together, these results indicate that the γ irradiation has changed the resonance condition for approximately 10-15 percent of the Cr^{3+} in a 0.05 wt% Cr_2O_3 sample. A likely inference is that the oxidation state of at least 99 percent of the chromium is unaltered, and that less than 10 ppm Cr has valence differing from three in the irradiated sample. These experiments are in essential agreement with other experiments on ruby.

Bower, V. E., **Determination of the Faraday by means of the iodine coulometer**, (Proc. 4th Int. Conf. on Atomic Masses and Fundamental Constants, Teddington, England, Sept. 6-10, 1971), Paper in *Atomic Masses and Fundamental Constants*, J. H. Sanders and A. H. Wapstra, Eds., pp. 516-520 (Plenum Press, London, England, 1972).

Key words: coulometry; Faraday; fundamental constants.

This paper describes briefly the work now in progress at NBS on the determination of the Faraday by means of the iodine coulometer. Results obtained to date are compared with a recent determination of the Faraday by means of the silver coulometer and with an adjusted value of the same constant derived from recent determinations of the gyromagnetic ratio of the proton and proton magnetic moment in nuclear magnetons.

Brennen, W., Brown, R. L., **Measurements on the nitrogen atom and pressure dependences of the visible nitrogen afterglow intensity in a nitrogen carrier using EPR**, *J. Chem. Phys. Letters to Editor* **52**, No. 9, 4910-4911 (May 1, 1970).

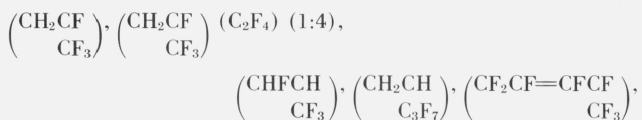
Key words: atom recombination; energy transfer; Lewis-Rayleigh afterglow; N-atoms; N_2 first positive bands; nitrogen afterglow.

The relative visible nitrogen afterglow intensity in a N_2 carrier was measured as a function of pressure and N-atom concentration using EPR detection over a range 0.12 to 75 torr. The specific intensity $I/[N]^2$ was found to be independent of pressure and $[N]$, within the experimental uncertainty.

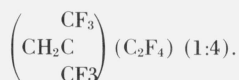
Brown, D. W., Florin, R. E., Wall, L. A., **The effect of dilute fluorine on certain fluoropolymers**, *Appl. Polym. Symp. No.* **22**, 169-180 (1973).

Key words: crosslinking; fluorine; fluoropolymers.

Various fluoropolymers were exposed to 5 percent fluorine in helium at 25 °C and one atmosphere. About 10-100 percent as many fluorine molecules were charged as monomer units in each polymer. Certain polymers degraded as shown by decreases in their intrinsic viscosities. Degrading polymers had the structures



and



The intrinsic viscosity of polyperfluoropropene was not changed. Other polymers cross-linked, as shown by formation of gel. These had the structures



and



In homopolymers the greater the hydrogen content the more likely the polymer was to crosslink, suggesting that crosslinking proceeds via abstraction of hydrogen atoms. However, an increased content of tetrafluoroethylene in copolymers also was associated with greater crosslinking or reduced degradation. Viton and a copolymer of 3,3,3-trifluoropropene gave highly crosslinked materials. The vulkanizates of Viton are quite resistive to stress relaxation at 250 °C in air. Those of the trifluoropropene copolymer are very unstable.

Brown, D. W., Lowry, R. E., Wall, L. A., **Radiation-induced polymerization at high pressure of *cis*- and *trans*-1,3,3,3-tetrafluoropropene in bulk and with tetrafluoroethylene**, *J. Polym. Sci. Part A-1*, **11**, 1973-1984 (1973).

Key words: copolymerization; high pressure; polymerization; radiation; tetrafluoroethylene; tetrafluoropropene.

The radiation-induced polymerization of *cis*- and *trans*-1,3,3,3-tetrafluoropropene in bulk and with tetrafluoroethylene was studied at pressures between 5000 and 15000 atm and temperatures between 21 and 100 °C. At 10^3 rad/hr the homopolymerization rates range from about 10^{-4} to 1 percent/hr. The activation enthalpy and volume are about 8 kcal/mole (33 kJ/mole) and -10 cm³/mole, respectively, for both isomers. The *cis* isomer polymerizes about twice as rapidly as the *trans* isomer. The latter freezes in the experimental range of temperature and pressure; the polymerization rate is very low in solid phase. Polymer intrinsic viscosities increase with polymerization pressure and decrease with polymerization temperature; the largest value obtained was 0.23 dl/g. In the copolymerizations all reactivity ratios favor incorporation of tetrafluoroethylene by factors of 6-16. The preference is stronger when the *trans* isomer is used.

Brown, R. L., **Effects of N-atom concentration, pressure, and carrier composition on some first positive band intensities in the yellow nitrogen afterglow**, *J. Chem. Phys.* **52**, No. 9, 4604-4617 (May 1, 1970).

Key words: energy transfer; first positive N_2 bands; Lewis-Rayleigh afterglow; nitrogen afterglow; nitrogen atoms; vibrational relaxation electronic quenching.

Absolute intensities of seven N_2 1st positive bands with $\nu' = 6-12$ were measured as a function of carrier pressure, carrier composition, and N-atom concentration in the range 4.5-0.06 torr. For an Ar carrier large pressure-dependent shifts in the $B^3\Pi_g$ vibrational distribution to higher levels were observed below 4 torr; similar but much smaller shifts were also found for N_2 and He carriers. With Ar, reducing the N-atom concentration shifted the vibrational distribution to lower levels. Changes in carrier composition produced large pressure dependent changes in the absolute and relative band intensities. An attempt was made to fit the results to a model involving vibrational relaxation and electronic quenching in $B^3\Pi$. While qualitatively successful, this model could not account quantitatively for the observed relative intensity changes over the whole pressure range for which data are available and, in addition, implied physically unreasonable vibrational relaxation rates. It is suggested that the observed changes in the $B^3\Pi_g$ vibrational distribution below 4 torr may arise from vibrational relaxation in some precursor state.

Camarda, H. S., ***P-wave neutron strength-function measurements and the low-energy optical potential***, *Phys. Rev. C* **9**, No. 1, 28-37 (Jan. 1974).

Key words: function; mass number; neutrons; optical potential; *R*-matrix; strength; time-of-flight.

Using the National Bureau of Standards electron linac and underground time-of-flight facility, precise average neutron-transmission measurements have been made in the energy range $1 \text{ keV} \leq E \leq 600 \text{ keV}$ on the elements As, Br, Nb, Rh, Ag, In, Sb, I, La, Ho, Au, and Th. The samples were "thick" in that the *s*-wave self-protection had to be accounted for at low energies. However, the samples were still sufficiently thin that any errors introduced by neglecting *p*-wave self-protection were negligible. The average *R*-matrix theory was employed in the analysis and the $l=0$ scattering length R' and the *p*-wave strength function S_1 were extracted from the data. The behavior of S_1 vs mass number A in the region of the $3P$ maximum was found to vary smoothly with no evidence of any splitting of the resonance. Using Moldauer's optical potential, which fits the $l=0$ data well, the behavior of S_1 vs A was calculated. The predicted behavior was found to differ significantly from experiment. In particular, experiment indicates S_1 peaks at a lower mass number and that the maximum is stronger than indicated by the calculations. When the constants of the potential were changed in order to reproduce the observed behavior of S_1 , a significant discrepancy with the $l=0$ data resulted. The results presented here imply an orbital angular momentum dependence of the low-energy optical potential.

Chang, S-S., ***Thermal relaxation and glass transition in polyethylene***, *J. Polym. Sci.*, No. 43, 43-54 (1973).

Key words: annealed; crystallinity; glass transition; polyethylene; relaxation; temperature drifts.

Thermal relaxations in the glass transition region can be observed as spontaneous temperature drifts of the sample under adiabatic conditions. Upon the heating of a quenched glass, positive drifts are observed reaching a peak at some temperature just below its T_g . An annealed glass produces a peak in the negative drift at temperatures just above its T_g . Heat capacity measurements have been made on three linear polyethylene samples having 71 to 96 percent crystallinity and on one branched polyethylene sample, in an adiabatic calorimeter from 2 to 360 K. In all four samples, temperature drifts were detected with peaks occurring around 235-240 K. The temperature of the peaks is not significantly affected by the degree of crystallinity. However, the magnitude of the peaks decreases as the crystallinity is increased.

Cohen, G. G., Alexandropoulos, N. G., Kuriyama, M., ***Relation between x-ray-Raman and soft-x-ray-absorption spectra***, *Phys. Rev. B* **8**, No. 12, 5427-5431 (Dec. 15, 1973).

Key words: energy transfer; lithium; momentum transfer; x-ray absorption; x-ray inelastic scattering.

A spectrum of x-ray inelastic scattering of copper $K\alpha_1 K\alpha_2$ radiation scattered by metallic lithium through $2\theta = 115^\circ$ was obtained. (These conditions correspond to a momentum transfer $k = 6.87 \times 10^{10} \text{ m}^{-1}$.) The spectrum is compared quantitatively to an experimental soft-x-ray-absorption spectrum of lithium. This comparison serves as an experimental verification of the relation between x-ray-Raman spectra and soft-x-ray-absorption spectra. The method renders possible the study of solid-state effects via x-ray Compton-Raman experiments without *ad hoc* assumptions concerning the wave functions of the inner electrons. Also presented is some evidence of the failure of a random-phase approximation and the impulse approximation in the region under investigation.

Costrell, L., Ed., ***CAMAC—organization of multi-crate system***, (AEC Committee on Nuclear Instrument Modules), *AEC Report No. TID-25876*, 42 pages (U.S. Atomic Energy Commission, Washington, D.C., Mar. 1972).

Key words: CAMAC; computer interfacing; control systems; instrumentation; instrumentation standards; nuclear instrumentation; standards.

CAMAC is a design for modular equipment systems used on-line with digital processors and computers and incorporates a comprehensive data transfer highway (Dataway). This extension to the CAMAC specifications defines a Branch Highway and a standard Crate Controller for communication between a system controller or computer and as many as seven crates. The specification has been developed by the ESONE Committee of European Laboratories and has been endorsed by the U.S. AEC Committee on Nuclear Instrument Modules (NIM Committee). Except for pages i-vii and page 30A, this report is identical to Euratom Report EUR 4600e dated October 1971. AEC Report TID-25877 constitutes a supplement to and is to be used in conjunction with this report. The basic CAMAC specifications are defined in AEC Report TID-25875.

Costrell, L., ***Highways for CAMAC systems—a brief introduction***, *IEEE Trans. Nucl. Sci.* **NS-21**, No. 1, 870-875 (Feb. 1974).

Key words: CAMAC; computer interfacing; control systems; instrumentation; instrumentation standards; nuclear instrumentation; standards.

The interconnection between CAMAC crates and between the crates and a computer is called the CAMAC highway. The purpose of this paper is to present a brief summary of CAMAC highway configurations to put in perspective the highway papers that follow and to serve as a starting point for the panel discussion on CAMAC highways.

Cowan, D. O., LeVanda, C., Collins, R. L., Candela, G. A., Mueller-Westerhoff, U. T., Eilbracht, P., ***Mössbauer and magnetic susceptibility studies of biferrocenylene (II, III) picrate***, *J. Chem. Soc. Chem. Commun.*, pp. 329-330 (1973).

Key words: biferrocenylene (2,3) picrate; magnetic susceptibility; Mössbauer.

Mössbauer and magnetic susceptibility studies of biferrocenylene (II, III) picrate show that extensive donor-acceptor interactions occur in this mixed-valence molecule which result in fractional oxidation states for the iron atoms.

Currie, L. A., DeVoe, J. R., ***The isotope separator as a tool for low-level radioassay and trace activation analysis***, (Proc. Symp. on Nuclear Techniques in Measurement and Control of Environmental Pollution, Salzburg, Austria, Oct. 26-30, 1970), Paper in *Nuclear Techniques in Environmental Pollution*, pp. 183-190 (International Atomic Energy Agency, Vienna, Austria, 1971).

Key words: activation analysis; iodine; mass separation; physical-radiochemical separation.

Determinations of environmental radioactivity and of low-level products of nuclear activation are frequently limited in sensitivity because of isotopic contamination. Sensitivity may be limited by radioisotopes because of interfering radiations and by stable isotopes because of decreased specific activity. To overcome these limitations, electromagnetic isotope separation, which is applicable to most elements, has been investigated as a complement to radiochemical separation and decay scheme resolution. An added advantage of mass separation in environmental studies is the physical separation of a diluting radioisotope—radioisotope dilution being desirable because of the possibility of unknown initial amounts of stable isotopes.

The characteristics of the relatively new class of laboratory isotope separators having moderately large beam currents, 1-5 mA, are particularly suitable, for they include reasonable throughput ($\sim \text{mg/h}$), yield ($\sim 10\%$) and resolution ($\sim 10^3$). Isotope separation was investigated in connection with the neutron activation analysis of trace

quantities ($\sim 10^9$ atoms) of iodine. The mass-separation step was found to be essential because of the production of interfering iodine fission products—even when uranium contamination was as low as 1 ppm. A particularly important result of our investigation was the absence of any detectable blank effect from prior separations. In addition, it has been shown that for certain problems electromagnetic separation, when combined with a high efficiency radiation detector, is far more sensitive and selective than a high resolution detector without mass separation.

Dehl, R. E., **NMR second moment of rotator-phase polycrystalline $n\text{-C}_{19}\text{H}_{40}$** , *J. Chem. Phys. Letters to Editor* **60**, No. 1, 339-340 (Jan. 1, 1974).

Key words: molecular rotation; NMR second moment; n -nonadecane; paraffin; rotator phase; wide-line NMR.

The proton NMR second moment of polycrystalline $n\text{-C}_{19}\text{H}_{40}$ in the rotator phase at 25 °C was measured for several spectra of the as-received ("98.5%") and the solution-recrystallized paraffin. The average second moment of the as-received paraffin (0.060 (mT)²) was considerably lower than that of the recrystallized paraffin (0.076 (mT)²), indicating the importance of chemical purity in obtaining accurate second moments of paraffins. The results for the recrystallized paraffin were significantly lower than Andrew's theoretical prediction (0.088 (mT)²), but significantly higher than the value predicted by Olf and Peterlin (0.064 (mT)²). Because of these discrepancies, the theoretical NMR second moment of the "rotator" paraffin was reevaluated, using exact calculations of the most important dipolar contributions and estimates of the smaller terms. The calculated and observed values were thus found to differ by only 4 percent. The NMR second moment is consistent with simple rotation or large-amplitude oscillation of the chains about their long axes.

Dehl, R. E., **The effect of salts on the nmr spectra of D_2O in collagen fibers**, *Biopolymers* **12**, 2329-2334 (1973).

Key words: collagen; D_2O in collagen; deuterium nmr; MgCl_2 in collagen; MgSO_4 in collagen; wide-line nmr.

The effects of two salts, MgCl_2 and MgSO_4 , on the wide-line nmr spectrum of D_2O in oriented, undenatured collagen fibers have been examined at four different D_2O contents. MgCl_2 was found to decrease the nmr doublet splitting, as compared with equal quantities of pure D_2O , while the major effect of MgSO_4 was to inhibit the adsorption of D_2O without significantly affecting its nmr spectrum. The results, together with a few observations of KCl and LiCl solutions, indicate that even fairly high concentrations of salt have only small effects on the nmr spectrum of D_2O in fibrous collagen. It is considered unlikely that either "two-state" or "structured-water" models can satisfactorily account for the D_2O -nmr doublet spectrum or the effects of salts on it, over the entire range of observed D_2O content.

Diamond, J. J., Calvano, N. J., **Ballistic resistance of police body armor**, *NILECJ-STD-0101.00*, 10 pages (U.S. Department of Justice, Law Enforcement Assistance Administration, National Institute of Law Enforcement and Criminal Justice, Washington, D.C., Mar. 1972).

Key words: armor (wearable); ballistic deformation; ballistic penetration; body armor; bullet proof vests.

This standard establishes performance requirements for ballistic penetration, and methods of test for ballistic penetration and deformation of police body armor intended to protect the torso against small arms gunfire. Standards are established for armors intended to provide three levels of protection: Armors protective against .30-06 armor piercing rifle fire, armors protective against .357 magnum revolver fire, and armors protective against .22 long rifle high velocity rifle fire.

Diamond, J. J., Weissler, P. G., **Hearing protectors for use on firing ranges**, *NILECJ-STD-0102.00*, 11 pages (U.S. Department of Justice, Law Enforcement Assistance Administration, National Institute of Law Enforcement and Criminal Justice, Washington, D.C., Mar. 1973).

Key words: earmuffs; earplugs; firing range noise; gunfire noise; hearing protectors.

This standard establishes performance requirements and methods of test for wearable devices used to protect the auditory system against the gunfire noise on firing ranges. The test method described measures hearing protection by psychoacoustic tests on human subjects, that is, the real-ear protection at threshold of audibility. It is based on ANSI Standard Z24.22-1957.

Douglas, W. M., Johannesen, R. B., Ruff, J. K., **Reactions of coordinated ligands. II. μ -oxo-bis(difluorophosphineiron tetracarbonyl)**, *Inorg. Chem.* **13**, No. 2, 371-374 (1974).

Key words: carbonyl compounds; coordination compounds; fluorophosphine; iron carbonyl; nmr; nuclear magnetic resonance.

Reaction of $\text{Fe}(\text{CO})_4\text{PF}_2\text{Br}$ with potential sources of the oxide ion (e.g., Ag_2O , Cu_2O , etc.) yielded the new complex compound, $\text{Fe}(\text{CO})_4\text{PF}_2\text{OPF}_2\text{Fe}(\text{CO})_4$. A more convenient preparation of this material involved the use of AgMnO_4 instead of the metal oxides. The ^{31}P and ^{19}F nmr parameters for the complex were obtained by analysis of the spectra as a $\text{AA}'\text{XX}'\text{-X}'\text{X}'$ spin system.

Dragoo, A. L., Paule, R. C., **Ultrapure materials: Containerless evaporation and the roles of diffusion and Marangoni convection**, (Proc. 12th Aerospace Sciences Meeting, Washington, D.C., Jan. 30-Feb. 1, 1974), *AIAA Paper No. 74-209*, pp. 1-8 (American Institute of Aeronautics and Astronautics, New York, N.Y., 1974).

Key words: Al_2O_3 ; complex equilibria; convective-diffusion; evaporative rate; purification (evaporative); solutal-capillary; thermal capillary convection; vacuum vaporization.

Contamination from containers is a major problem in preparing ultrapure refractory materials. Space with its zero gravity and its high vacuum offers an opportunity for containerless purification of these materials. The evaporation of impurities from a melt will involve many complex chemical equilibria. Thermodynamic calculations have been modified to describe these equilibria when impurities in the melt evaporate into vacuum. The contributions of diffusion and Marangoni convection to mass transfer rates in the bulk liquid have been estimated. Calculations for the evaporative purification of molten alumina are given.

Dragoo, A. L., **Diffusion**, Chapter IV in *Beryllium: Physico-Chemical Properties of Its Compounds and Alloys*, *Atomic Energy Review Special Issue*, O. Kubaschewski, Ed., No. 4, pp. 173-175 (International Atomic Energy Agency, Vienna, Austria, 1973).

Key words: chemical interdiffusion; grain-boundary diffusion; intrinsic diffusion; lattice diffusion; self-diffusion; tracer diffusion.

The tracer diffusion coefficient, the self-diffusion coefficient, the intrinsic diffusion coefficient and the interdiffusion coefficient are briefly described. Grain boundary and lattice (volume) diffusion are contrasted. The frequency factors (D_0) and activation energies (Q) are tabulated for diffusion in the borides, carbides, and oxides of Be, Hf, Mo, Nb, Ta, Th, Ti, and Zr and for diffusion of C, N, and O in these metals. The purity of the solvent media, the preparation and properties of the samples, the method, the type of diffusion coefficient measured and the temperature range are also specified.

Dragoo, A. L., **Diffusion**, Chapter IV in *Tantalum: Physico-Chemical Properties of Its Compounds and Alloys*, *Atomic Energy Review*

Special Issue, O. Kubaschewski, Ed., No. 3, pp. 131-133 (International Atomic Energy Agency, Vienna, Austria, 1972).

Key words: chemical interdiffusion; grain-boundary diffusion; intrinsic diffusion; lattice diffusion; self-diffusion; tracer diffusion.

The tracer diffusion coefficient, the self-diffusion coefficient, the intrinsic diffusion coefficient and the interdiffusion coefficient are briefly described. Grain boundary and lattice (volume) diffusion are contrasted. The frequency factors (D_0) and activation energies (Q) are tabulated for diffusion in the borides, carbides, and oxides of Be, Hf, Mo, Nb, Ta, Th, Ti, and Zr and for diffusion of C, N, and O in these metals. The purity of the solvent media, the preparation and properties of the samples, the method, the type of diffusion coefficient measured and the temperature range are also specified.

Evans, A. G., Fuller, E. R., **Crack propagation in ceramic materials under cyclic loading conditions**, *Met. Trans.* **5**, 27-33 (Jan. 1974).

Key words: ceramics; cyclic failure; relation to static failure; slow crack growth; tension/compression; time to failure.

An analysis is presented which enables crack propagation rates under cyclic loading conditions to be predicted from static slow crack growth parameters. A comparison of the predicted times to failure under cyclic conditions with available measured failure times, for several ceramic materials at ambient temperatures, suggests that there is no significant enhancement of the slow crack growth rate due to cycling. This is verified in a series of measurements of slow crack growth rates under static and cyclic conditions.

Evans, A. G., Linzer, M., **Failure prediction in structural ceramics using acoustic emission**, *J. Amer. Ceram. Soc.* **56**, No. 11, 575-581 (Nov. 1973).

Key words: acoustic emission; ceramics; failure prediction; fracture.

Crack propagation in a typical structural ceramic (porcelain) is accompanied by acoustic emission. Two types of emission are detected. The first type is caused by slow growth of the fracture-initiating flaw; the emission rate depends primarily on crack velocity. Failure prediction using this source of emission can be effective, however, only if low-level emission, which may be related exclusively to crack growth, can be detected. The second source of emission, which occurs during bulk stressing, is the cracking associated with second-phase particles (quartz particles in porcelain) as a result of the combined action of the applied stress and local thermal and mechanical stresses. An analysis for predicting emission rates is developed and forms the basis for using this source of acoustic emission in failure prediction.

Fanconi, B., **Low-frequency vibrational spectra of some homopolypeptides in the solid state**, *Biopolymers* **12**, 2759-2776 (1973).

Key words: far infrared spectroscopy; interchain hydrogen bonding; low frequency vibrations; polypeptides; Raman spectroscopy.

Low-frequency Raman and far-infrared spectra of polyglycine, poly-L-alanine, and poly-L-valine have been measured. The Raman spectra exhibit an intense band near 100 cm^{-1} for these homopolypeptides. Lattice calculations of the polyglycines are used to assign the intense Raman band to a rotatory lattice mode. For homopolypeptides in the β conformation, an infrared band is observed whose frequency varies inversely with the square root of the mass of the peptide repeating unit. This infrared band is assigned to the hydrogen bond stretching lattice vibration.

Farabaugh, E. N., Parker, H. S., Armstrong, R. W., **Skew-reflection x-ray microscopy of the vapor-growth surface of an Al_2O_3 single crystal**, *J. Appl. Crystallogr.* **6**, Part 6, 482-486 (Dec. 1973).

Key words: Al_2O_3 ; Berg-Barrett; single crystal; skew reflection; vapor growth; x-ray diffraction microscopy.

The most commonly used geometry for the Berg-Barrett x-ray microscopy uses the zero-layer reflections as described by Newkirk. It can be shown that non-zero-layer reflections, skew-plane reflections, can be used equally well to obtain x-ray micrographs. The analysis of the stereographic representation of the skew-reflection geometry demonstrates the many usable reflections and gives the conditions for minimum image distortion. In these x-ray micrographs the contributions to diffraction contrast from shadowing and sub-boundaries can be identified. An estimate of the height of steps occurring on the crystal surface can also be made.

Feldman, A., Horowitz, D., Waxler, R. M., **Mechanisms for self-focusing in optical glasses**, *IEEE J. Quantum Electron.* **QE-9**, No. 11, 1054-1061 (Nov. 1973).

Key words: absorption coefficient; damage threshold; electrostriction; electrostrictive self-focusing; Kerr effect; laser damage; nonlinear index of refraction; self-focusing; thermal self-focusing.

The relative contributions of the Kerr, electrostrictive, and thermal effects to the self-focusing thresholds of borosilicate crown glass, fused silica, and dense flint glass have been estimated from an analysis of damage-threshold data for linearly polarized and circularly polarized radiation. The measurements were made with a Nd:glass laser operating in the TEM₀₀ mode with a temporal pulsewidth of 25 ns. The Kerr effect appears to be the largest effect. The thermal effect is also significant. The electrostrictive effect is smallest. Reasonable values of the absorption coefficient are calculated from the thermal contribution. The results are in qualitative agreement with the work of others.

Field, B. F., Finnegan, T. F., Toots, J., **Volt maintenance at NBS via $2e/h$: A new definition of the NBS volt**, *Metrologia* **9**, No. 4, 155-166 (1973).

Key words: Josephson effect; standard cell; tunnel junction; voltage comparator; voltage standard.

This paper describes in detail the procedures, methods and measurements used to establish a new definition of the U.S. legal volt via the ac Josephson effect. This new definition has been made possible by the use of thin film tunnel junctions (capable of producing 10 mV outputs) and high accuracy voltage comparators. The Josephson junction is used as a precise frequency-to-voltage converter with a conversion factor equal to $2e/h$. A series of measurements of $2e/h$ have been carried out at NBS referenced to the as-maintained unit of emf based on a large group of standard cells. Measurements made at regular intervals over a one year period (1971 to 1972) indicate that the mean emf of this group of standard cells has decreased about 4 parts in 10^7 . Primarily to remove the effects of this drift, on July 1, 1972 a new as-maintained unit was defined by choosing a value of $2e/h$ consistent with the existing unit of emf. The adopted value of $2e/h$ is 483593.420 GHz/VNBS. The precision (one standard deviation) with which the new unit of emf can be maintained with the present techniques and apparatus is about 2 parts in 10^8 . The accuracy of the present system is estimated to be 4 parts in 10^8 . Comparisons of $2e/h$ systems at different national laboratories have been limited by uncertainties associated with the physical transfer of standard cells. In order to determine the relative agreement of the various $2e/h$ systems with precision better than 1 or 2 parts in 10^7 , it appears desirable to compare $2e/h$ systems directly by transporting one of them.

Frommer, M. A., Shporer, M., Messalem, R. M., **Water binding and irreversible dehydration processes in cellulose acetate membranes**, *J. Appl. Polym. Sci.* **17**, 2263-2276 (1973).

Key words: adsorption of water; cellulose acetate; dehydration; free induction decay; freezing of water; irreversible processes; membranes; NMR; porous membranes.

The relative amounts of freezing and nonfreezing water in various water-wet cellulose acetate (CA) membranes were determined by NMR techniques, from the initial heights of the water component in the free induction decay (NMR intensity). The results suggest that (1) a significant fraction of the water in various wet CA membranes does not freeze, probably because of strong interaction with the polymer; (2) the relaxation times T_2 of the nonfreezing water are of the order of milliseconds indicating that they are still highly mobile compared with ice; (3) all the water contained in dense CA films or in membranes equilibrated at relative humidity of 0.93 does not freeze upon cooling the membranes from room temperature to -60°C ; (4) the amounts of nonfreezing bound water in membranes is higher than the total amount of water absorbed from liquid water by a dense film of the same polymer. However, the amounts of nonfreezing water in various CA membranes as calculated from the "relative NMR intensities" is substantially lower than those calculated from DSC melting endotherms by assuming the heat of fusion of water in membranes to be identical to that of pure water. Various possible reasons for this discrepancy are discussed. Measurements on the first desorption-adsorption cycle of *wet* CA membranes have also been performed. They suggest that during the first dehydration process, irreversible changes are induced in the structure of the membrane which result in a significantly lower accessibility of the polymer to interact with water. The extent of these irreversible changes in membrane structure is dependent on the details of the dehydration process being more pronounced at higher temperatures.

Gallagher, A., Lewis, E. L., **Determination of the vapor pressure of rubidium by optical absorption**, *J. Opt. Soc. Amer.* **63**, No. 7, 864-869 (July 1973).

Key words: rubidium; vapor pressure.

The vapor pressure of rubidium was determined in the neighborhood of 330 K from measurements of optical absorption of the resonance lines. A narrow-line source was used and a full analysis of the line profiles was done. Measurements of resonance-broadening depolarization give another check on the Rb vapor pressure in the 430-K range, assuming that theoretical cross section is correct. The results are very close to the analytic compromise previously suggested by Nesemeyanov.

Galy, J., Roth, R. S., **The crystal structure of $\text{Nb}_2\text{Zr}_6\text{O}_{17}$** , *J. Solid State Chem.* **7**, 277-285 (1973).

Key words: anion excess fluorite; crystal structure; $\text{Nb}_2\text{Zr}_6\text{O}_{17}$; square anti-prism.

$\text{Nb}_2\text{Zr}_6\text{O}_{17}$ is orthorhombic, space group *Ima2*, with $a = 40.91$, $b = 4.93$, $c = 5.27$ Å. The asymmetric structural unit contains one octahedron, three sevenfold coordinated ions, and one square antiprism, and its relations to the fluorite and ZrO_2 structures are discussed. Variations in compositions can be accounted for by increasing or decreasing the number of sevenfold coordinated ions in the structure.

Gebbie, K. B., Steinitz, R., **On spatial variations in the intensity of chromospheric H_α** , *Astrophys. J.* **188**, No. 2, 399-406 (Mar. 1, 1974).

Key words: features observed in H_α ; H_α filtergrams; lateral contrasts in intensity; profile variation mechanism.

We investigate the formation of patterns in H_α spectroheliograms and filtergrams. Introducing a *source-sink-control diagram*, we conclude that the H_α line source function in the quiet solar chromosphere is indirectly controlled by the photospheric radiation fields in the Balmer and Paschen continua. We demonstrate that in producing the observed patterns, horizontal spatial variations in the shape of the absorption profile are extremely effective compared to changes in the source and sink terms. Applying this mechanism, we compute asymptotic values for the contrasts and visibilities in chromospheric H_α .

Geist, J., Blevin, W. R., **Chopper-stabilized null radiometer based upon an electrically calibrated pyroelectric detector**, *Appl. Opt.* **12**, No. 11, 2532-2535 (Nov. 1973).

Key words: ac power measurements; electrically calibrated radiometer; pyroelectric detector; radiometer; radiometry.

In this paper we will describe a new type of radiometric system that combines the high-accuracy characteristics of electrical calibration and null detection with the noise and background discrimination of chopper-stabilized, synchronous detection. We start by outlining those characteristics required for high accuracy and those required for good noise discrimination. Next we show that these requirements are mutually inconsistent for certain types of detectors (thermopiles), but that they can all be well satisfied by electrically-calibrated pyroelectric detectors. Then we discuss the special requirements for a chopper-stabilized null radiometer, including wave-form independent, lock-in detection, and lastly we describe the performance of a system that we have constructed.

Geist, J., Schmidt, L. B., Case, W. E., **Comparison of the laser power and total irradiance scales maintained by the National Bureau of Standards**, *Appl. Opt.* **12**, No. 11, 2773-2776 (Nov. 1973).

Key words: intercomparison; irradiance scale; laser power scale.

The paper describes an intercomparison of the instrument used to realize and maintain the NBS laser power and energy scale with the instrument used to realize and maintain the upper end of the NBS total irradiance scale. The intercomparison was conducted by performing simultaneous measurements of the average power from a cw krypton laser with both instruments. The procedure and apparatus of the comparison are described. The measured difference between the two instruments was well within the ~ 1.5 percent limit of error associated with the intercomparison.

Geltman, S., Teague, M. R., **Atomic absorption of ultra intense laser radiation**, *J. Phys. B: At. Mol. Phys. Letter to Editor* **7**, No. 1, L22-L27 (1974).

Key words: atoms; free-free absorption; ultra-intense laser radiation.

We derive an expression for the rate of absorption by an atomic system (bound or free) of radiation from an ultra intense laser beam. The absorption characteristics are radically different from those of conventional weak-field absorption theory.

Glaze, D. J., Hellwig, H., Jarvis, S., Jr., Wainwright, A. E., Allan, D. W., **Recent progress on the NBS primary frequency standard**, *Proc. 27th Annual Symp. on Frequency Control, Philadelphia, Pa., June 12-14, 1973*, pp. 347-356 (Electronic Industries Association, Washington, D.C., 1973).

Key words: cesium beam standard; Doppler effect; frequency accuracy; frequency stability; power shift; primary frequency standard.

The design of NBS-5 is discussed in detail including its relation to previous NBS primary cesium beam frequency standards. The application of pulsed microwave excitation, and the use in the accuracy evaluation of frequency shifts due to known changes in the exciting microwave power are discussed. Significant changes in the measured atomic velocity distribution with the beam alignment are reported and compared with measured Ramsey patterns. Stabilities of 3×10^{-14} for one-day averaging are reported and data on accuracy are given. Preliminary results give an evaluated accuracy of 2×10^{-13} with indications that this figure may be improved in the future.

The bias-corrected frequency of NBS-5 agrees to within 1×10^{-13} with the value obtained with NBS-III in 1969 which is preserved in the rate of the NBS Atomic Time Scale.

Goldberg, R. N., Armstrong, G. T., **Microcalorimetry: A tool for biochemical analysis**, *Med. Instrum.* **8**, No. 1, 30-36 (Jan.-Feb. 1974).

Key words: analytical chemistry; bacterial identification; biochemistry; cellular processes; clinical chemistry; enzyme activity; immunochemistry; medical instrumentation; microcalorimetry; thermochemistry.

In order for the application of heat measurements to analysis and clinical chemistry to be feasible, three requirements must be met: (1) specificity of reaction, (2) knowledge of the thermochemistry involved, and (3) adequate instrumentation. Instrumentation requirements are met by devices known as heat conduction microcalorimeters. Some of the principles underlying these instruments are reviewed. The current status of microcalorimetry regarding requirements of sensitivity, sample volume, accuracy, reproducibility, and speed is considered. A brief review of analytical applications that have utilized microcalorimetry is given. These applications include assays for enzymes and substrates, bacterial identifications, and investigation of cellular processes. The advantages and disadvantages of the method as well as possibilities for future development are considered.

Goldman, A. J., **Approximate localization theorems for optimal facility placement**, *Transp. Sci.* **6**, No. 2, 195-201 (May 1972).

Key words: facility location; optimal location.

The problem is that of locating a flow-receiving facility in a region, so as to minimize the weighted sum of distances between sources and facility. It is shown here that if a subregion S both generates "sufficiently much" of the region's total flow, and admits entry via specified "gate" points without "too much" circuitry, then (a) S contains at least one "near-optimal" location for the facility, and (b) no strictly optimal location can lie "too far" from S .

Goldman, A. J. **Minimax location of a facility in a network**, *Transp. Sci.* **6**, No. 4, 407-418 (Nov. 1972).

Key words: facility location; network theory; optimal location.

The problem is that of locating a facility in a network N so as to minimize the largest of its distances from the vertices of N . A method is given that either solves the problem, or else reduces it to an analogous problem for a single "cyclic component" of N . When N is acyclic (a tree), a very efficient solution algorithm results. Partial analogs of these results are given for a "weighted-distance" extension of the problem.

Goldman, D. T., Logan, D. A., **Solid wastes—a technological assessment**, *Chem. Eng. Progr.* **69**, No. 9, 33-35 (Sept. 1973).

Key words: engineering education; solid waste disposal; technology assessment.

A technology assessment is performed on the problem of the disposal of municipal refuse. Various alternative methods are considered including proposed methods for the utilization of solid waste. The identification of those affected by the various alternatives and an evaluation of the impacts these alternatives have on the affected parties are presented. The conclusions of this simple assessment is that sanitary landfills is the most desirable form of presently available disposal methods. For the future, new methods for the utilization of solid waste are required.

Haber, S., **Numerical evaluation of multiple integrals**, *SIAM Rev.* **12**, No. 4, 481-526 (Oct. 1970).

Key words: best integration formulas; diophantine approximation; Gaussian quadrature; integration; Monte Carlo; multiple integration; multiple quadrature; numerical analysis; numerical integration; optimal formulas; quadrature.

This paper is an expository survey of the main methods that have been developed for numerical evaluation of multiple integrals. Among the approaches discussed are: the Monte Carlo method and its generalizations; number-theoretical methods, based essentially on the ideas of diophantine approximation and equidistribution modulo 1; the functional analysis approach, in which the quadrature error is regarded as a linear functional and one attempts to minimize its norm; and the classical approach of designing formulas to be exact for polynomials of high degree while using as few values of the integrand as possible. Most of the research in this field is quite recent.

Halford, D., **Infrared-microwave frequency synthesis design: Some relevant conceptual noise aspects**, (Proc. Frequency Standards and Metrology Seminar, Quebec, Canada, Aug. 30-Sept. 1, 1971), Paper in *Proceedings of the Frequency Standards and Metrology Seminar*, pp. 431-466 (Quantum Electronics Laboratory, Laval University, Quebec, Canada, 1972).

Key words: Allan variance; base units; fast linewidth; frequency multiplication; infrared frequency metrology; Josephson effect; linewidth; methane frequency standard; phase noise; unified standard.

Extremely accurate and precise frequency synthesis into the infrared and visible radiation regions will allow new vistas of metrology. Frequency and time measurements are the basic operations which will be affected, and impact is expected in such diverse areas as length standards and metrology, spectroscopy, timekeeping, communications, and relativistic tests. In addition the set of independent base units of measurement may change, and the speed of light may become a conventional (defined) quantity. The attainment of the desired high accuracy and precision will be easiest and cheapest if there is careful optimization of the synthesis design aspects involving noise. When frequencies in the terahertz region are considered, the linewidth of the signal becomes an important parameter. Due to the low-frequency-divergence of the instability of good signal sources, the concept of the *fast linewidth* becomes of particular importance. Some of the properties and importance of the *fast linewidth* in system design are discussed in this paper.

Halford, D., Shoaf, J. H., Risley, A. S., **Spectral density analysis: Frequency domain specification and measurement of signal stability**, *Proc. 27th Annual Symp. on Frequency Control, Cherry Hill, N.J., June 12-14, 1973*, pp. 421-431 (Electronic Industries Association, Washington, D.C. 10006).

Key words: amplitude fluctuations; cross-spectral density; frequency domain; frequency noise; modulation noise; noise specification and measurement; oscillator noise; phase noise; radio frequency power spectral density; script $\mathcal{L}(f)$; script $\mathcal{M}(f)$; script \mathcal{N} ; sidebands; signal stability; spectral density.

Stability in the frequency domain is commonly specified in terms of spectral densities. The spectral density concept is simple, elegant, and very useful, but care must be exercised in its use. There are several different but closely related spectral densities, which are relevant to the specification and measurement of stability of the frequency, phase, period, amplitude, and power of signals. Concise, tutorial descriptions of useful spectral densities are given in this survey. These include the spectral densities of fluctuations of (a) phase, (b) frequency, (c) fractional frequency, (d) amplitude, (e) time interval, (f) angular frequency, and (g) voltage. Also included are the spectral densities of radio frequency power and its two normalized components, Script $\mathcal{L}(f)$ and Script $\mathcal{M}(f)$, the phase modulation and amplitude modulation portions, respectively. Some of the simple, often-needed relationships among these various spectral densities are given. The use of one-sided spectral densities is recommended. The relationship to two-sided spectral densities is explained. The concepts of cross-spectral densities, spectral densities of time-dependent spectral densities, and smoothed spectral densities are discussed.

Hastie, J. W., Hauge, R. H., Margrave, J. L., **Infrared spectra of matrix-isolated species in the gallium-fluorine system**, *J. Fluorine Chem.* **3**, 285-291 (1973/74).

Key words: aluminium; fluorides; gallium; infrared spectra; matrix isolation.

The species GaF₃, GaF, AlF₃, AlF and (AlF)₂ have been isolated in inert-gas matrices and their infrared absorption spectra obtained over the range 33-4000 cm⁻¹. The following techniques were used to generate these species; (i) co-deposition of Ga or GaF and molecular F₂ or F atoms with an excess of inert gas; (ii) Knudsen cell effusion and matrix isolation of the vapors over GaF₃, GaF₃+Ga and GaF₃+Al.

Hellwig, H., Jarvis, S., Jr., Halford, D., Bell, H. E., **Evaluation and operation of atomic beam tube frequency standards using time domain velocity selection modulation**, *Metrologia* **9**, No. 3, 107-112 (1973).

Key words: atomic beams; cavity phase shift; cesium beam; frequency accuracy; frequency standard; pulsed excitation; second-order Doppler shift; velocity distribution.

Pulsed excitation of atomic and molecular beam devices with separated Ramsey-type interaction regions allows the observation of signals due to very narrow atomic velocity groups. The theoretical background of this method is discussed. Experimental operation of a near mono-velocity cesium beam tube is demonstrated. The velocity distribution of a commercial cesium beam tube is obtained using the pulse method. The normal Ramsey pattern of this beam tube is calculated from the velocity distribution and compared with the measured Ramsey pattern. The pulse method allows the direct determination of the cavity phase shift and of the second-order Doppler correction in beam devices. The pulse method thus shows promise for the evaluation of existing laboratory as well as commercial cesium beam tubes with respect to these effects.

Hellwig, H., Bell, H. E., **Some experimental results with an atomic hydrogen storage beam frequency standard**, *Metrologia* **8**, 96-98 (1972).

Key words: atomic hydrogen beam; dispersion; frequency stability; frequency standard; hydrogen maser.

A frequency standard is described in which a quartz crystal oscillator is locked to the hydrogen hyperfine transition using the dispersion of this resonance. The hydrogen storage beam apparatus closely resembles a hydrogen maser with a low-Q cavity below oscillation threshold. Cavity pulling can be reduced to a point where environmental temperature fluctuations limit the stability mainly via the second-order Doppler effect. Locking to the dispersion feature of the resonance eliminates the need for frequency modulation in order to find line-center. The stability of the frequency standard was measured against crystal oscillators and cesium beam frequency standards; stabilities of 4×10^{-13} were recorded for sampling times of 30 seconds and of 3 hours.

Hellwig, H., Jarvis, S., Jr., Glaze, D. J., Halford, D., Bell, H. E., **Time domain velocity selection modulation as a tool to evaluate cesium beam tubes**, *Proc. 27th Annual Symp. on Frequency Control, Philadelphia, Pa., June 12-14, 1973*, pp. 357-366 (Electronic Industries Association, Washington, D.C., 1973).

Key words: atomic beams; cavity phase shift; cesium beam; frequency standard; pulsed excitation; second-order Doppler shift; velocity distribution.

Pulsed excitation of atomic and molecular beam devices with separated Ramsey-type interaction regions allows the observation of signals due to very narrow atomic velocity groups. The theoretical background of this method is discussed. Experimental operation of a near mono-velocity cesium beam tube is demonstrated. The velocity distribution of a commercial cesium beam tube and of the primary

laboratory standard NBS-5 are obtained using the pulse method. The normal Ramsey patterns are calculated from the velocity distribution and compared with the measured Ramsey patterns. The pulse method allows the direct determination of the cavity phase shift and of the second-order Doppler correction in beam devices. Velocity distributions obtained via the pulse method allow the use of microwave power shift results for accuracy evaluations. These aspects as well as the effects of modulation and different velocity distributions are discussed in detail. The pulse method thus shows promise for the evaluation of existing laboratory as well as commercial cesium beam tubes with respect to these effects.

Howell, B. F., Margolis, S., Schaffer, R., **Residual fluorescence as an index of purity of reduced nicotinamide adenine dinucleotide**, *Clin. Chem.* **19**, No. 11, 1280-1284 (1973).

Key words: alcohol dehydrogenase; fluorescence studies; nicotinamide adenine dinucleotide; optical rotation.

Determination of fluorescence remaining after reduced nicotinamide adenine dinucleotide (NADH) has reacted with excess acetaldehyde in the presence of alcohol dehydrogenase (EC 1.1.1.1) is useful as a criterion of NADH purity when used in conjunction with other methods for determining purity such as the rate of reaction, the ratio of ultraviolet absorbances at 260 nm and 340 nm, the color, and the chromatographic homogeneity of the preparation. Measurement of residual fluorescence monitors the enzymatically inactive material which absorbs at 340 nm. The specific optical rotations of NADH at several wavelengths are also reported.

Huie, R. E., Herron, J. T., Davis, D. D., **Absolute rate constants for the addition and abstraction reactions of atomic oxygen with 1-butene over the temperature range 190-491 K**, *J. Phys. Chem.* **76**, No. 23, 3311-3313 (1972).

Key words: abstraction reactions; addition reactions; atomic oxygen; reaction kinetics; 1-butene.

Using the technique of flash photolysis-resonance fluorescence, absolute rate constants have been measured for the reaction of ground-state atomic oxygen with 1-butene over the temperature range 190-491 K. With a measured precision of 3-5 percent at each temperature, it was found that the data could not be fit by a single straight line. It was concluded that the curvature in the Arrhenius plot was due to concurrent abstraction and addition reactions, the former process representing approximately 15 percent of the total reaction at 300 K and 39 percent at 500 K. The rate expressions derived were $k_{\text{addition}} = (3.7 \pm 1.8) \times 10^{-12} \exp(-50 \pm 210 \text{ cal mol}^{-1}/RT) \text{ cm}^3 \text{ molecule}^{-1} \text{ sec}^{-1}$ and $k_{\text{abstraction}} = (1.6 \pm 0.9) \times 10^{-11} \exp(-1970 \pm 430 \text{ cal mol}^{-1}/RT) \text{ cm}^3 \text{ molecule}^{-1} \text{ sec}^{-1}$.

Johnson, C. R., **Gersgorin sets and the field of values**, *J. Math. Anal. Appl.* **45**, No. 2, 416-419 (Feb. 1974).

Key words: D-stable matrix; diagonal; doubly stochastic matrix; field of values; Gersgorin circles; numerical radius; positive definite; spectrum.

Two links are drawn between two well-known inclusion sets for the characteristic roots of a complex matrix: the field of values and the Gersgorin circles. An application is made to the theory of D-stable matrices.

Kaufman, V., Artru, M.-C., Brillet, W.-U. L., **Revised analysis of the 2p³3s, 3p, 3d, and 4s configurations of triply ionized aluminum (Al IV)**, *J. Opt. Soc. Amer.* **64**, No. 2, 197-201 (Feb. 1974).

Key words: aluminum; energy levels; spectra; ultraviolet; wavelengths.

The spectrum of triply ionized aluminum (Al IV) was observed between 700 and 2200 Å. About 60 new lines have been identified as transitions between the 2p³3s, 3p, 3d, and 4s configurations. The ground-state combinations have been remeasured (124-161 Å). Ener-

gies and designations are given for all levels of these configurations, and several changes and additions to the previous analysis have been made. Results of calculations of these configurations are included to support the level identifications. An isoelectronic comparison is discussed.

Kayser, B., Lipkin, H. J., Meshkov, S., **Tests of higher symmetries**, *Phys. Rev. D* **8**, No. 11, 4193-4198 (Dec. 1, 1973).

Key words: cross sections; reactions; Regge pole; SU(3); symmetry breaking; trajectory.

Model-independent cross-section relations predicted by unbroken SU(3) symmetry, and some predicted by SU(6)_{w, strong}, are compared with experiment. The relations are found to be satisfied, apart from deviations which follow, in every case, the pattern and rough size of symmetry breaking expected from Regge-pole exchange. Interestingly, this Regge symmetry breaking diverges with increasing energy. It is argued that this behavior, though contrary to intuition, is reasonable.

Kelleher, D. E., Wiese, W. L., **Observation of ion motion in hydrogen Stark profiles**, *Phys. Rev. Lett.* **31**, No. 24, 1431-1434 (Dec. 10, 1973).

Key words: Balmer; broadening; dynamic; ion; plasma; Stark.

We have measured the central part of the Balmer H_β or D_β line in similar stabilized arc plasmas, but of different chemical compositions. We have found an ion-motion effect which appears to scale with the inverse square root of the reduced mass of the radiator-perturber system and which, for H_β at least, essentially removes one of the largest remaining discrepancies between experiment and Stark-broadening theory.

Kessler, K. G., **Absolute measurements of differential cross sections for electron scattering at intermediate energies (50-500 eV)**, *Comments At. Mol. Phys.* **1**, No. 3, 70-72 (Aug.-Sept. 1969).

Key words: differential cross sections; elastic cross sections; electron scattering.

Technological improvements in the design and construction of electron impact spectrometers now make possible more reliable absolute measurements of elastic and inelastic differential cross sections for the scattering of electrons by atoms and molecules. Cross sections can now be determined with an imprecision of 5 percent or less, depending upon the degree to which systematic errors are brought under control.

Kranbuehl, D. E., Verdier, P. H., Spencer, J. M., **Relaxation of fluctuations in the shape of a random-coil polymer chain**, *J. Chem. Phys. Letter to Editor* **59**, No. 7, 3861-3862 (Oct. 1, 1973).

Key words: lattice-model polymer chains; Monte Carlo; polymer chain dynamics; relaxation times.

The relaxation times of deviations from spherical symmetry of random-coil polymer chains in dilute solution have been investigated by dynamical Monte Carlo studies of lattice-model chains without excluded volume. The deviations are found to persist for times of the order of the longest relaxation times of the internal motions of the chains.

Kuriyama, M., Early, J. G., Burdette, H. E., **Fluid flow effects on crystalline perfection**, (Proc. 12th Aerospace Sciences Meeting, Washington, D.C., Jan. 30-Feb. 1, 1974), *AIAA Paper No. 74-204*, pp. 1-10 (American Institute of Aeronautics and Astronautics, New York, N.Y., 1974).

Key words: copper single crystals; crystal perfection; dislocations; fluid flow; thermal convection; x-ray topography.

In the absence of gravity, thermal convection, i.e., convection induced by gravity acting on density differences in the melt, would be

expected to be negligible. Fluid flow in the melt, including thermal convection, probably affects the perfection of crystals grown from the melt. At present, the relationship between crystal growth conditions, in particular, fluid flow conditions, and the degree of crystal perfection has not been well established for metals. It is, therefore, highly desirable to document the perfection of crystals grown from the melt in terms of directly controllable process parameters, before one even begins to analyse the fluid flow conditions in the melt in terms of thermodynamical variables. In this paper, optimum solidification parameters for the production of highly perfect copper crystals by Czochralski growth are sought along with documentation of crystal imperfections under various growth conditions. A vital part of research of this type is the assessment of crystal perfection. X-ray techniques which do not in their application produce defects and which allow the characterization of imperfections in single crystals are chosen to assess crystal perfection. The properties of crystals grown from the melt are anticipated to vary over a large range, since the growth conditions, especially the fluid flow conditions, are deliberately changed. The x-ray techniques employed ranged from ordinary Laue photography through Borrmann topography to double-crystal scanning diffractometry, thus allowing crystals with a wide variation in perfection to be studied. As a set of controllable solidification parameters, the rotation of the seed and of the melt and the diameter of the bottle-neck are chosen. X-ray diffraction topographs are analysed along with the data obtained from rocking curve measurements. Tables of growth conditions and quantitative data of rocking curve widths are presented.

Kurylo, M. J., **Kinetics of the reactions OH(v=0) + NH₃ → H₂O + NH₂ and OH(v=0) + O₃ → HO₂ + O₂ at 298 K**, *Chem. Phys. Lett.* **23**, No. 4, 467-471 (Dec. 15, 1973).

Key words: ammonia; kinetics; OH radical; ozone; stratosphere.

The rate constants for the reactions OH(X²Π, v=0) + NH₃^{k₁} → H₂O + NH₂ and OH(X²Π, v=0) + O₃^{k₂} → HO₂ + O₂ were measured at 298 K by the flash photolysis resonance fluorescence technique. The values of the rate constants thus obtained are k₁ = (4.1 ± 0.6) × 10⁻¹⁴ and k₂ = (6.5 ± 1.0) × 10⁻¹⁴ in units of cm³ molecule⁻¹ sec⁻¹. The results are discussed in terms of understanding the dynamics of the perturbed stratosphere.

Laughlin, D. E., Cahn, J. W., **The crystal structure of the metastable precipitate in copper-based copper-titanium alloys**, *Scr. Met.* **8**, 75-78 (1974).

Key words: coherency; copper-titanium; D1_a; electron diffraction; L1₂.

Knight and Wilkes recently reported that the metastable ordered phase which forms by precipitation from copper-rich copper-titanium binary alloys is of the type L1₂. This note shows that this indexing is incorrect, and that the previously assigned structure of D1_a is fully consistent with all experimental findings.

Ledbetter, H. M., Naimon, E. R., **Relationship between single-crystal and polycrystal elastic constants**, *J. Appl. Phys.* **45**, No. 1, 66-69 (Jan. 1974).

Key words: Debye temperature; elastic constants; lattice-vibrational properties; polycrystal; single crystal; Voigt-Reuss-Hill.

A new method is given for computing effective polycrystalline elastic constants from single-crystal elastic coefficients. Agreement with observation is good. The method is based on the assumed equivalence of the lattice-vibrational properties of single crystals and polycrystals of the same material; single-crystal and polycrystal Debye temperatures are equated. Present predictions of polycrystal elastic moduli differ significantly from those of most other averaging methods by being lower than the familiar Voigt-Reuss-Hill results.

Lee, P. H., Broida, H. P., Braun, W., Herron, J. T., **Direct observation of vibrationally excited hydrogen produced by colli-**

sional energy transfer from electronically excited sodium, rubidium, caesium, and mercury, *J. Photochem.* **2**, 165-172 (1973/74).

Key words: absorption spectra; apparatus and method; energy transfer; gases; kinetics of reaction; photochemistry; vacuum u.v.

Hydrogen has been vibrationally excited by direct energy transfer from electronically excited sodium, rubidium and caesium, and mercury. The vibrational excitation of the $B^1\Sigma^+_u \leftarrow X^1\Sigma^+_g$ transitions in hydrogen was detected by absorption of the vacuum u.v. radiation from a low pressure molecular hydrogen lamp.

Lenzi, M., McNesby, J. R., Mele, A., Xuan, C. N., **Collisional deactivation of $NH_2(\tilde{A}^2A_1)$** , *J. Chem. Phys.* **57**, No. 1, 319-323 (July 1, 1972).

Key words: ammonia; fluorescence; Jovian; vacuum ultraviolet.

$NH_2(\tilde{A}^2A_1)$ was produced by photolysis of ammonia in the vacuum ultraviolet. Deactivation rates of this radical were measured by the quenching of fluorescence in NH_3 , CH_4 , H_2 , N_2 , He, Ne, Ar, Kr, Xe. An estimate of the lifetime of spontaneous radiative decay of 0.8×10^{-5} sec is suggested. Application of the results to the dynamics of the Jovian atmosphere is reported.

Levin, E. M., Benedict, J. T., Sciarello, J. P., Monsour, S., **The system K_2SO_4 - Cs_2SO_4** , *J. Amer. Ceram. Soc.* **56**, No. 8, 427-430 (Aug. 1973).

Key words: Cs_2SO_4 ; density K_2SO_4 - Cs_2SO_4 solid solutions; equilibrium diagram Cs_2SO_4 - K_2SO_4 ; hexagonal solid solutions; K_2SO_4 ; phase diagram Cs_2SO_4 - K_2SO_4 ; polymorphism Cs_2SO_4 - K_2SO_4 solid solutions; solid solutions.

The phase diagram for the system K_2SO_4 - Cs_2SO_4 was determined by using DTA for melting relations and DTA and high-temperature x-ray diffractometry for subsolidus relations. At the solidus the system shows complete solid solubility, with a minimum at 940 °C and 50 mol% Cs_2SO_4 . Orthorhombic K_2SO_4 and Cs_2SO_4 , the stable low-temperature forms, show mutual solid solubility and form a eutectoid at 50 mol% Cs_2SO_4 and 430 °C, the lowest temperature of stability of the high-temperature hexagonal solid-solution phase. Isothermal plots of the a and c dimensions of this hexagonal phase vs composition show large positive deviations from linearity for c . These deviations are interpreted on the basis of the crystal structure of $KNaSO_4$ with a similar unit cell.

Lyon, G., **Syntax-directed least-errors analysis for context-free languages: A practical approach**, *Commun. ACM* **17**, No. 1, 3-14 (Jan. 1974).

Key words: arbitrary input strings; context-free grammars; dynamic programming; parsing.

A least-errors recognizer is developed informally using the well-known recognizer of Earley, along with elements of Bellman's dynamic programming. The analyzer takes a general class of context-free grammars as drivers, and any finite string as input. Recognition consists of a least-errors count for a corrected version of the input relative to the driver grammar. The algorithm design emphasizes practical aspects which help in programming it.

Madey, T. E., Yates, J. T., Jr., Erickson, N. E., **ESCA study of fractional monolayer quantities of chemisorbed gases on tungsten**, *Chem. Phys. Lett.* **19**, No. 4, 487-492 (Apr. 15, 1973).

Key words: carbon monoxide; ESCA; monolayer; oxygen; photoyields; sensitivity; tungsten.

X-ray photoelectron spectroscopy (ESCA) has been used in a study of CO and O_2 chemisorbed on a polycrystalline tungsten sample. Working under ultrahigh vacuum conditions, the surface was cleaned and then covered with known monolayer and fractional monolayer

quantities of adsorbed CO and O_2 . The O(ls) and C(ls) spectral features were detected, and the influence of an adsorbed layer on the tungsten spectral features was determined. A chemical shift of 3.4 eV in the O(ls) line from chemisorbed CO is related to the different modes of bonding of CO to tungsten. A model calculation of the photoelectron yields expected from an adsorbed monolayer is in good agreement with the experimental results.

Mandel, J., Lashof, T. W., **Interpretation and generalization of Youden's two-sample diagram**, *J. Qual. Technol.* **6**, No. 1, 22-36 (Jan. 1974).

Key words: collaborative reference programs; interlaboratory tests; test method evaluation; Youden diagram.

Youden's two sample diagram is a useful method for certain types of interlaboratory comparisons of test results. Generally, points in the plot fall within an elongated ellipse, the major axis of which makes a 45° angle, approximately, with the x, y axes. Occasionally it happens that the axes are not the bisectors of the coordinate axes. This paper (1) examines more closely the assumptions underlying the Youden diagram and presents a more general method of interpreting it and (2) generalizes the diagram to situations where the two samples do not have the same level and/or the axes of the ellipse definitely do not bisect the coordinate axes.

Mauer, F. A., Hubbard, C. R., **Evaluation of the energy dispersive powder diffraction method for the determination of quartz in dust samples**, (Proc. Roundtable Discussion on Analytical Techniques for Quartz, Cincinnati, Ohio, Dec. 6-7, 1972), Paper in *Analytical Techniques for Quartz*, pp. 17-23 (National Institute for Occupational Safety and Health, American Conference of Governmental Industrial Hygienists, Cincinnati, Ohio, Jan. 1974).

Key words: analytical methods; industrial hygiene; quartz; silicosis; x-ray diffraction.

An energy dispersive powder diffractometer was assembled and used to determine the amount of quartz on six silver membrane filters, such as those used in sampling airborne dust. The amount of quartz, which varied from 24 to 531 μg , was also determined by weighing. The results obtained indicate that the overall uncertainty in the weight of quartz obtained by the energy dispersive x-ray method is at least 50 μg . The method, therefore, does not meet the National Institute for Occupational Safety and Health requirement for a practical lower limit of detection of 20 μg and an analytical range of 20 μg to 4 mg.

Mazur, J., Guttman, C. M., McCrackin, F. L., **Monte Carlo studies of self-interacting polymer chains with excluded volume. II. Shape of a chain**, *Macromolecules* **6**, No. 6, 872-874 (Nov.-Dec. 1973).

Key words: asymmetry of polymer configurations; excluded volume; principal moments; radius of gyration; self-interacting polymer chains.

The principal moments of the squared radius of gyration of polymer chains with excluded volume were computed for chains on the simple cubic and face-centered cubic lattices. The moments were ordered for each configuration by their magnitude, then averaged over a large number of chain configurations and divided by the squared radius of gyration to yield shape factors of the chain. These shape factors were found to be independent of chain length for long chains. The shape factors showed that the instantaneous shape of a polymer chain is very asymmetrical. With increasing interaction energy between the segments of the chains, the chains became less asymmetrical; at the Θ point the shape factors became equal to those of the random coil as previously calculated by Solc and Stockmayer. The relative variations of the principal moments were also calculated. The largest principal moments were found to have the largest relative variations.

Mazur, J., Rubin, R. J., **Average span of self-avoiding walks on the simple cubic lattice**, *J. Chem. Phys. Letters to Editor* **60**, No. 1, 341-342 (Jan. 1, 1974).

Key words: polymer chains; ratio method; self-avoiding walks; span.

In a recent publication, Bellemans concluded that the average span of a self-avoiding walk has a different asymptotic dependence on the number of steps than does the root-mean-square end-to-end distance. In this paper, we reanalyze Bellemans' data and show that there is no basis for his conclusion.

McAlister, A. J., Cuthill, J. R., Dobbyn, R. C., Williams, M. L., **Soft x-ray study of the *d*-bands in AuAl₂**, (Proc. Int. Conf. on Band Structure Spectroscopy of Metals and Alloys, Strathclyde, Glasgow, Scotland, Sept. 26-30, 1971), Paper in *Band Structure Spectroscopy of Metals and Alloys*, D. J. Fabian and L. H. Watson, Eds., pp. 191-203 (Academic Press, London, England, 1973).

Key words: Au; AuAl₂; *d*-bands; emission spectrum; N_{6,7}; soft x-ray.

The N_{6,7} soft x-ray emission spectrum (5d to 4f transition) of Au in AuAl₂ has been measured. This work, together with the x-ray photoemission results of Chan and Shirley, shows the *d*-bands to be distributed over a range of approximately 4 eV, with maxima at 5.0 and 7.1 eV below the Fermi level. These results raise some questions about the interpretation of the Al L emission spectrum from the compound, which appeared to offer strong confirmation of nonrelativistic band calculations of the electronic structure of AuAl₂, and again raise the possibility of *d*-band participation in the strong coloring of the compound, an effect which the Al emission spectrum and nonrelativistic band calculations appeared to exclude.

McCarter, R. J., **A new technique for thermal analysis of vapor-producing reactions**, *J. Appl. Polym. Sci.* **17**, 1833-1846 (1973).

Key words: differential thermal analysis; DTA; kinetics; pyrolysis; TGA; thermal analysis; thermal degradation; thermogravimetric analysis.

An apparatus was developed for measuring the rate at which vapors are evolved during the thermal degradation of materials and thereby deriving the kinetics of such reactions. Requisite to the operating scheme of the apparatus is the provision of a high-temperature zone to convert condensable or tarry vapors into noncondensable form. The apparatus yields a direct measure of reaction velocity, rather than the integrated indication obtained with thermogravimetric analysis. This simplifies the identification and calculation of kinetic parameters. Increases in sensitivity and operating range are also achieved. Flexibility in operation is obtained that permits the separate recording of reactions that tend to overlap. Although the apparatus principally has been operated using a combustible gas indicator to meter the evolved vapors, a number of options are available for the latter function, including flowmeters and various continuous gas analyzers. The applicability of the method appears promising.

McCrackin, F. L., Mazur, J., Guttman, C. M., **Monte Carlo studies of self-interacting polymer chains with excluded volume. I. Squared radii of gyration and mean-square end-to-end distances and their moments**, *Macromolecules* **6**, No. 6, 859-871 (Nov.-Dec. 1973).

Key words: excluded volume; Monte Carlo; polymer solution; radii of gyration; theta point.

Random walks that are not allowed to intersect themselves were generated on the simple cubic and face-centered cubic lattices and used as a model of a linear polymer chain in dilute solution with excluded volume and attractive energies between chain elements. The mean-square end-to-end distances and mean squared radii of gyration and their moments were computed for chain lengths up to 2000 segments and for a wide range of attractive energies. The partition func-

tions of the chains were also computed. The attractive energy required for a given property of the chain to be the same as the given property of a random coil, the θ point, was investigated. The required attractive energy depended slightly on the particular property chosen for comparison, so rather than a unique θ point, a narrow range of θ points was found.

McDaniel, C. L., **Phase relations in the systems Na₂O-IrO₂ and Na₂O-PtO₂ in air**, *J. Solid State Chem.* **9**, 139-146 (1974).

Key words: compounds; dissociation; Na₂O-IrO₂ system; Na₂O-PtO₂ system; phase relations.

The equilibrium phase relations for the Na₂O-IrO₂ and Na₂O-PtO₂ systems were determined in air using the quenching technique. The Na₂O-IrO₂ system contains two stable compounds Na₂O·IrO₂ and 2Na₂O·3IrO₂, which dissociate at 1235 and 1040 °C, respectively. The Na₂O-PtO₂ system contains three compounds: Na₂O·PtO₂, metastable 2Na₂O·3PtO₂, and Na_xPt₃O₄ (0 ≤ x ≤ 1). Their dissociation temperatures are 890, 710, and 810 °C, respectively. Indexed x-ray diffraction powder patterns for Na₂O·IrO₂ and 2Na₂O·3IrO₂ are given.

Merris, R., Newman, M., **An explicit isomorphism with applications to inequalities for matrix functions**, *J. Algebra* **25**, No. 3, 468-474 (June 1973).

Key words: central idempotents; group algebras; irreducible representations; matrix functions.

Inequalities for matrix functions are derived in a uniform way for an explicit isomorphism.

Mielenz, K. D., **Eureka! Appl. Opt.** **13**, No. 2, A14 and A16 (Feb. 1974).

Key words: Archimedes; Buffon; burning mirrors; feasibility; history of optics; Second Punic War; solar energy.

In view of the recently renewed controversy whether Archimedes could have used mirrors to defer the attacking Roman fleet during the siege of Syracuse in the Second Punic War, it is pointed out that the feasibility of this has been demonstrated by Buffon in 1747. Additional facts are presented which also suggest that the use of burning mirrors could have presented a serious threat to the blockading Romans.

Morrissey, B. W., Stromberg, R. R., **The conformation of adsorbed blood proteins by infrared bound fraction measurements**, *J. Colloid Interface Sci.* **46**, No. 1, 152-164 (Jan. 1974).

Key words: blood proteins; infrared bound fraction; protein adsorption; protein conformation.

The likelihood that surface-induced blood coagulation results from specific protein-material interactions has led to a study of the conformation of adsorbed blood proteins. Infrared difference spectroscopy was used to determine the bound fraction, i.e., the fraction of carbonyl groups of an adsorbed molecule directly interacting with the surface, of serum albumin, prothrombin, and fibrinogen *in situ*. Measurements were carried out on individual proteins as a function of the amount adsorbed, time of absorption, pH, and ionic strength using a silica surface.

The results obtained for serum albumin and prothrombin indicate that the internal bonding of these globular proteins is sufficient to prevent changes in the structure while adsorbed, even at low surface population. The bound fraction of fibrinogen increases with increasing adsorbance, suggesting possible interfacial aggregation. The conformation of all three proteins was found to be independent of the time of adsorption, although major differences in the rates of adsorption were observed.

Studies of cross-linked and denatured serum albumin have provided information on the conformational changes concomitant with

adsorption of the native protein. Qualitatively, such changes, if they occur, are small. This conclusion is supported by computer simulation studies of lysozyme adsorption. Studies of the effect of pH and ionic strength on the adsorbance and bound fraction of serum albumin show that caution must be exercised when identifying the plateau adsorbance of a protein isotherm with a close-packed monolayer.

Mount, G. H., Linsky, J. L., Shine, R. A., **One- and multi-component models of the upper photosphere based on molecular spectra. I: The violet system of CN (0,0)**, *Solar Phys.* **32**, No. 1, 13-30 (Sept. 1973).

Key words: best-fit model; carbon abundance; molecular spectra; upper photosphere.

Spectroheliograms taken in the CN(0,0) violet band near $\lambda 3883 \text{ \AA}$ show very small scale network and cell structures with high contrast. The bandhead itself, which is a broad feature due to overlap of several CN lines, allows the diagnostic simplicity of a continuum since motions, magnetic fields, and broadening mechanisms are unimportant. We have obtained spectroheliograms in the bandhead and center-to-limb photoelectric spectra of CN(0,0) at Kitt Peak National Observatory. From the photoelectric spectra and a detailed analysis of the formation of the CN(0,0) spectrum we derive a best-fit one-component upper photospheric model differing from that of the HSRA and recommend a change in solar carbon abundance from the HSRA value of $\log A_c = 8.55$ to $\log A_c = 8.25$. From the calibrated spectroheliograms we consider a multi-component model to account for the observed fine structure intensity variations.

Mozer, B., De Graaf, L. A., Le Neindre, B., **Neutron-diffraction studies in liquid ^4He** , *Phys. Rev. A* **9**, No. 1, 448-459 (Jan. 1974).

Key words: condensate fraction; density and temperature; liquid helium; neutron diffraction; pair correlation and three-atom correlation function; structure factor.

Structure factors of liquid helium have been determined from neutron-diffraction measurements of high statistical accuracy. Diffraction measurements were performed out to momentum transfers of 7 \AA^{-1} for three different densities of liquid helium at a constant temperature above the helium λ transition and at a nearly constant temperature below the λ transition for the same three densities. Statistically significant differences in the structure factors are observed as the density is varied at constant temperature and for temperatures above and below the λ transition at constant density. The radial pair-correlation functions have been calculated from the liquid-structure factors. The structure factors or the related radial pair-correlation functions can be used to obtain information about three-atom correlations in liquid helium above and below the λ transition from a construction of their isothermal density derivative. The temperature dependence of the constant-density structure factors or their derived pair-correlation functions can also be used to test a current theoretical estimate of the condensate fraction in liquid helium.

Naimon, E. R., **Elastic constants of the perovskite RbMnF_3 using a Born model**, *Phys. Rev. B* **9**, No. 2, 737-740 (Jan. 15, 1974).

Key words: Born-Mayer repulsion; Born model; elastic constants; electrostatic interactions; perovskite; RbMnF_3 .

The elastic constants of RbMnF_3 were calculated using a Born model, which consists of electrostatic and Born-Mayer repulsive interactions. This model has two adjustable parameters; these were determined from the equilibrium volume and one of the three second-order elastic constants. Calculated third-order elastic constants agreed reasonably well with experiment. Also calculated were the electrostatic contributions to the first-, second-, and third-order elastic constants of the cubic perovskite structure for several values of ionic charge. Relationships of these constants to those of the NaCl- and CsCl-type structures are given.

Newbury, D. E., Yakowitz, H., Yew, N. C., **Observation of magnetic domains in nickel using the scanning electron microscope**, *Appl. Phys. Lett.* **24**, No. 2, 98 (Jan. 15, 1974).

Key words: bitter patterns; contrast mechanisms; magnetic domains; nickel; scanning electron microscopy; transformer alloy.

Scanning electron microscope (SEM) observation of magnetic domains in a polycrystalline pure nickel sheet was made possible through the use of a 50-kV accelerating potential. The contrast was unobservable in an SEM capable of only a 30-kV accelerating potential.

Newman, M., **Symmetric completions and products of symmetric matrices**, *Trans. Amer. Math. Soc.* **186**, 191-201 (Dec. 1973).

Key words: fields; principal ideal rings; symmetric completion; symmetric matrices; unimodular matrices.

We show that any vector of n relatively prime coordinates from a principal ideal ring R may be completed to a symmetric matrix of $\text{SL}(n, R)$, provided that $n \geq 4$. The result is also true for $n = 3$ if R is the ring of integers Z . This implies for example that if F is a field, any matrix of $\text{SL}(n, F)$ is the product of a fixed number of symmetric matrices of $\text{SL}(n, F)$ except when $n = 2$, $F = \text{GF}(3)$, which is a genuine exception.

Olsen, P. T., Driscoll, R. L., **Determination of γ_p' at the National Bureau of Standards**, (Proc. 4th Int. Conf. on Atomic Masses and Fundamental Constants, Teddington, England, Sept. 6-10, 1971), Paper in *Atomic Masses and Fundamental Constants*, J. H. Sanders and A. H. Wapstra, Eds., pp. 471-484 (Plenum Press, London, England, 1972).

Key words: fine structure constant; gyromagnetic ratio of proton; nuclear induction; precision solenoid.

The gyromagnetic ratio of the proton, γ_p' is one of our most important fundamental physical constants. (The prime indicates that the protons are in a spherical sample of pure H_2O .) Not only is it used for calibration purposes in nuclear magnetic resonance experiments, but it plays a crucial role in determining the fine structure constant from the measurement of $2e/h$ via the ac Josephson effect. Additionally the continued measurement of γ_p' can be used to monitor as-maintained units of current.

The precision of γ_p' measurements at the National Bureau of Standards (NBS) has improved significantly since the early measurements of the 1950's, from several parts per million (ppm) to the present 0.1 to 0.2 ppm. Current efforts are now being directed towards improving the present 3 to 4 ppm accuracy of the experiment by an order of magnitude. It is the purpose of this paper to briefly report the progress being made in this direction. First, a general discussion of the experiment is given, including (a) use of the method of nuclear induction to determine the precession frequency; (b) a description of a new and improved series of pitch measurements using a laser interferometer; (c) a discussion of the effect of the change in original winding tension on the effective diameter of the windings; and (d) an analysis of the effect of the finite susceptibility of the solenoid and water sample support structure on the calculated magnetic field. All of the known corrections to the field are then summarized, and finally, a brief analysis of the uncertainties in the experiment is given along with a value for γ_p' .

Penn, D. R., **An improved Anderson model**, *Phys. Rev. B* **9**, No. 3, 839-843 (Feb. 1, 1974).

Key words: adsorbates on metal surfaces; density of states; impurity wave function; magnetic impurities; phase shift; reformulation of the Anderson model.

The Anderson model has been very successful in the study of (magnetic) impurities in metals and has also proved useful for atoms adsorbed on metal surfaces. The model as originally formulated is phenomenological in that the position and width of the resonant impurity state cannot be calculated within the context of the model even in the absence of correlation effects. Anderson and McMillan and also Kanamori have proposed theories which are more quantitative. We show that the results of both theories follow from very simple assumptions. Moreover, we show that for the case of a free-electron-like metal and a spherical impurity potential both theories will give a correct density of states for the metal plus impurity if the wave function associated with the impurity is chosen properly. This is particularly important for the theory of Kanamori where the use of a non-Hermitian Hamiltonian raises questions about its validity. The best choice for the impurity wave function requires it to be energy dependent, unlike that one which appears in the usual Anderson model. However, it is shown that an energy-independent wave function can be chosen such that the Anderson-McMillan and Kanamori theories will yield a good density of states.

Perlstein, J. H., Ferraris, J. P., Walatka, V. V., Jr., Cowan, D. O., Candela, G. A., **Electron transport and magnetic properties of new highly conducting TCNQ complexes**, (Proc. 18th AIP Conf. on Magnetism and Magnetic Materials, Denver, Colo., Nov. 28-Dec. 1, 1972), Paper in *Magnetism and Magnetic Materials*, C. D. Graham, Jr., and J. J. Rhyne, Eds., No. 10, 1494-1498 (American Institute of Physics, New York, N.Y., 1973).

Key words: electron transport; magnetic properties; metallic; TCNQ complexes.

Single crystals of the 1:1 complexes tetrathiafulvalinium tetracyanoquinodimethane (TTF-TCNQ) and tetrathianaphthacinium tetracyanoquinodimethane (TTN-TCNQ) have been synthesized and the electron transport properties and magnetic susceptibility have been measured from 2 K to room temperature. For TTN-TCNQ, σ at room temperature is $1\Omega^{-1}\text{cm}^{-1}$. For TTF-TCNQ, σ at room temperature along the long axis (σ_{\parallel}) is in the range $192\text{--}652\Omega^{-1}\text{cm}^{-1}$ depending on sample whereas perpendicular to the long axis σ_{\perp} is $1\Omega^{-1}\text{cm}^{-1}$. The conductivity remains metallic down to 66 K in both directions whereupon a continuous metal to insulator transition occurs. The activation energy in the insulating state is 0.0062 eV. The transition is associated with a small hysteresis between the heating and cooling curves suggesting a possible structural change. In the metallic region, ρ_{\parallel} follows a T^2 dependence whereas ρ_{\perp} follows a T^{-1} behavior. The magnetic susceptibility is diamagnetic below 20 K becoming increasingly more paramagnetic with increasing T even in the metallic region. It is suggested that spin disorder scattering may account for the anomalous temperature dependence of ρ_{\parallel} .

Piermarini, G. J., Block, S., Barnett, J. D., **Hydrostatic limits in liquids and solids to 100 kbar**, *J. Appl. Phys.* **44**, No. 12, 5377-5382 (Dec. 1973).

Key words: diamond-anvil pressure cell; glass transition pressures; hydrostaticity; pressure gradients; pressure measurements; ruby fluorescence.

The hydrostatic properties of the materials methanol, isopropyl alcohol, water, sodium chloride, silver chloride, and the binary mixtures pentane-isopentane and methanol-ethanol have been determined in the diamond-anvil pressure cell up to 180 kbar by line-broadening and line-shift measurements of the sharp R_1 ruby fluorescence line. A liquid mixture 4:1 by volume of methanol:ethanol remains hydrostatic to almost 100 kbar at room temperature. This mixture exceeds the hydrostatic limit of the previous generally accepted fluid, 1:1 pentane:isopentane which has a hydrostatic limit of about 70 kbar. Silver chloride and water (ice VII) are better than sodium chloride as pressure-transmitting media, but do not even qualitatively approach hydrostatic conditions much above 70 kbar. The stress sensitivity level of the ruby limits the ex-

tent to which slight deviations from hydrostatic conditions can be determined in solid systems and suggests the qualitative nature of the method in characterization of quasihydrostatic states. The equilibrium freezing pressure of methanol at 24 °C was redetermined to be 35.8 ± 0.8 kbar.

Rains, T. C., Epstein, M. S., Menis, O., **Automatic correction system for light scatter in atomic fluorescence spectrometry**, *Anal. Chem.* **46**, No. 2, 207-210 (Feb. 1974).

Key words: atomic fluorescence spectrometry; automatic correction; electrodeless discharge lamp; light scatter; standard reference material.

Light scattering of incident radiation by solvent droplets and unvaporized solute particles in the flame is a major interference in atomic fluorescence spectrometry (AFS). A technique for the automatic correction of light scatter is described which increases the speed and accuracy of analysis. The light from an electrodeless discharge lamp and a 150-W xenon lamp is alternately passed through the flame. The resulting signal from the multiplier phototube is fed to a lock-in amplifier which corrects for the contribution of the light scattering to the fluorescence signal. The principles of the technique and apparatus for making the automatic correction are described. To accomplish this correction, scatter of the incident radiation from the electrodeless discharge and xenon lamps is balanced initially while aspirating a 1 percent lanthanum solution. The method has been applied to the determination of 0.11 and 0.26 μg Cd/gram in SRM's Orchard Leaves and Liver, respectively, without any prior separation or preconcentration.

Raveché, H. J., Mountain, R. D., **Structure studies in liquid ^4He** , *Phys. Rev. A* **9**, No. 1, 435-447 (Jan. 1974).

Key words: condensate fraction; ground state wave function; neutron diffraction; pair correlation function; triplet correlation function; ^4He .

We investigate, using neutron-diffraction data, several properties of the local atomic structure in liquid ^4He , both above and below the superfluid transition. Distinguishing features of the pair-correlation function are summarized and the diffraction data are employed to investigate a proposed form for the condensate fraction as a function of temperature. The pair-correlation function is used to examine an inequality that gives an upper bound that is close to the observed values, and also to examine the use of approximate integral equations for the ground-state wave function. Triplet correlations and closure approximations are studied from the isothermal density derivative of the pair-correlation function. The results suggest that, analogous to the pair-correlation function, the triple-correlation function shows a temperature dependence that is not observed in simple classical fluids.

Richmond, J. C., **A standard for night vision devices for law enforcement**, (Proc. of the Society of Photo-Optical Instrumentation Engineers, San Diego, Calif., Aug. 27-29, 1973), Paper in *Image Intensifiers: Technology, Performance, Requirements and Applications*, A. D. Schnitzler and M. W. Klein, Eds., **42**, 109-115 (1974).

Key words: contrast transfer function; distortion; flare; image intensifiers; law enforcement; light equivalent background; light induced background; night vision; optical gain.

A draft Standard for Passive, Hand-Held Night Vision devices has been developed for the Law Enforcement Standards Laboratory of the National Bureau of Standards. This Standard is now being circulated for comment prior to adoption as a Standard of the National Institute of Law Enforcement and Criminal Justice of the Law Enforcement Assistance Administration of the Department of Justice.

The paper mentions some of the philosophy behind the standard, lists the performance requirements and describes briefly the test procedures for (A) focus adjustment, curvature of field and distortion

of the eyepiece lens, (B) optical gain, optical gain stability, light equivalent background, light induced background, luminance of output screen, luminance uniformity, cathode and screen quality, contrast transfer function, distortion and flare of a night vision device complete with objective lens, but with the eyepiece removed, and (C) for resistance to vibration, high and low temperature storage, operation and thermal shock and humidity of night vision devices complete with both objective and eyepiece lenses, and (D) boresight adjustment, click movement and resistance to mechanical shock of night vision devices intended for use as rifle sights.

Risley, A. S., **The Josephson junction as applied to the measurement of the frequencies of several laser lines**, (Proc. Frequency Standards and Metrology Seminar, Quebec, Canada, Aug. 30-Sept. 1, 1971), Paper in *Proceedings of the Frequency Standards and Metrology Seminar*, pp. 325-328 (Quantum Electronics Laboratory, Laval University, Quebec, Canada, 1972).

Key words: harmonic generation; Josephson junction; laser frequencies; methane; microwave frequency stability.

The Josephson junction has been applied to the measurement of laser frequencies as high as 3.8 THz by direct multiplication from an X-band source. An attempt is being made to extend this technique to frequencies as high as 10.7 THz.

Roberts, R. W., **Energy research: Scientists seek to ease the pinch**, *The Futurist VIII*, No. 1, 19-22 (Feb. 1974).

Key words: buildings; conservation, energy.

In this period of energy shortage, intensive research and development efforts are required for the development of viable alternatives to traditional energy sources. During the inevitable lag time between energy need and new supply, conservation measures can do much to reduce the energy gap. This is especially true in buildings, where vast amounts of energy are currently wasted. Various NBS programs bearing on the design and operation of more energy efficient buildings are summarized.

Rowe, J. M., Livingston, R. C., Rush, J. J., **Neutron quasielastic scattering study of SH⁻ reorientation in rubidium hydrosulfide in the intermediate temperature trigonal phase**, *J. Chem. Phys.* **59**, No. 12, 6652-6655 (Dec. 15, 1973).

Key words: neutron scattering; orientational disorder; phase transition; reorientation; residence time; rubidium hydrosulfide; vibration amplitude.

The reorientation of (SH)⁻ ions in the trigonal phase of RbSH has been investigated by neutron quasielastic scattering at 373 and 393 K. The quasielastic peaks show a distinct two-component (elastic and broadened) structure, the behavior of which is used to establish that the ions are reorienting between two equilibrium sites (presumably by 180° flips along the trigonal axis) with average times between reorientation of 5.4 ± 0.4 psec and 4.0 ± 0.4 psec at 373 and 393 K. Mean square amplitudes of hydrogen vibration are determined from the momentum transfer dependence of the total intensity, and found to be higher than that found in the high temperature fcc phase, even though the rate of reorientation is an order magnitude faster in the cubic phase.

Scavennec, A., Nahman, N. S., **A simple passively mode-locked CW dye laser**, *IEEE J. Quantum Electron.* **QE-10**, No. 1, 95-96 (Jan. 1974).

Key words: DODCI; dye laser; laser; mode-lock; picosecond; rhodamine 6 G.

The operation of a simple passively mode-locked 5800-Å dye laser is reported. A single active medium, solution of rhodamine 6 G and diethyloxadicarbocyanine iodide (DODCI) in glycol flowing as an unconfined liquid film, is used for the simultaneous production of gain and nonlinear absorption.

Sharman, L. J., Tovey, H., Vickers, A. K., **Current status and national priorities for flammable fabric standards**, *Proc. 6th Annual Meeting of Information Council on Fabric Flammability*, New York, N.Y., Dec. 7, 1972, pp. 265-306 (Information Council on Fabric Flammability, New York, N.Y., May 1, 1973).

Key words: blankets; children's sleepwear; fabric fires; fabric flammability standards; FFACTS; fire injuries; flammable fabrics; flammability standards priorities; garment flammability; garments; sampling plans; upholstered furniture.

The present status (calendar year 1972) of flammability standards issued by the Department of Commerce is described. During 1972, a sampling plan was developed for the Standard for the Flammability of Children's Sleepwear, DOC FF 3-71. The Standard was reissued with this plan included. A Flammability Standard for Mattresses was also issued. Work is in progress on a proposed flammability standard for blankets and flammability test methods for upholstered furniture. The approaches used in development of the standard and the current status of the work are discussed.

The results of a recent analysis of information available to the Fire Technology Division, National Bureau of Standards, on the relative need for specific flammability standards for wearing apparel are discussed. The system used for developing "candidate priorities" for standards is briefly described. A list of high priority garment types is presented, along with examples of compilations of data from the NBS-Flammable Fabrics Accident Case and Testing System (F-FACTS) and other sources supporting the placement of the individual garment types on the list.

Shumaker, J. B., **A spectroscopic study of equilibrium in nitrogen arcs**, *J. Quant. Spectrosc. Radiat. Transfer* **14**, 19-26 (1974).

Key words: arc plasma; equilibrium; LTE; nitrogen.

Nitrogen arc measurements of the intensity of the 4915 Å — 4935 Å NI doublet and of the 3995 Å NII line show that local thermodynamic equilibrium cannot be assumed in nitrogen arcs at electron densities below 1×10^{17} cm⁻³. Below this point, the results suggest that gas and electron temperatures differ significantly and that ground states are overpopulated with respect to upper electronically excited states.

Simmonds, M. B., **Using the semiconductor junction in quantum interference devices**, *J. Appl. Phys.* **45**, No. 1, 366-368 (Jan. 1974).

Key words: Josephson junctions; quantum interference; SQUID.

We have fabricated small-area tunnel junctions of a lead-tellurium-lead structure. These have been used in conjunction with bulk superconductors to make hybrid interference devices. We have successfully operated these devices at bias frequencies of 30 MHz, 300 MHz, and 10 GHz.

Straty, G. C., Goodwin, R. D., **Dielectric constant and polarizability of saturated and compressed fluid methane**, *Cryogenics* **13**, No. 12, 712-715 (Dec. 1973).

Key words: dielectric constant; methane; polarizability.

Accurate measurements of the dielectric constant of methane have been made on the saturated liquid from near the triple point to 188 K and on the compressed fluid along selected isotherms from 100 K to 300 K and at pressures to 345 bar. The data are combined with accurate densities to obtain the molar polarizability and its dependence on density and temperature. The density range examined extends to nearly three times the critical density. The molar polarizability is found to increase initially with density and then decrease in qualitative agreement with theoretical predictions and the behaviour of other fluids.

Thrower, P. A., Nagle, D. C., Horton, W. S., **The anisotropy of pyrolytic graphite**, *J. Appl. Crystallogr.* **6**, Part 5, 347-351 (Oct. 1973).

Key words: magnetic susceptibility; orientation function; preferred orientation; pyrolytic graphite.

Two proposed expressions, $I_1(\phi) = \cos^m \phi$ and $I_2(\phi) = (1 + b^2 \sin^2 \phi)^{-1}$, for the orientation function, $I(\phi)$, of pyrolytic graphites have been shown analytically to give quite different values for the Bacon anisotropy factor (BAF) for oriented materials. BAF values derived from the angle of half-maximum intensity using $I_1(\phi)$ are within 20 percent of numerically calculated values for the BAF range 10-90, whereas values obtained using $I_2(\phi)$ are smaller by as much as a factor of twenty. The effect of sample preparation on such measurements has been found to be negligible. Diamagnetic-susceptibility measurements on the graphites investigated validated the calculated BAF values in that the derived single-crystal susceptibilities were in reasonable agreement with known values. BAF values calculated via $I_2(\phi)$ produced unacceptable paramagnetic values parallel to the basal plane. It is suggested that $I_1(\phi)$ be used for rapid BAF determinations; although numerical calculation is preferred, the difficulty of measuring $I(\phi)$ at large ϕ , for highly oriented materials, may make the full numerical procedure impracticable and this approximate procedure the more desirable.

Verdier, P. H., **Monte Carlo studies of lattice-model polymer chains. III. Relaxation of Rouse coordinates**, *J. Chem. Phys.* **59**, No. 11, 6119-6127 (Dec. 1, 1973).

Key words: excluded volume; lattice-model polymer chains; Monte Carlo; polymer chain dynamics; relaxation times.

The relaxation of the seven lowest Rouse coordinates for simple lattice models of polymer chains of up to 64 beads, with and without excluded volume, is studied by simulation on a digital computer. The similarity between the relaxation of the lattice-model chains without excluded volume and that of a statistical-bead model, noted in previous studies of end-to-end length, is confirmed and examined in greater detail. The effect of excluded volume in slowing down the relaxation of the Rouse coordinates is examined, and a simple picture is suggested which accounts qualitatively for the results obtained. The nonnormal coordinate nature of the Rouse coordinates for chains with excluded volume is demonstrated by their nonexponential autocorrelation functions. However, the results suggest that for each chain length, there is a unique longest internal relaxation time, corresponding to an internal coordinate closely resembling the lowest Rouse coordinate.

Wampler, R. H., **Some recent developments in linear least-squares computations**, (Proc. Computer Science and Statistics 6th Annual Symp. on the Interface, University of California, Berkeley, Calif., Oct. 16-17, 1972), Paper in *Proceedings of the Computer Science and Statistics Sixth Annual Symposium on the Interface*, M. E. Tarter, Ed., 94-110 (Western Periodicals Co., North Hollywood, Calif., Oct. 1972).

Key words: analysis of variance; computer programs; Gram-Schmidt orthogonalization; Householder transformations; ill-conditioned test problems; iterative refinement; least squares computations; linear equations; OMNITAB; regression; rounding errors; statistics.

The results of an evaluation of linear least-squares computer programs (Wampler (174, 175)) are briefly summarized. Subsequent work, including problems encountered, to provide a more accurate least-squares routine for the OMNITAB II program is discussed. In this connection, the comparative results of running a number of ill-conditioned problems on OMNITAB II and two other reliable programs are presented. A bibliography of the recent literature on least-squares analysis has been prepared with special emphasis on the computational aspects of obtaining least-squares solutions.

Weiss, A. W., **Correlation in excited states of atoms**, *Advan. At. Mol. Phys.* **9**, 1-46 (1973).

Key words: correlation; energy levels; oscillator strengths; spectroscopy; wave functions.

This article reviews the current status of work on electron correlation in excited states of light atoms through approximately $Z=20$. The primary orientation is towards *ab initio* correlation calculations, so that semiempirical methods are not discussed except insofar as they relate directly to the correlation problem. Furthermore, the discussion is restricted to the effects of correlation on only two properties, namely energies and oscillator strengths. After a brief statement and description of the correlation problem in general, we concentrate on 1) methods currently employed to attack excited state correlation, and 2) a description of some of the results obtained so far which appear to be peculiar to excited states.

Since most excited state correlation calculations have relied on the multiconfiguration expansion, this method is described at some length. For convenience the variety of such approaches are classified according to the choice of zeroth order, or reference state, starting point, which may be the Hartree-Fock, Hartree-Fock-Slater, or statistical model. Allowing the reference state orbitals to relax in the field of the virtual configuration leads to the multiconfiguration self-consistent field approximation, and this method is described as well. The charge expansion scheme and the pair correlation approach are also discussed from the standpoint of providing a framework for analyzing much of the results which have been obtained.

Some of the more striking effects of excited state correlation are related to the readjustment of energy levels along an isoelectronic sequence. Not only are there anomalies associated with level crossings, but the asymptotic degeneracy effects predicted by the charge expansion theory appear, very often, to persist along an entire sequence. One of the large correlation corrections in the ground state involves orbital polarization, and this also happens with excited states, where it can often be understood as a series perturbation phenomenon. Series perturbations represent a large and important correlation correction not only for the series but for the perturbing state as well. These effects are all discussed by way of examples. Finally, some discussion is given of the role of pair correlations in excited states.

Wiese, W. L., **Experimental studies of the Stark broadening of hydrogen lines**, (Proc. VI Yugoslav Symp. and Summer School on the Physics of Ionized Gases, Miljevac by Split, Yugoslavia, July 16-21, 1972), Paper in *Physics of Ionized Gases*, M. V. Kurepa, Ed., pp. 559-596 (Institute of Physics, Beograd, Yugoslavia, 1972).

Key words: atomic line shapes; critical review; hydrogen lines; plasma sources; Stark broadening.

Recent experimental investigations on the Stark broadening of hydrogen lines by high density plasma sources are critically viewed. The principal requirements for accurate Stark broadening experiments are discussed, and plasma sources, line profile measurements, and diagnostic techniques are reviewed in detail. The most recent experimental results are presented, compared with theory, and their significance for future theoretical work on Stark broadening is pointed out.

Wiese, W. L., **Regularities in atomic oscillator strengths**, (Proc. VI Yugoslav Symp. and Summer School on the Physics of Ionized Gases, Miljevac by Split, Yugoslavia, July 16-21, 1972), Paper in *Physics of Ionized Gases*, M. V. Kurepa, Ed., pp. 627-649 (Institute of Physics, Beograd, Yugoslavia, 1972).

Key words: atomic oscillator strengths; perturbation theory; regularities; systematic trends.

A review of the recently detected regularities and systematic trends among atomic oscillator strengths is presented. The quantum mechanical background for the existence of these regularities is discussed and, in particular, the relationship between oscillator strengths and nuclear charge as derived from perturbation theory is derived in detail. All regularities are illustrated by some typical graphical or tabular examples.